Magnetic Calorimeters for Neutrino Physics

Loredana Gastaldo

Kirchhoff Institute for Physics, Heidelberg University

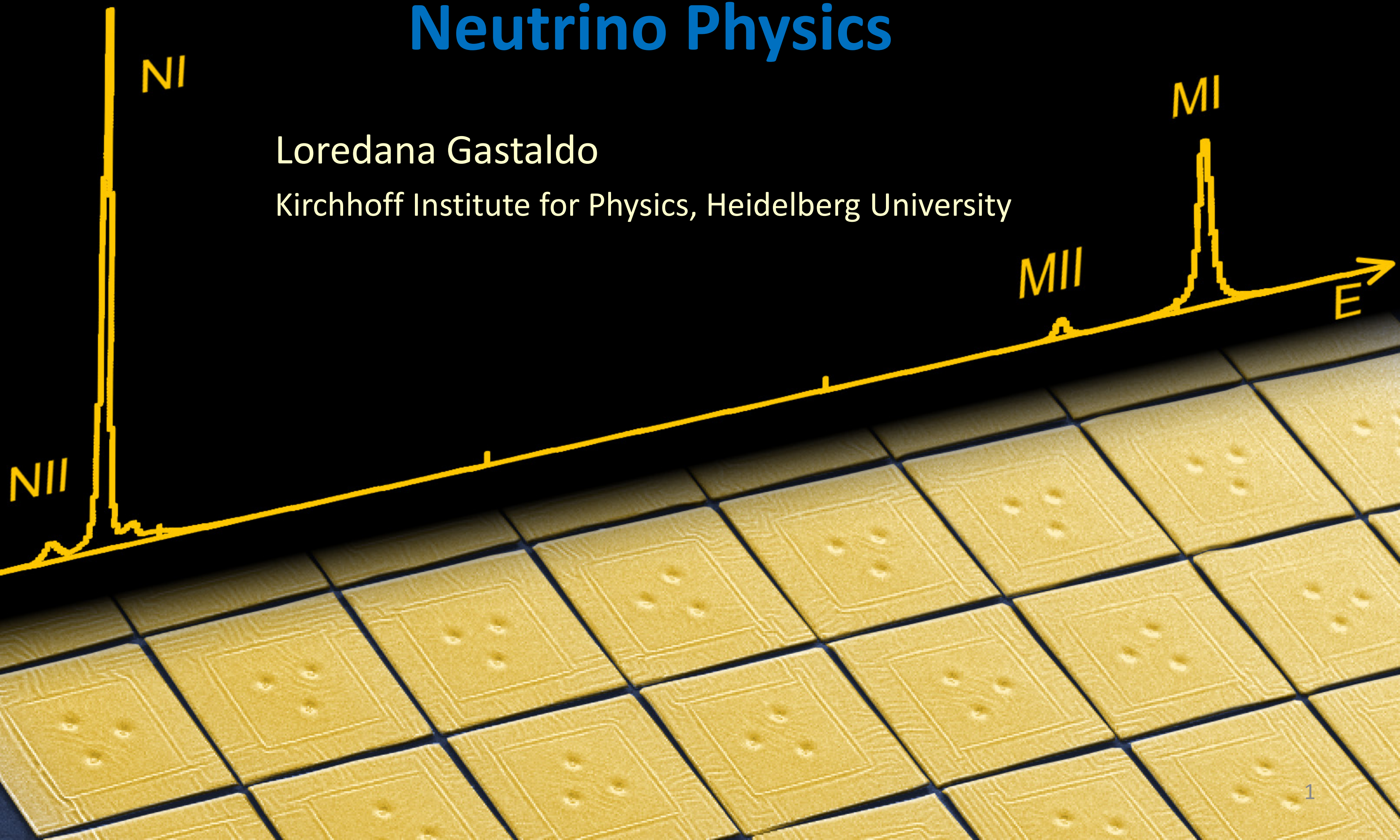

Contents

- Metallic Magnetic Calorimeters
- Direct neutrino mass determination
  The ECHo neutrino mass experiment
- Sterile neutrinos searches in electron capture spectra
- $0\nu2\beta$ with scintillating crystals
- Conclusions and outlook

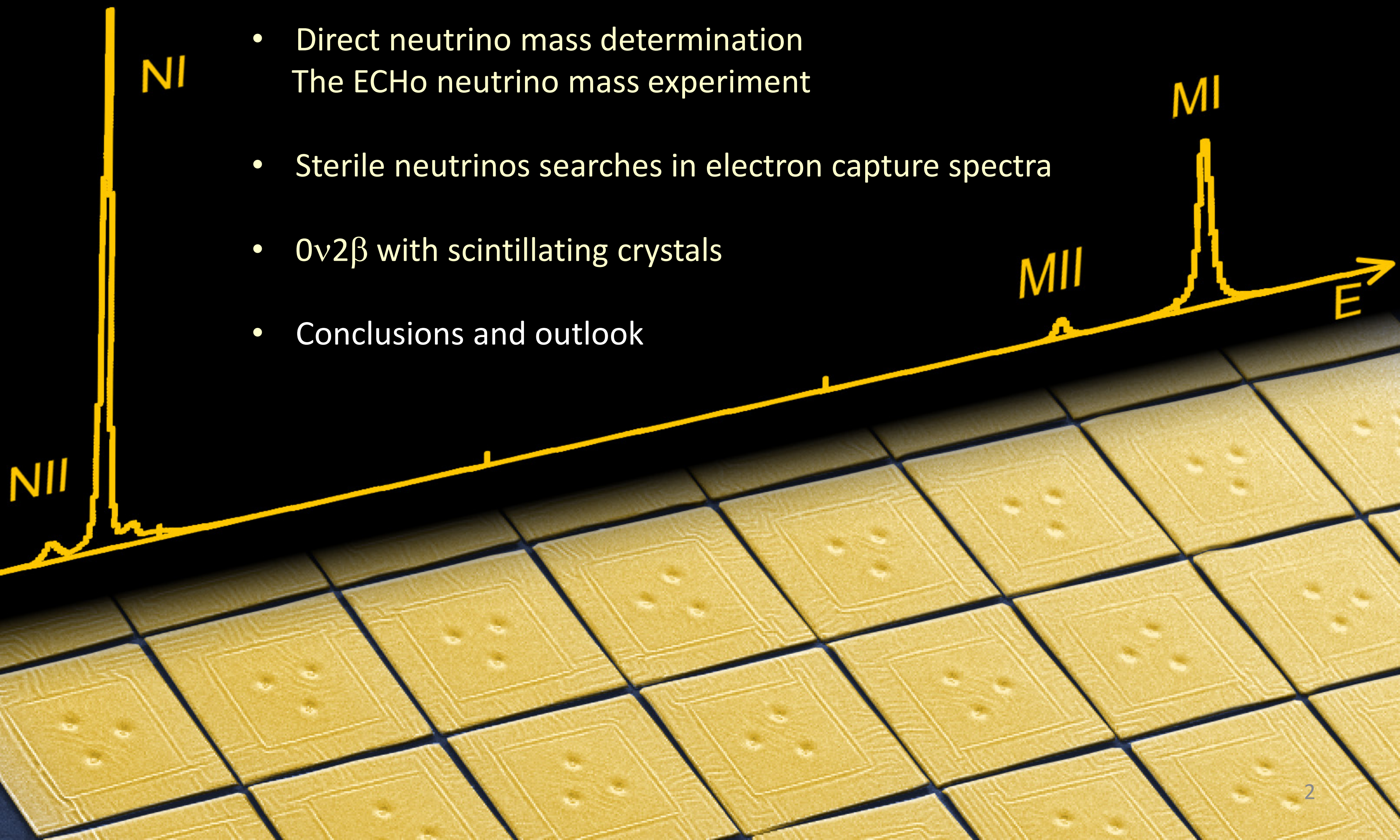

Take-home messages

- Working principle of MMCs and their performance
- Where a finite electron neutrino mass affects the ^{163}Ho EC spectrum
  Experimental methods (advantages and disadvantages)
- How to search for sterile neutrino signature in EC spectra
- Benefits of scintillating crystals and
  detector requirements for DBD experiments

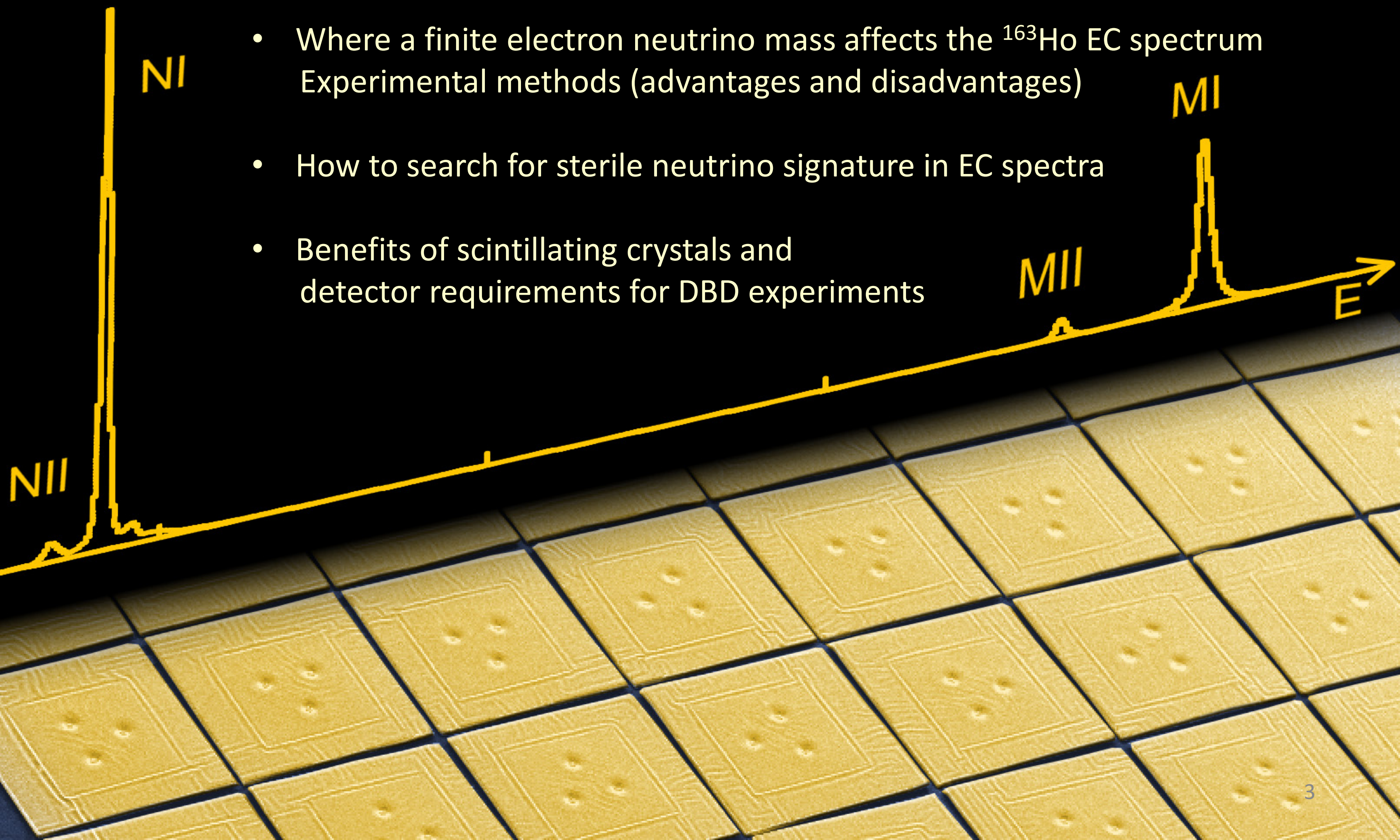

Low temperature micro-calorimeters

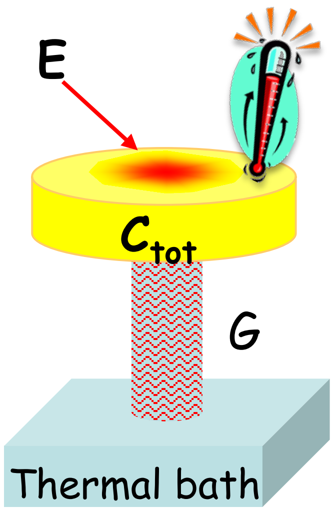

$$\Delta T \cong \frac{E}{C_{tot}}$$

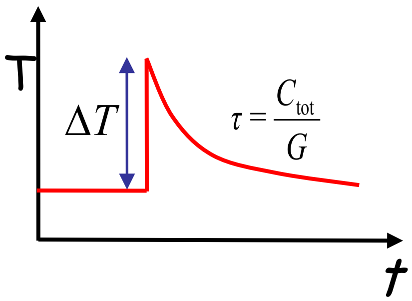

Low temperature micro-calorimeters

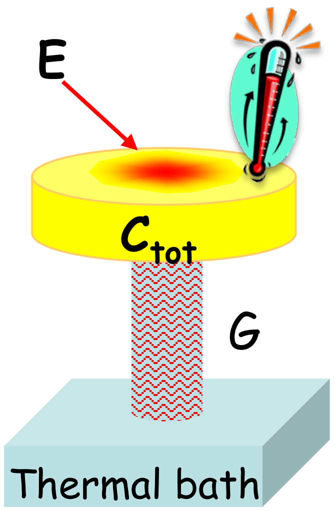

$$\Delta T \cong \frac{E}{C_{tot}}$$

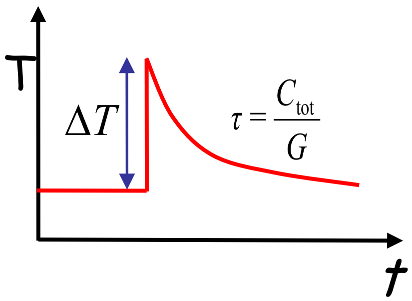

***E* = 10 keV**

C_{tot} = 4.18 J/K

→~ 3.8 10^{-16} K

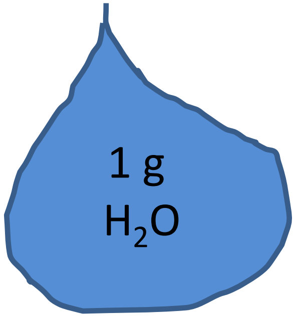

Low temperature micro-calorimeters

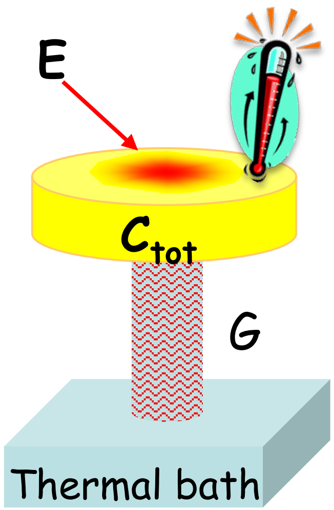

$$\Delta T \cong \frac{E}{C_{tot}}$$

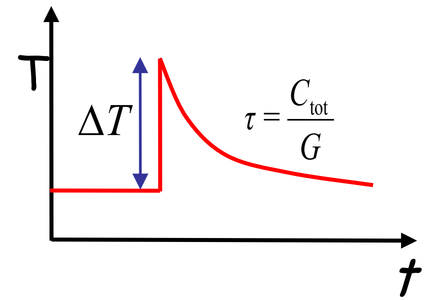

E = 10 keV
C_{tot} = 1 pJ/K
→ ~ 1 mK

- Very small volume
- Working temperature below 100 mK
  small specific heat
  small thermal noise
- **Very sensitive temperature sensor**

Temperature sensors

Resistance of highly doped semiconductors, NTD-Ge

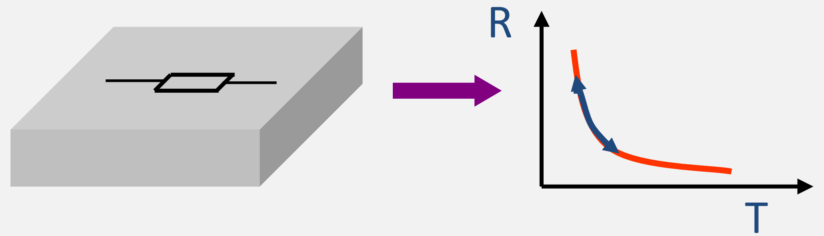

Resistance at superconducting transition,TES

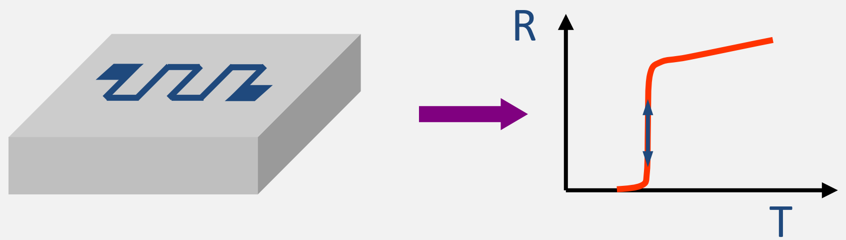

Magnetization of paramagnetic material, MMC

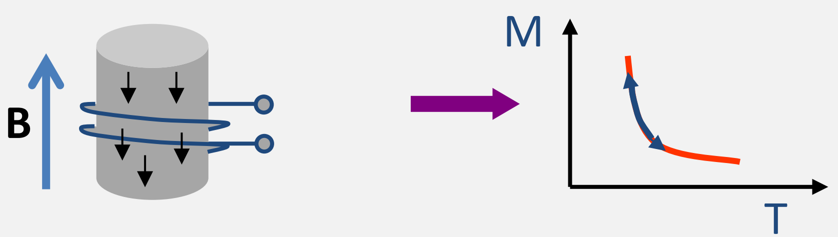

Metallic Magnetic Calorimeters - MMC

Paramagnetic sensor: **Au**:Er
Ag:Er

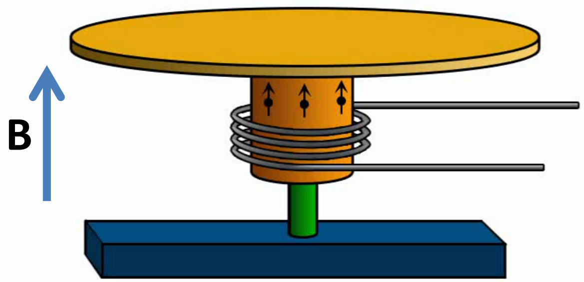

Sensor temperature

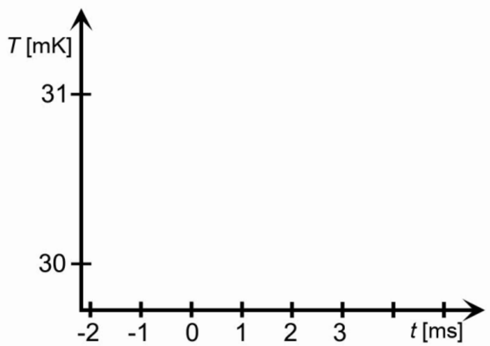

Sensor magnetization

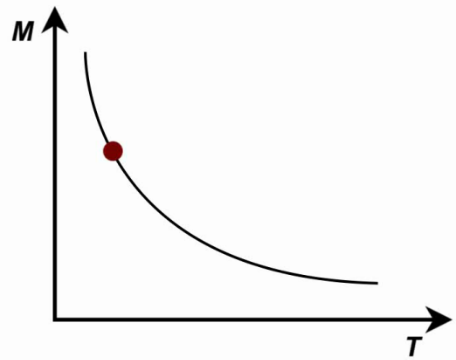

Pulse: 6 keV photon in
$C_{abs} \sim 1$ pJ/K

$$\delta M = \frac{\partial M}{\partial T} \delta T = \frac{\partial M}{\partial T} \frac{E_\gamma}{C_{\text{tot}}}$$

main differences to calorimeters with resistive thermometers

no dissipation in the sensor

no galvanic contact to the sensor

MMC: signal size

Numerical calculations based on mean field approximation are used to describe thermodynamical properties of interacting spins (RKKY)

$$\delta\Phi_{\mathrm{S}} \propto \frac{\partial M}{\partial T} \frac{1}{C_{\mathrm{tot}}} \delta E$$

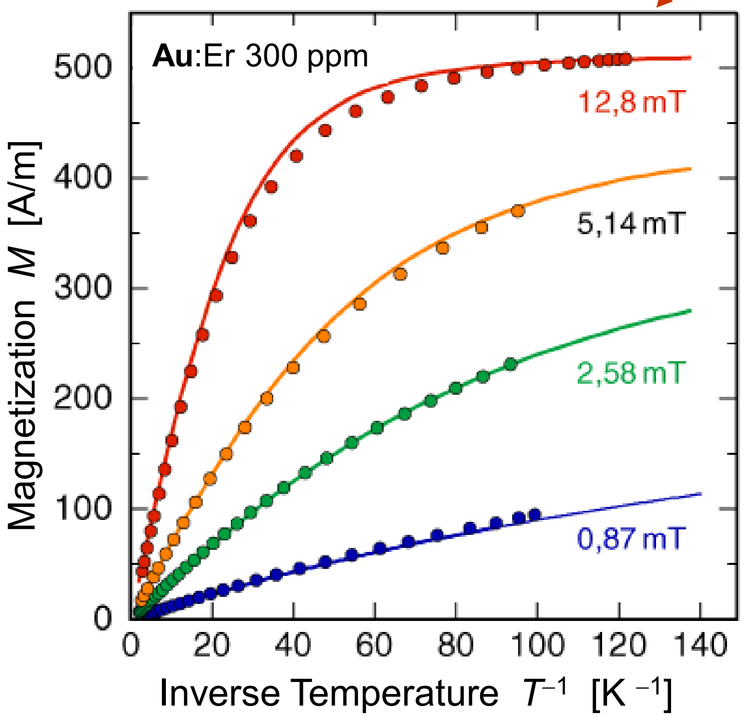

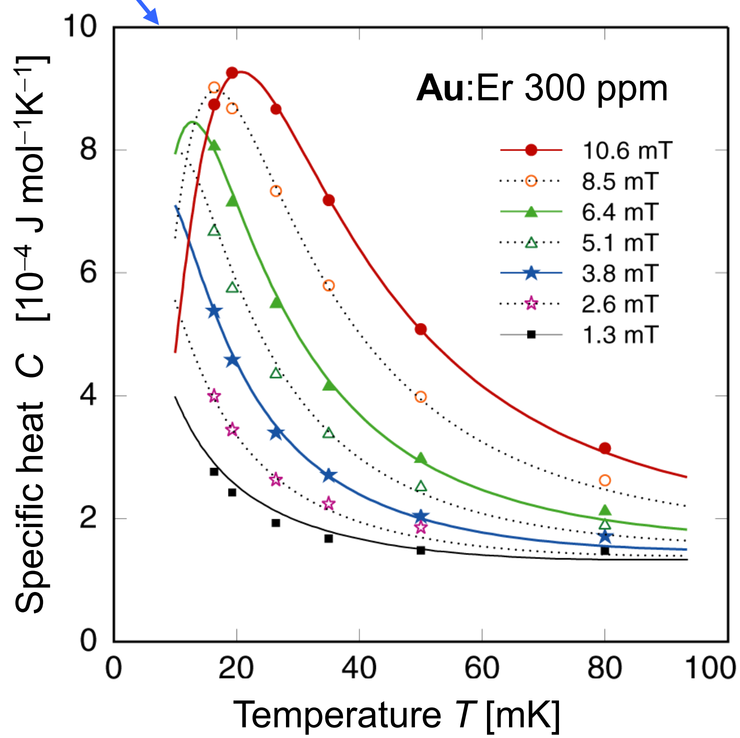

MMCs: Readout

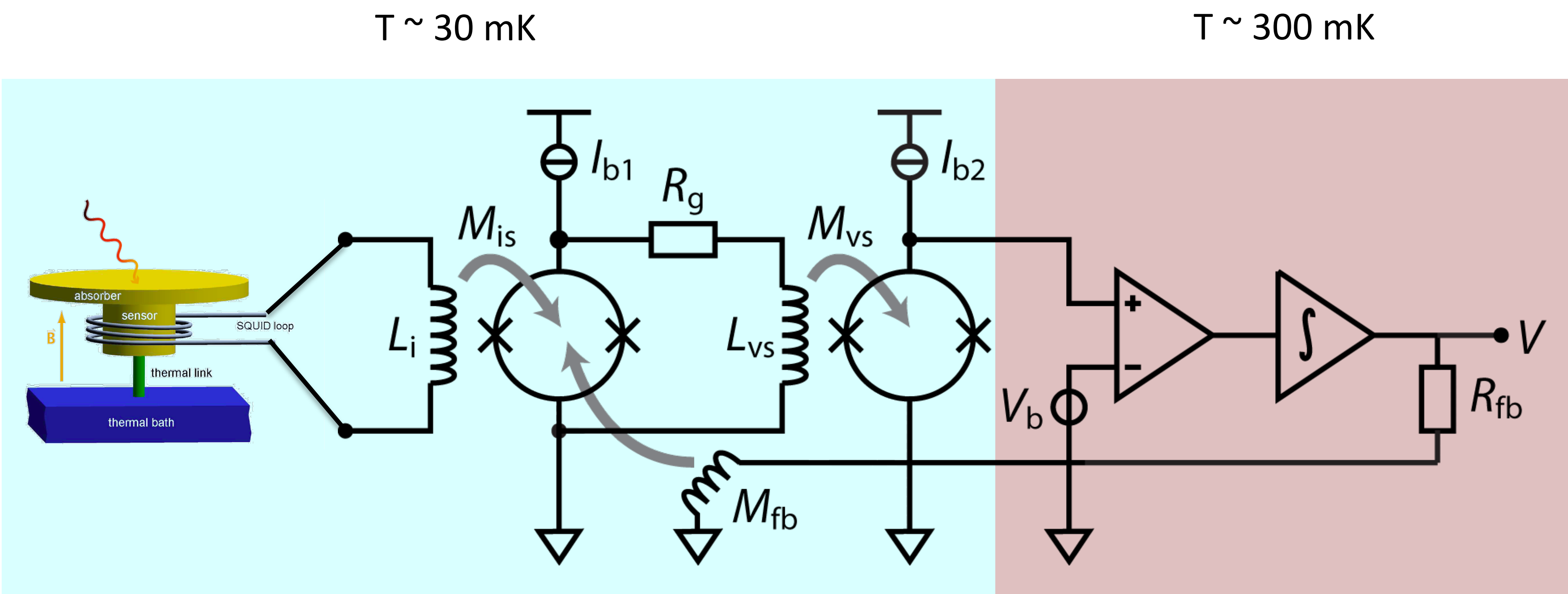

Two-stage SQUID setup with flux locked loop allows for:

- low noise
- large bandwidth / slewrate
- small power dissipation on detector SQUID chip (voltage bias)

MMCs: Planar Geometries

- Planar temperature sensor
- B-field generated by persistent current
- transformer coupled to SQUID

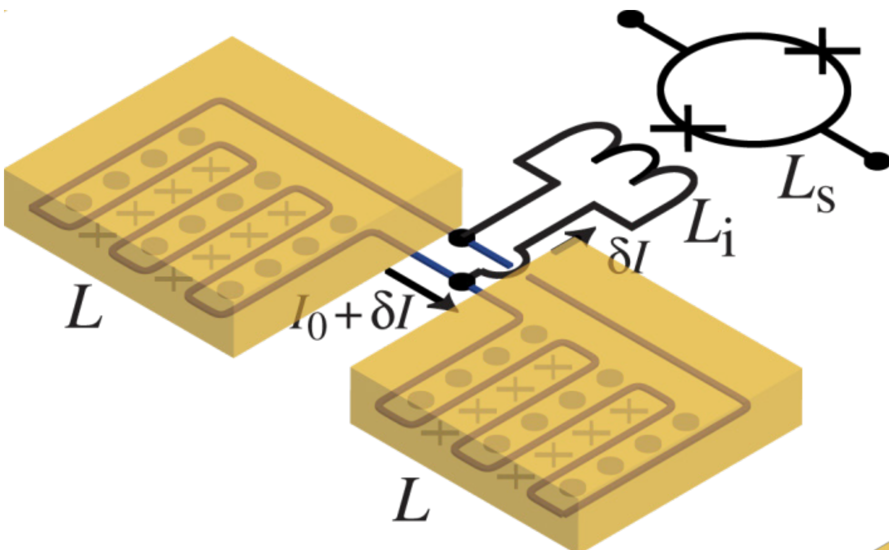

Sandwich design:
Filling factor ~1

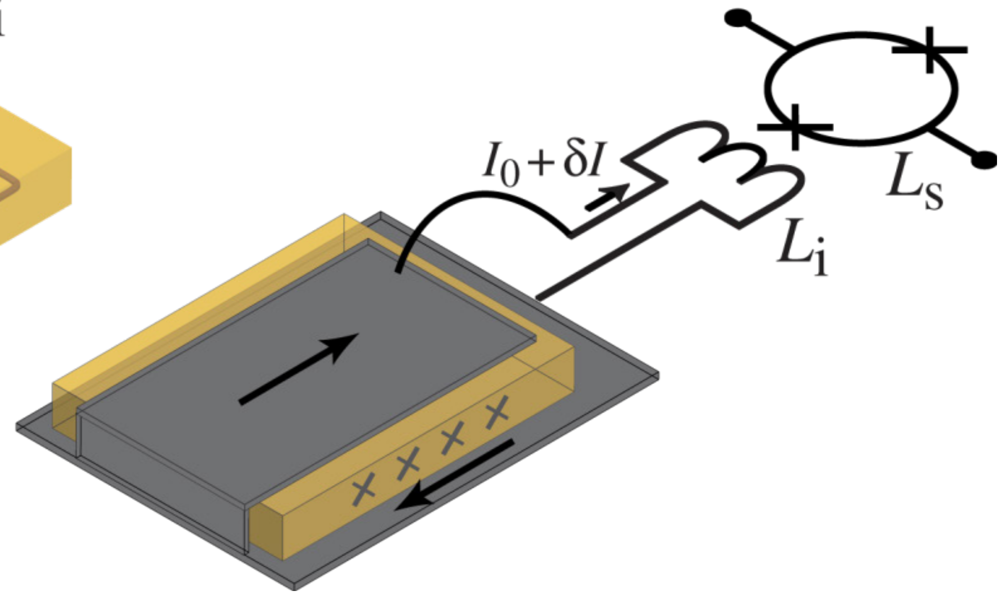

Meander-shaped pick-up coil:
Filling factor ~0.5

maXs20: 1d-array for soft x-rays

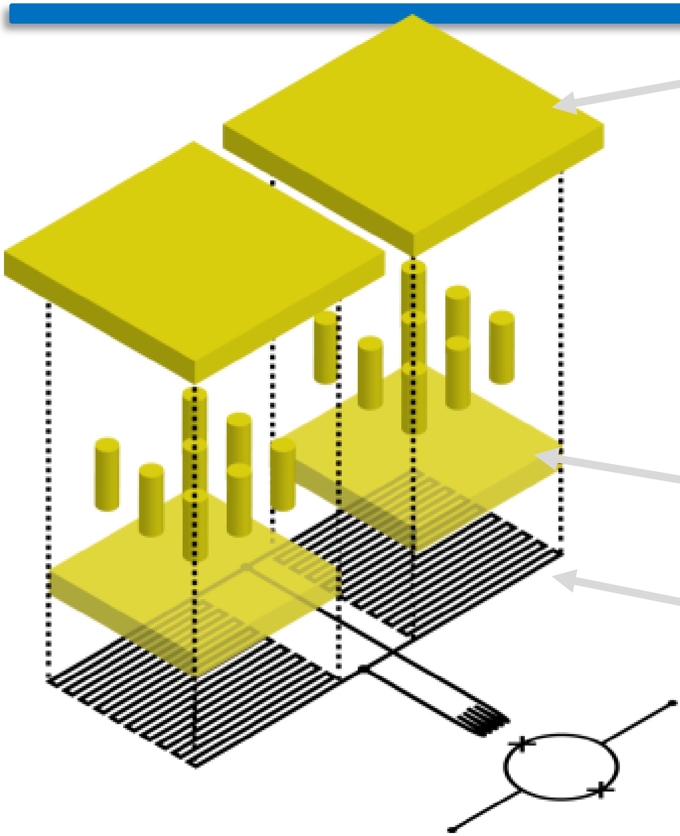

- **1×8 x-ray absorbers**
  - **250µm×250µm** gold**, 5µm thick**
  - **98%** Qu.-Eff. @ 6 keV
  - electroplated into photoresist mold (RRR>15)
  - **mech/therm contact to sensor by stems**
    to prevent loss of initially hot phonons
- **Au:^{168}Er$_{300ppm}$ temperature sensors**
  - co-sputtered from pure Au and high conc. AuEr target
- **Meander shaped pickup coils**
  - 2.5 µm wide Nb lines
  - I_c **≈ 100mA**
- **On-chip persistent current switch** (AuPd)

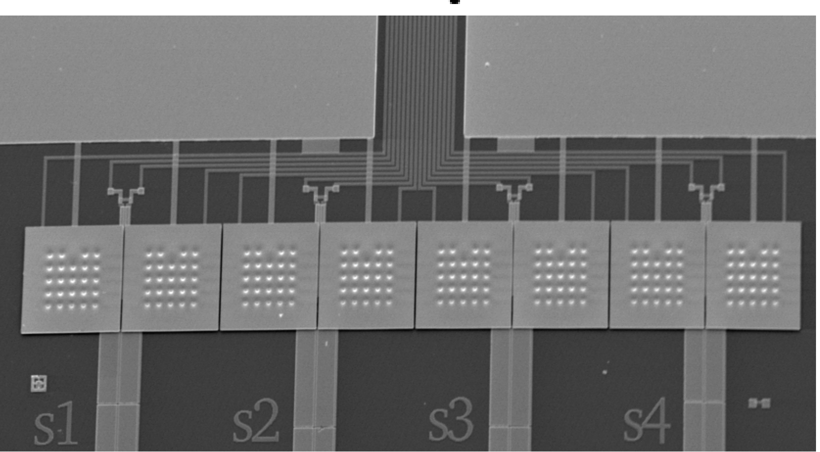

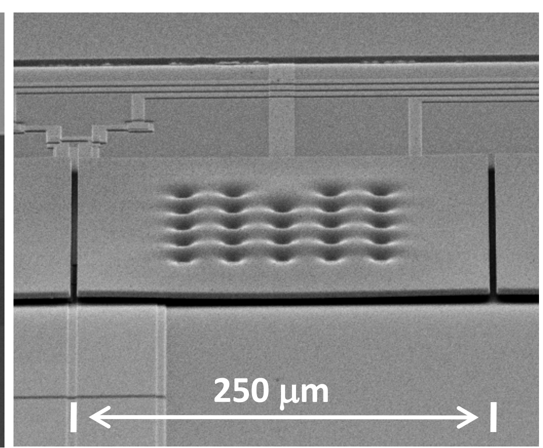

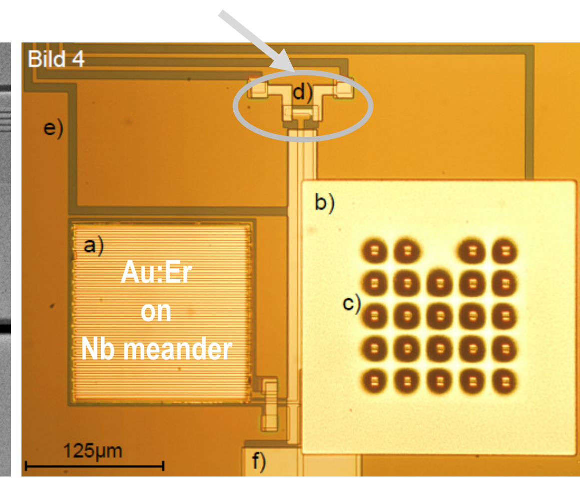

MMCs: Microfabrication

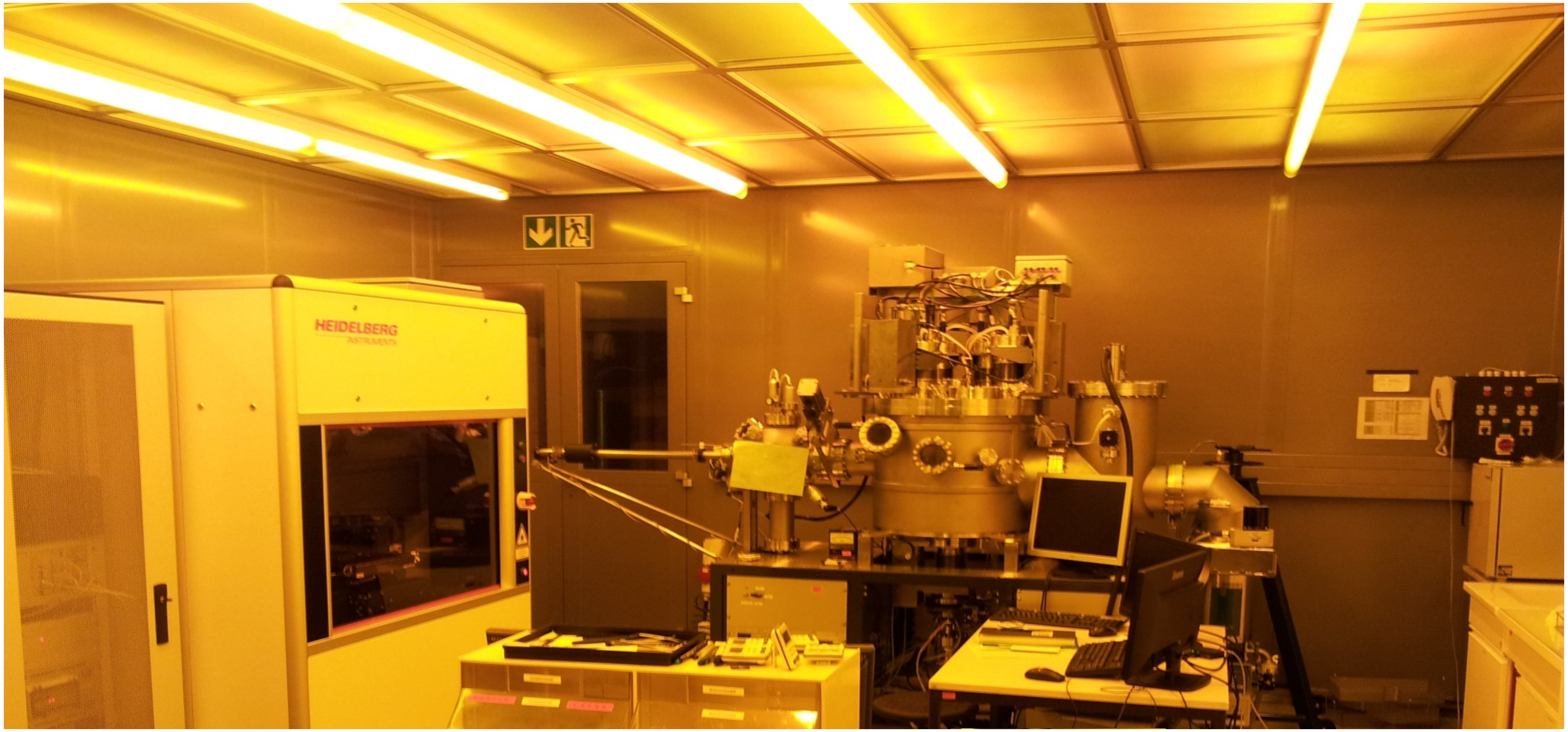

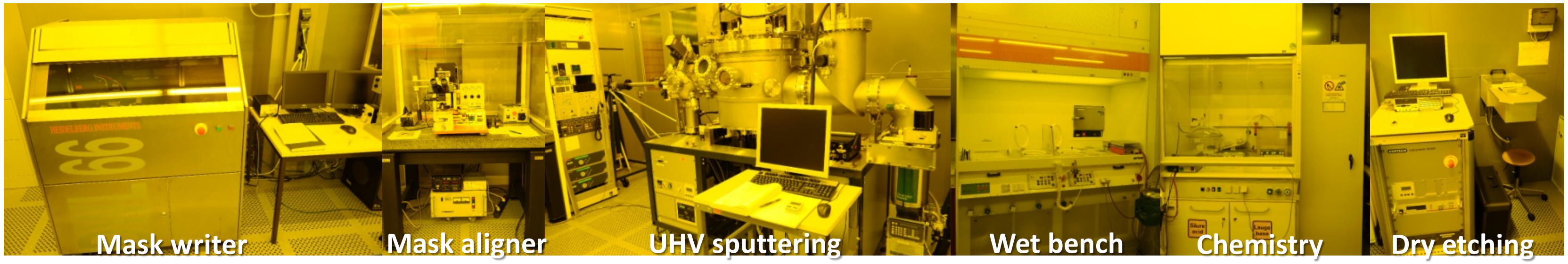

maXs20: 1d-array for soft x-rays

- **rise time: 90 ns** @ 30 mK,

  as expected for the **spin-electron-relaxation**

  from Korringa-constant of Er in Au

Fastest rise-time among µ-cal for x-ray detection

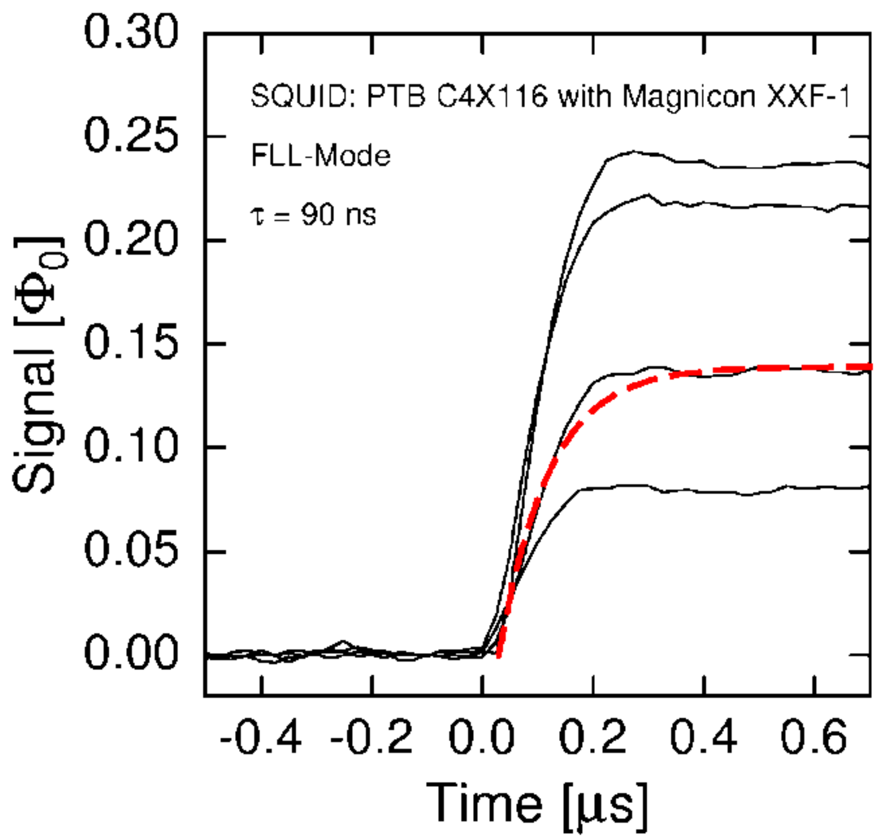

maXs20: 1d-array for soft x-rays

- **decay time** here: **3 ms @ 30 mK**
- nearly single exponential decay

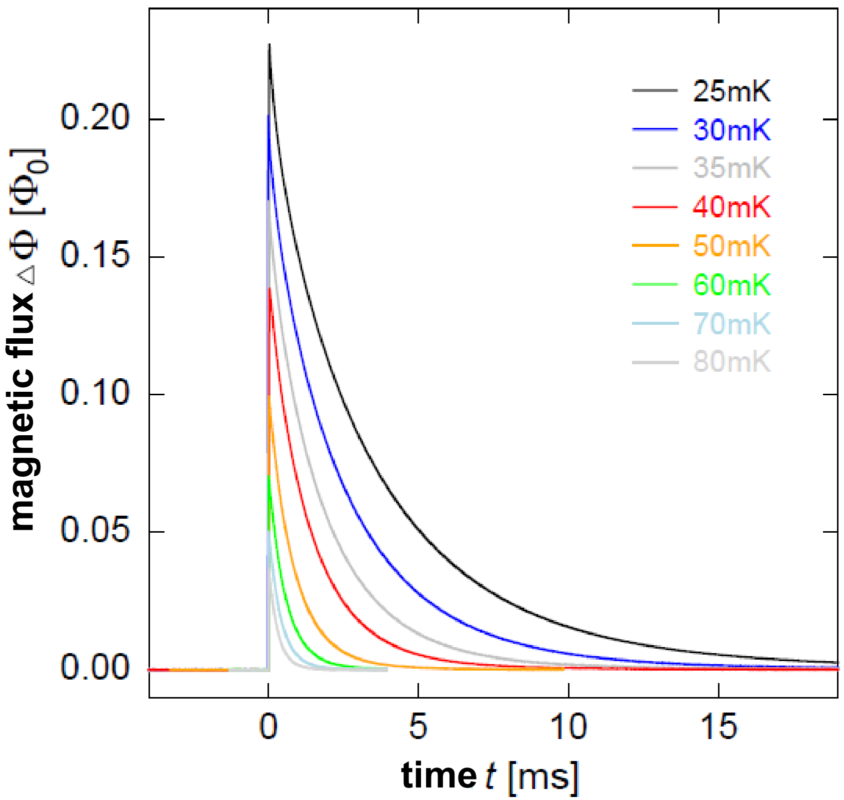

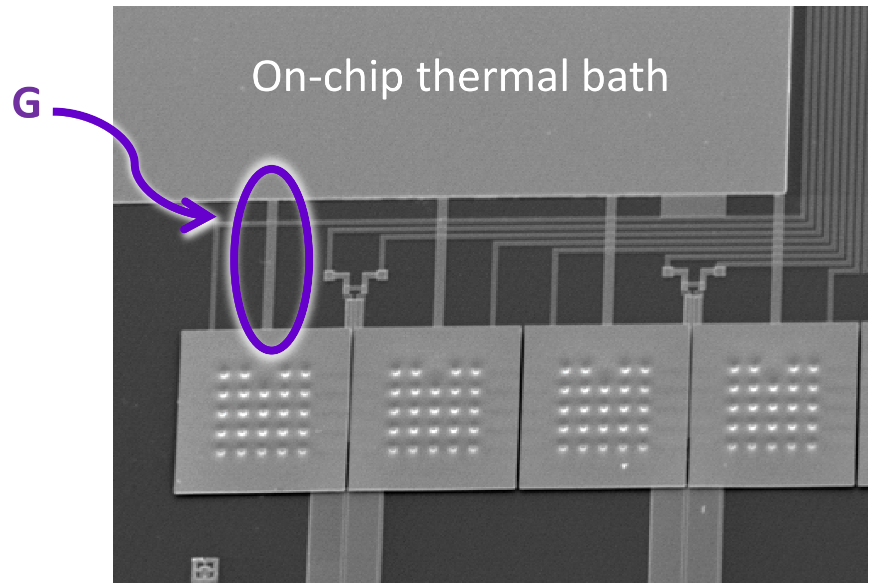

adjusted by sputtered thermal link (Au)

maXs20: 1d-array for soft x-rays

- **non-linearity: 1%** at **6 keV**
- well described by quadratic term

The energy scale is defined with high precision

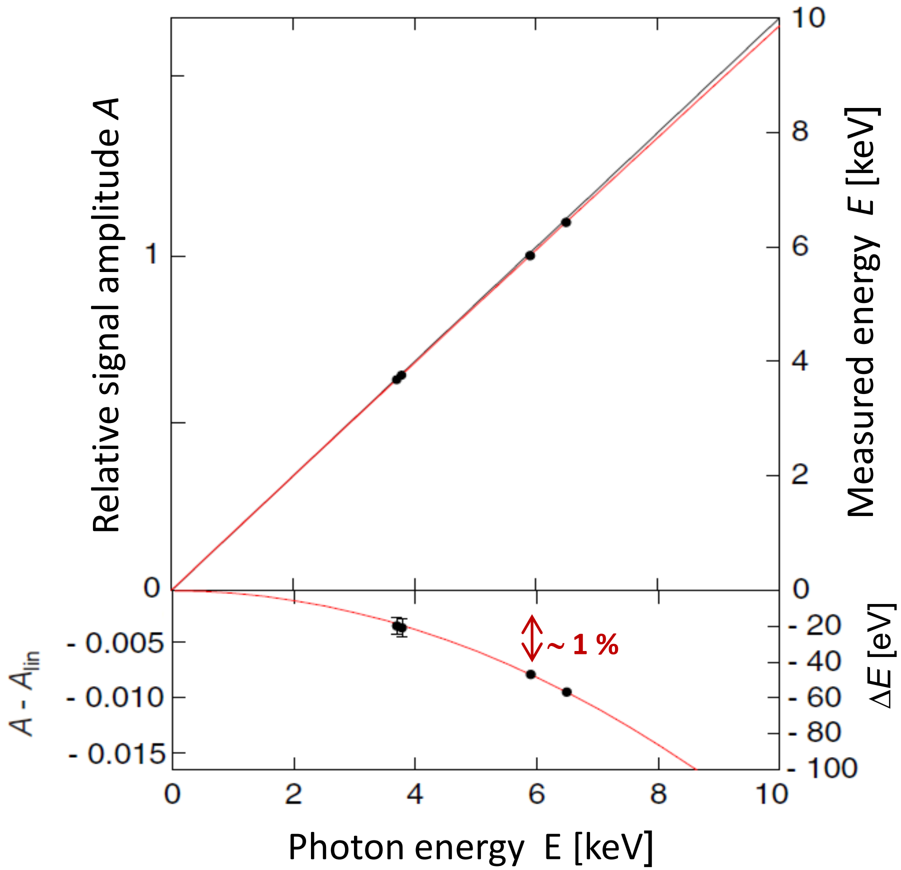

maXs20: 1d-array for soft x-rays

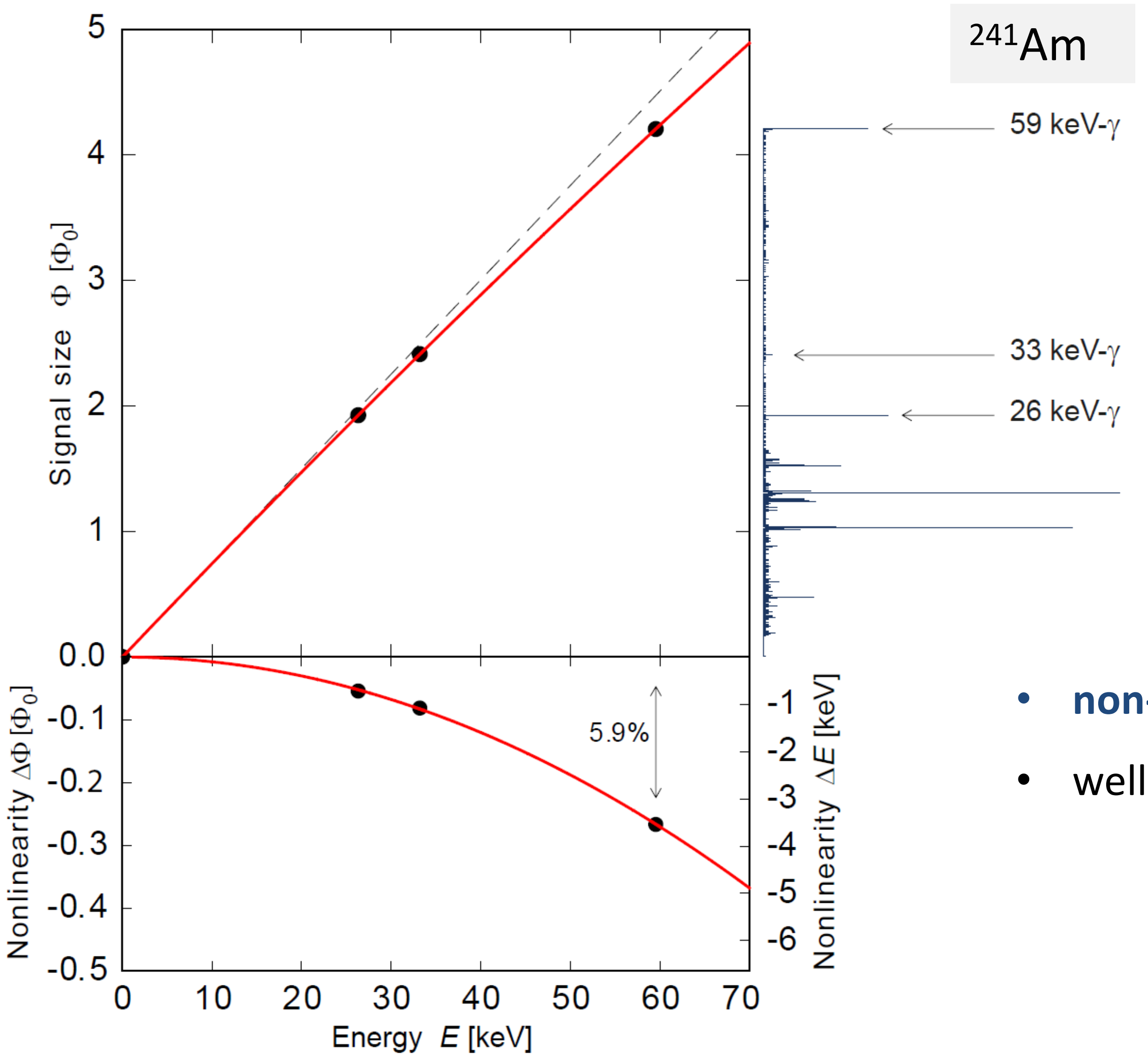

- **non-linearity: 6%** at **60 keV**
- well described by quadratic term

maXs20: 1d-array for soft x-rays (T=20 mK)

- Very good energy resolution

ΔE_{FWHM}= 1.6 eV @ 6 keV

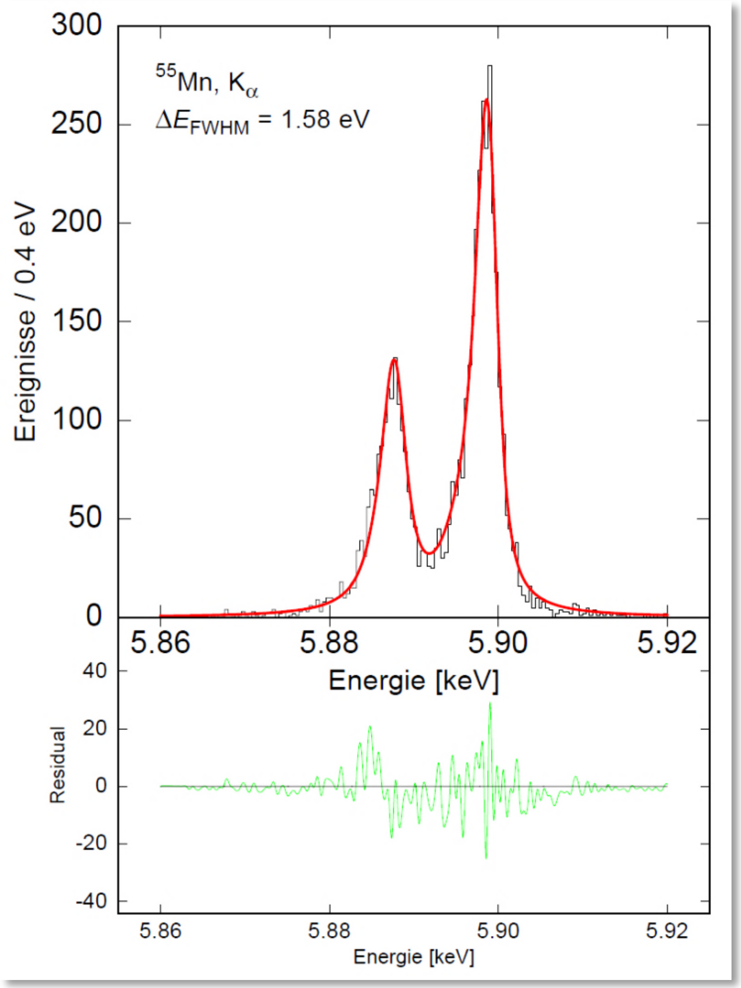

maXs20: 1d-array for soft x-rays (T=20 mK)

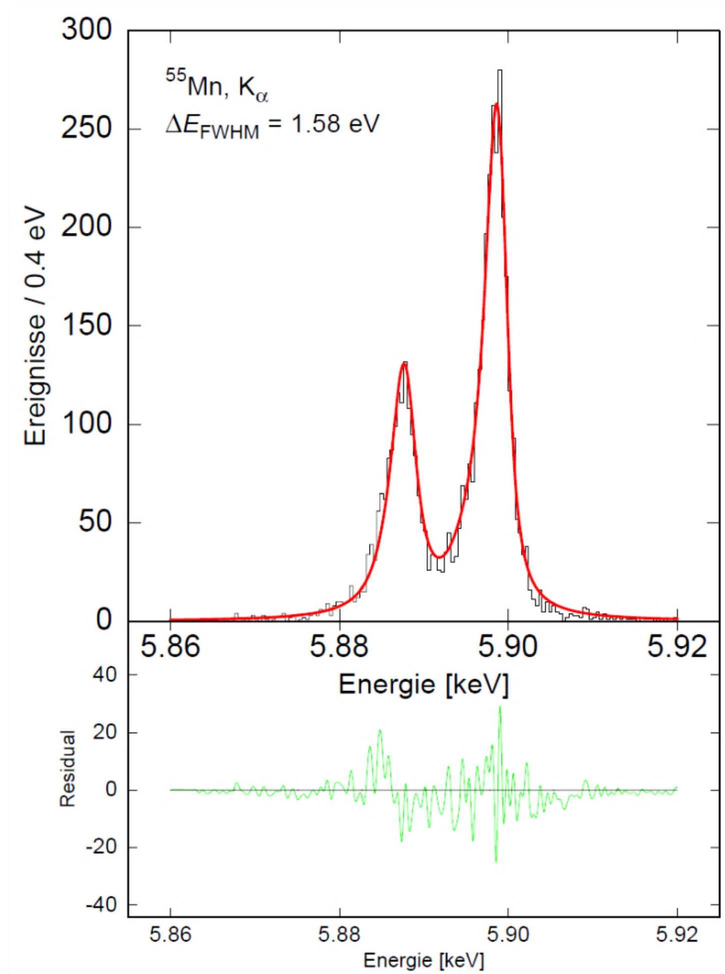

MMCs: Microwave SQUID multiplexing

Single HEMT amplifier and 2 coaxes
to read out 100 - 1000 detectors

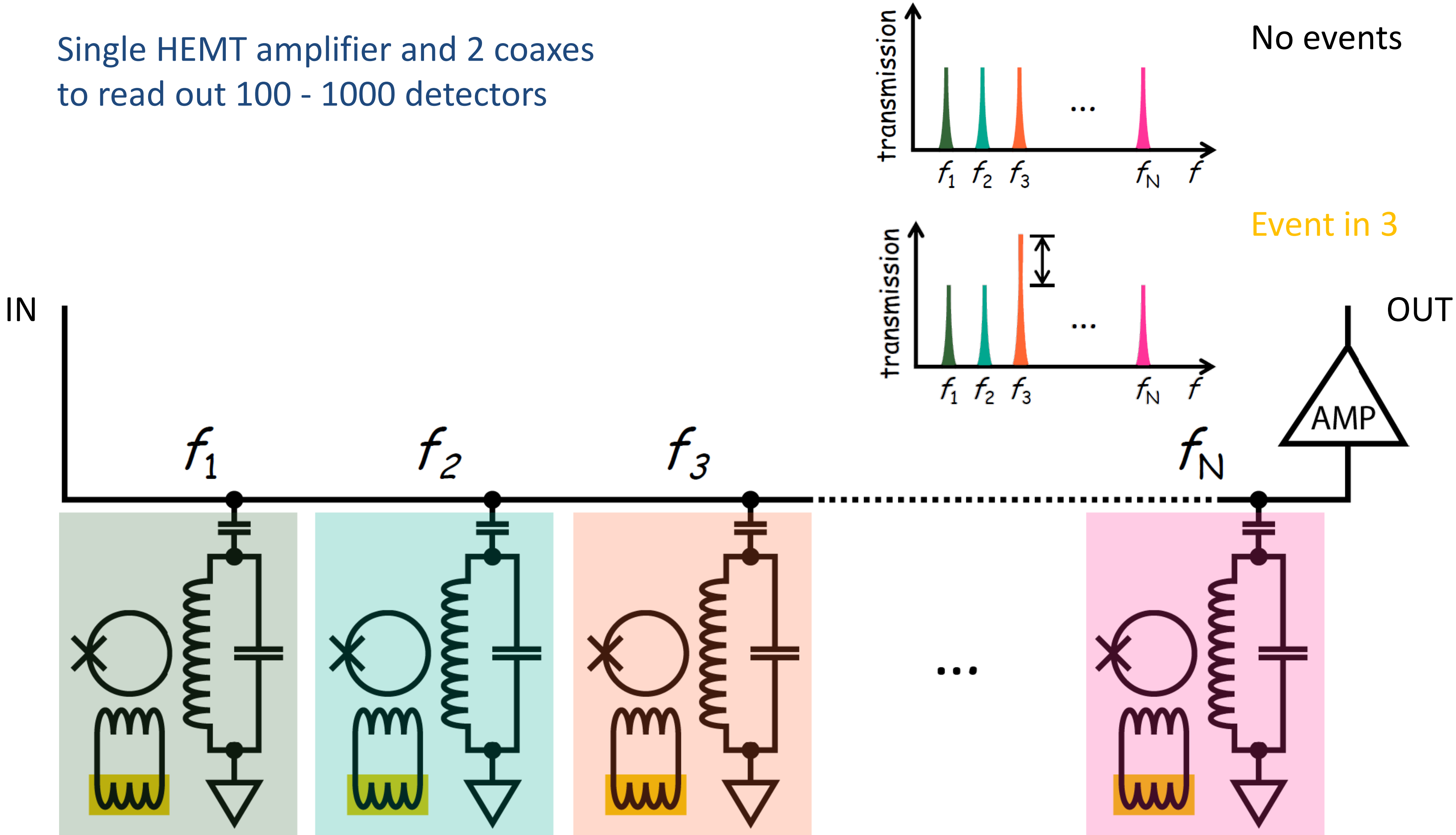

Microwave SQUID Multiplexer for the Readout of Metallic Magnetic Calorimeters
S.Kempf et al., *J. Low. Temp. Phys.* **175** (2014) 850-860

MMCs: Microwave SQUID multiplexing

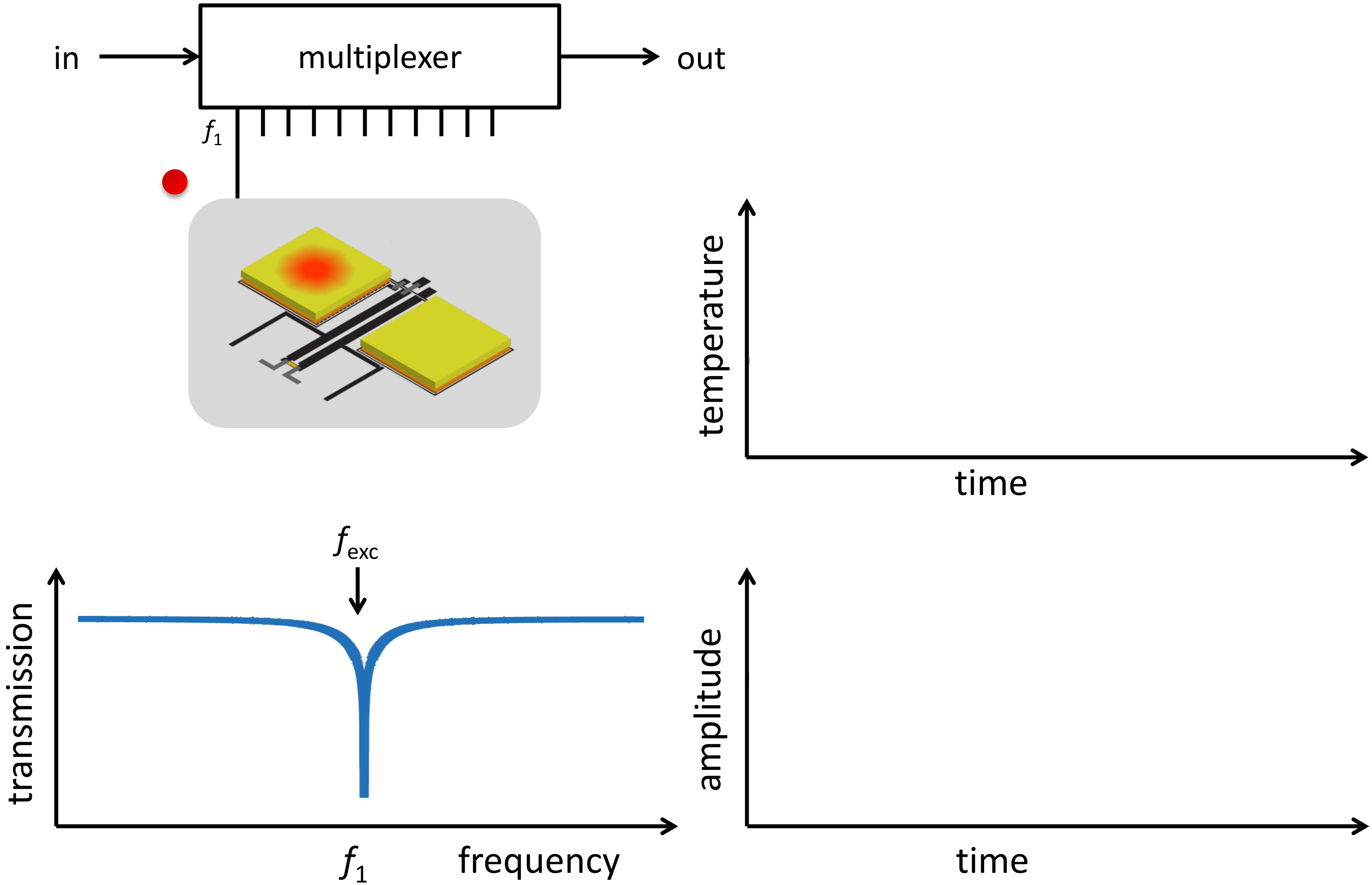

Massive neutrinos

Neutrino mass determination

Cosmology	Neutrinoless Double beta decay	Kinematics of β-decay and electron capture
$M_\nu = \sum m_i$	$m_{\beta\beta} = \left\| \sum_i U_{ei}^2 m_i \right\|$	$m^2(\nu_e) = \sum_i \|U_{ei}\|^2 m_i^2$

Cosmology

- Model dependent
- Need of satellites
- Present limit 0.12 – 1 eV
- Next future 15-50 meV

Neutrinoless Double beta decay

- Model dependent
- Laboratory experiments
- Present limit 0.1 – 0.4 eV
- Next future 15-50 meV

Kinematics of β-decay and electron capture

- Model independent
- Laboratory experiments
- Present limit 2 eV
- Next future 200 meV

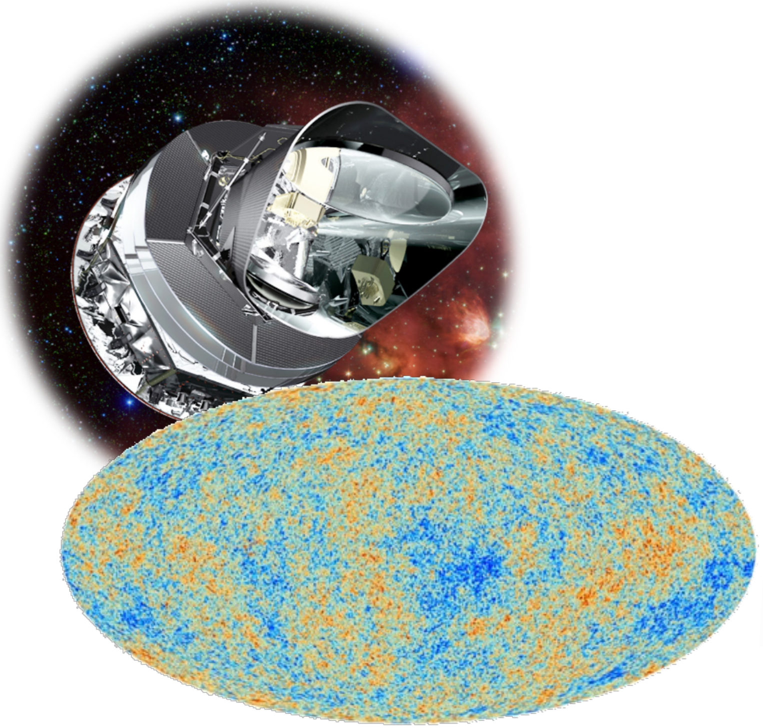

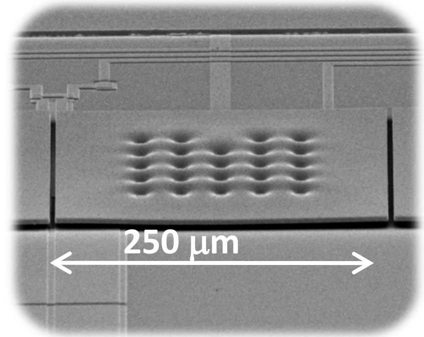

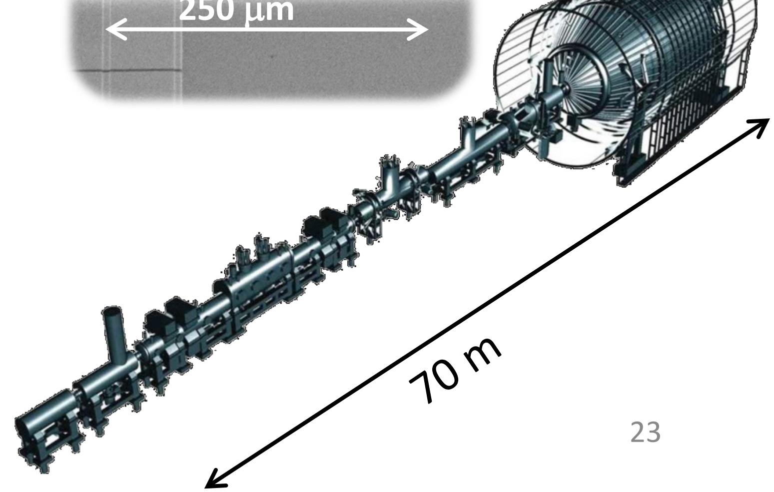

Direct neutrino mass determination

Kinematics of beta decay

$$m^2(\nu_e) = \sum_i |U_{ei}|^2 m_i^2$$

- Model independent
- Laboratory experiments

$$m(\overline{\nu}_e) < 2\ eV$$ ^3H (1)

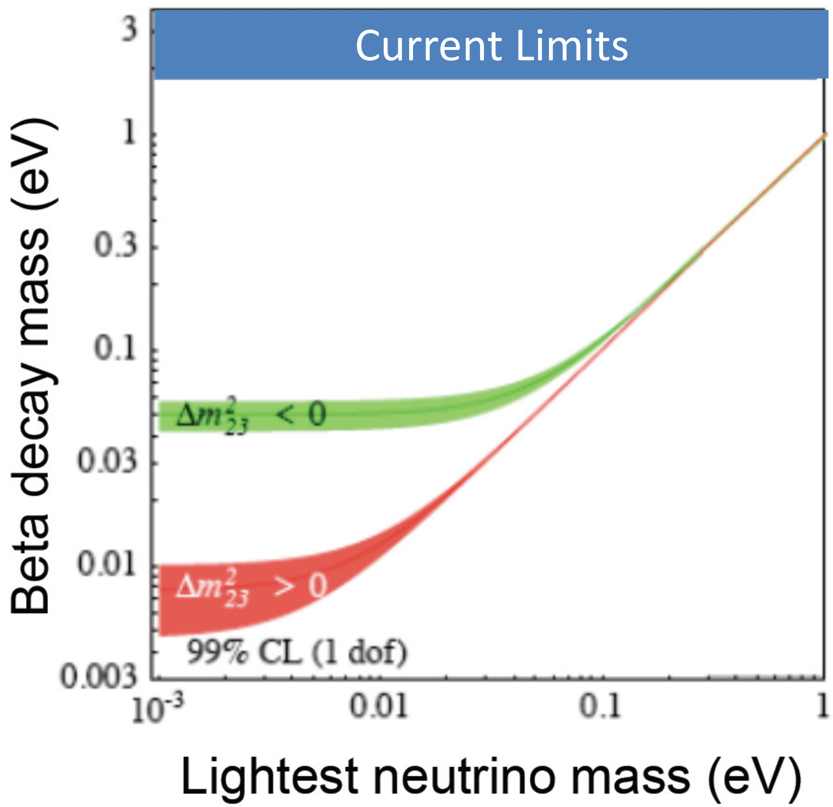

(1) Ch. Kraus *et al.*, Eur. Phys. J. C **40** (2005) 447
N. Aseev *et al.*, Phys. Rev D **84** (2011) 112003

Direct neutrino mass determination

Kinematics of beta decay

$$m^2(\nu_e) = \sum_i |U_{ei}|^2 m_i^2$$

- Model independent
- Laboratory experiments

$$m(\bar{\nu}_e) < 2\ eV$$ ^3H (1)

$$m(\nu_e) < 225\ eV$$ ^{163}Ho (2)

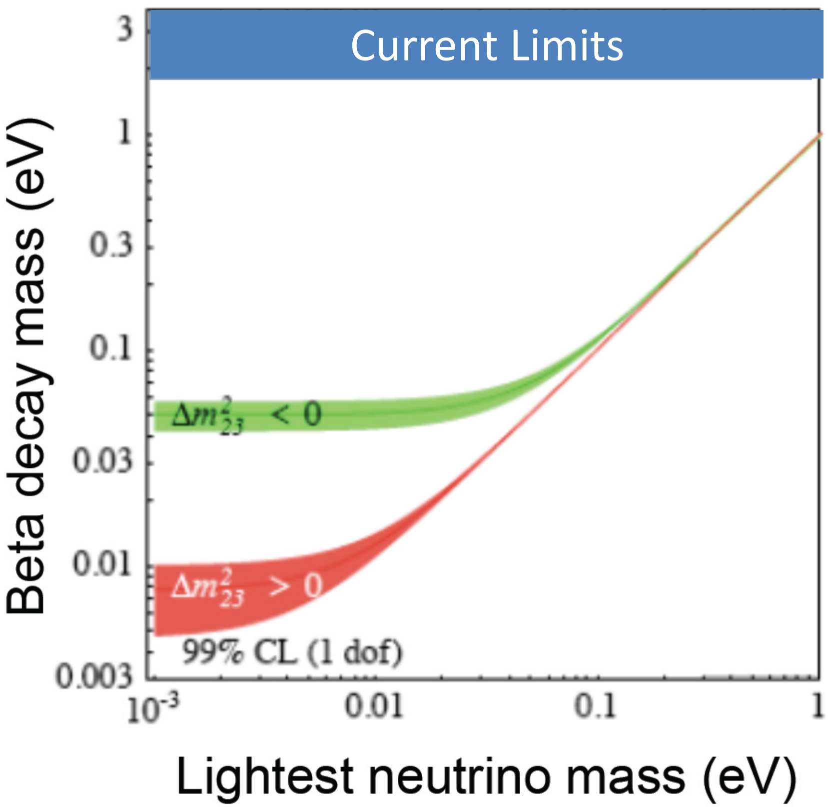

(1) Ch. Kraus *et al.*, Eur. Phys. J. C **40** (2005) 447
N. Aseev *et al.*, Phys. Rev D **84** (2011) 112003

(2) P. T. Springer, C. L. Bennett, and P. A. Baisden Phys. Rev. A 35 (1987) 679

Direct neutrino mass determination

Kinematics of beta decay

$$m^2(\nu_e) = \sum_i |U_{ei}|^2 m_i^2$$

- Model independent
- Laboratory experiments

$$m(\bar{\nu}_e) < 2 \ eV$$ ^3H (1)

$$m(\nu_e) < 225 \ eV$$ ^{163}Ho (2)

- **Next future 200 meV**

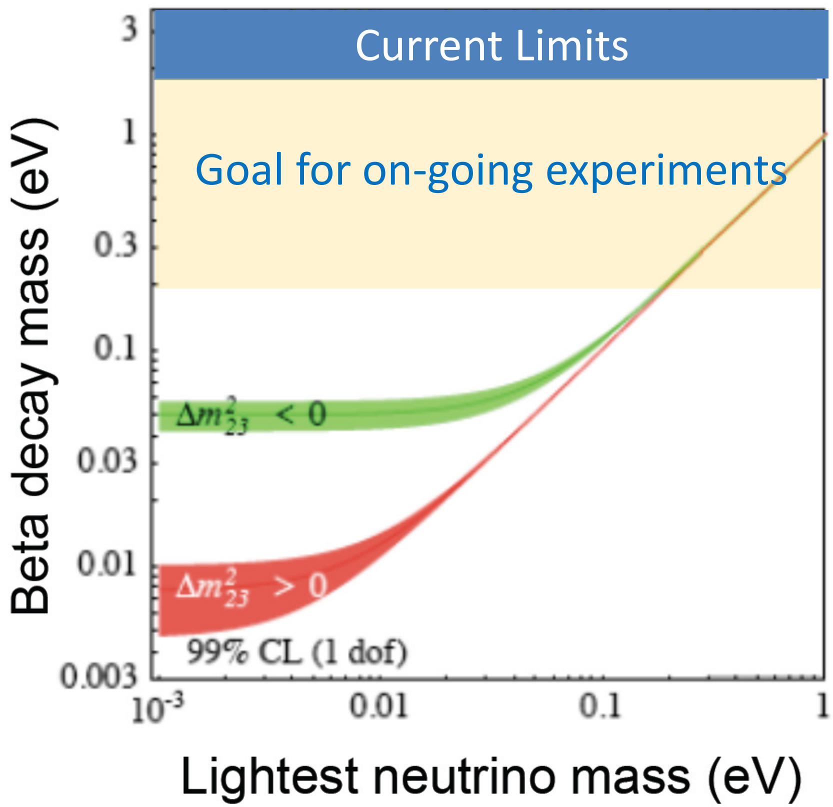

(1) Ch. Kraus *et al.*, Eur. Phys. J. C **40** (2005) 447
N. Aseev *et al.*, Phys. Rev D **84** (2011) 112003

(2) P. T. Springer, C. L. Bennett, and P. A. Baisden Phys. Rev. A 35 (1987) 679

Beta decay and electron capture

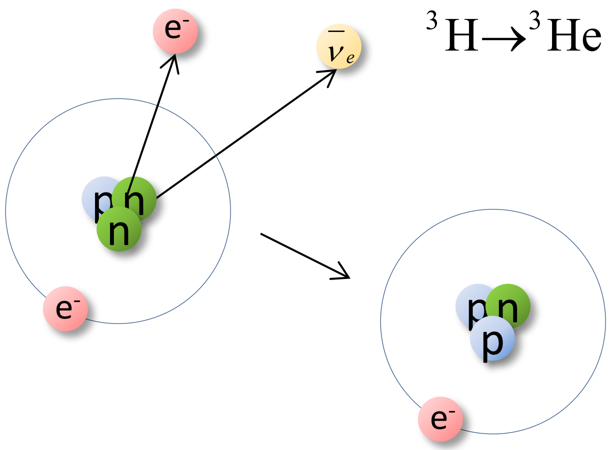

$$^{3}\mathrm{H} \rightarrow {}^{3}\mathrm{He} + e^{-} + \overline{\nu}_e$$

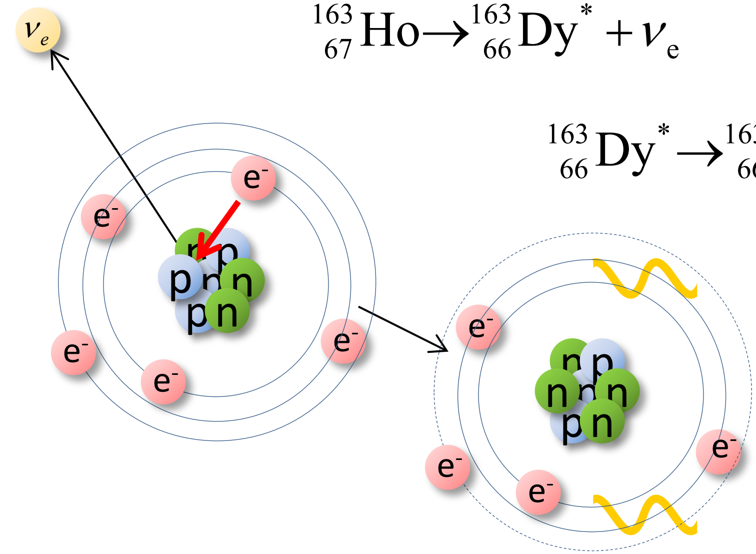

$$^{163}_{67}\mathrm{Ho} \rightarrow {}^{163}_{66}\mathrm{Dy}^{*} + \nu_{\mathrm{e}}$$

$$^{163}_{66}\mathrm{Dy}^{*} \rightarrow {}^{163}_{66}\mathrm{Dy} + E_{\mathrm{C}}$$

- $\tau_{1/2} \cong$ 12.3 years (4*10^8 atoms for 1 Bq)
- Q_β = 18 592.01(7) eV

E.G. Myers et al., *Phys. Rev. Lett.* **114** (2015) 013003

- $\tau_{1/2} \cong$ 4570 years (2*10^{11} atoms for 1 Bq)
- Q_{EC} = $(2.833 \pm 0.030^{stat} \pm 0.015^{syst})$ keV

S. Eliseev et al., *Phys. Rev. Lett.* **115** (2015) 062501

Beta decay and electron capture

$$^{3}\mathrm{H} \rightarrow {}^{3}\mathrm{He} + e^{-} + \bar{\nu}_e$$

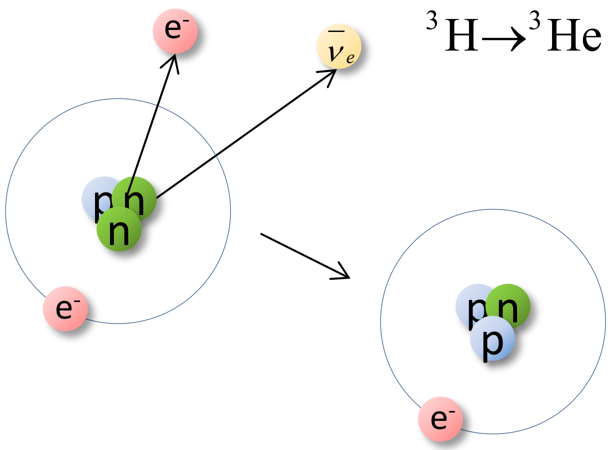

$$^{163}_{67}\mathrm{Ho} \rightarrow {}^{163}_{66}\mathrm{Dy}^{*} + \nu_{\mathrm{e}}$$

$$^{163}_{66}\mathrm{Dy}^{*} \rightarrow {}^{163}_{66}\mathrm{Dy} + E_{\mathrm{C}}$$

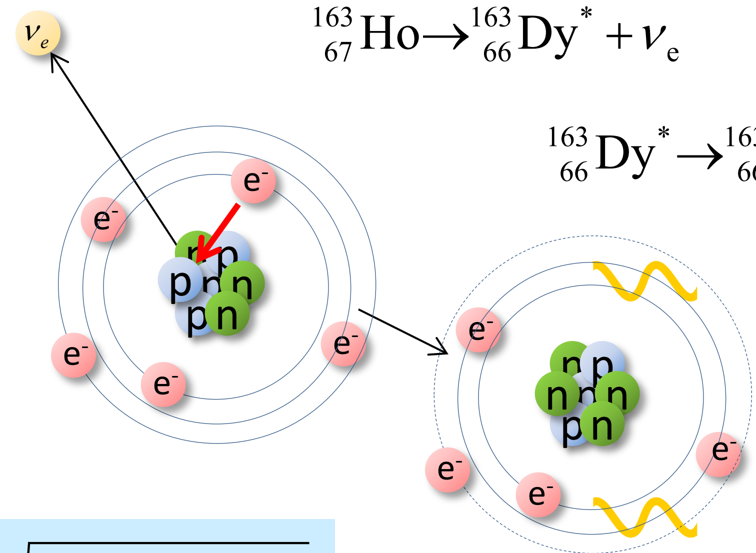

$$\frac{dW}{dE} \propto (Q - E)^2 \sqrt{1 - \frac{m_\nu^{\ 2}}{(Q - E)^2}}$$

- $\tau_{1/2} \cong$ 12.3 years (4*10^8 atoms for 1 Bq)
- Q_β = 18 592.01(7) eV

E.G. Myers et al., *Phys. Rev. Lett.* **114** (2015) 013003

- $\tau_{1/2} \cong$ 4570 years (2*10^{11} atoms for 1 Bq)
- Q_{EC} = $(2.833 \pm 0.030^{stat} \pm 0.015^{syst})$ keV

S. Eliseev et al., *Phys. Rev. Lett.* **115** (2015) 062501

Beta decay of ^3H

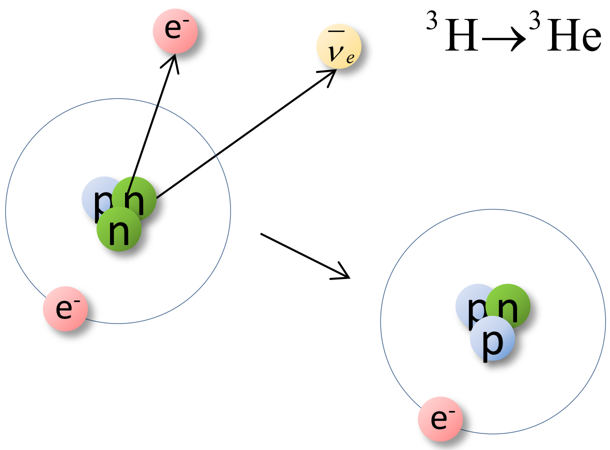

$$^{3}\mathrm{H} \rightarrow {}^{3}\mathrm{He} + e^{-} + \overline{\nu}_e$$

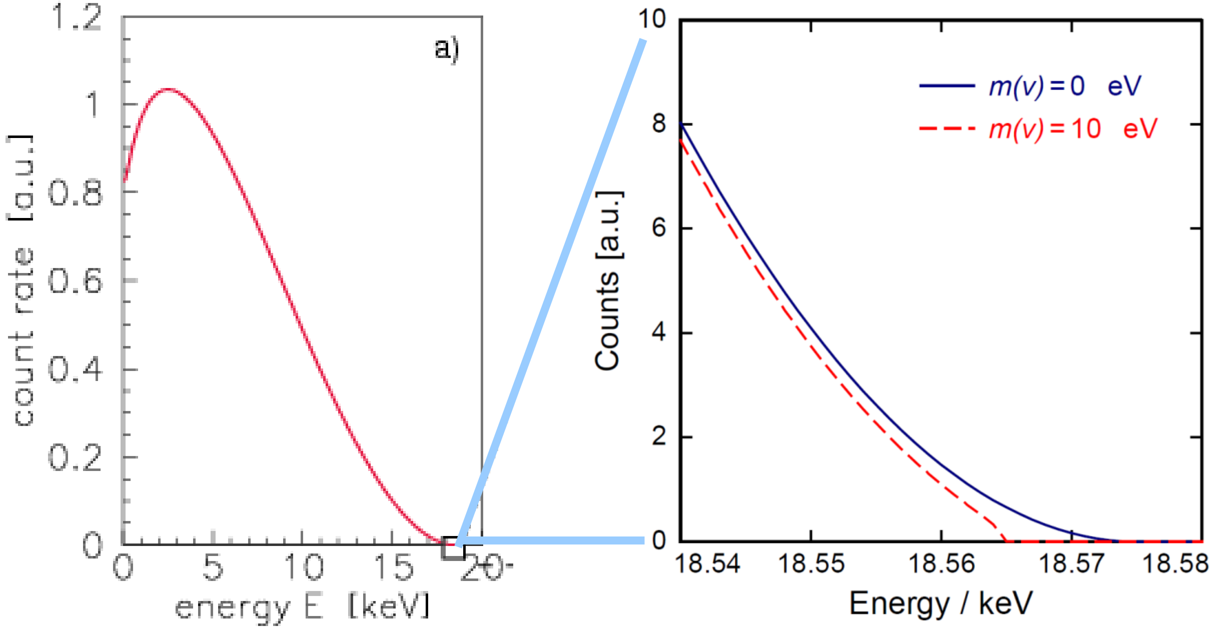

Beta decay of ^{3}H

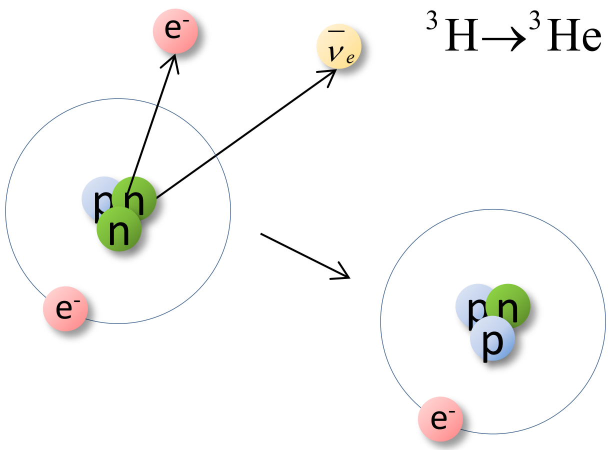

$$^{3}\mathrm{H} \rightarrow {}^{3}\mathrm{He} + e^{-} + \overline{\nu}_{e}$$

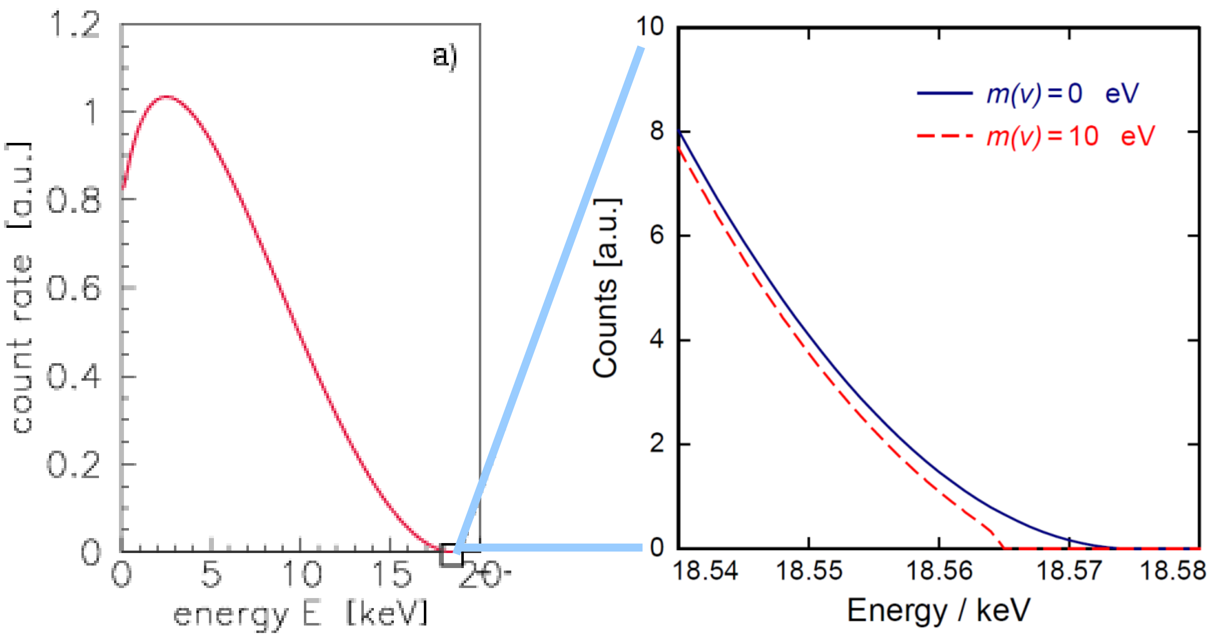

Only a small fraction of events in the last eV below the endpoint: **$2 * 10^{-13}$**

Very low background is required

The KATRIN experiment

❖ **KATRIN** - **Ka**rlsruhe **Tri**tium **N**eutrino Experiment

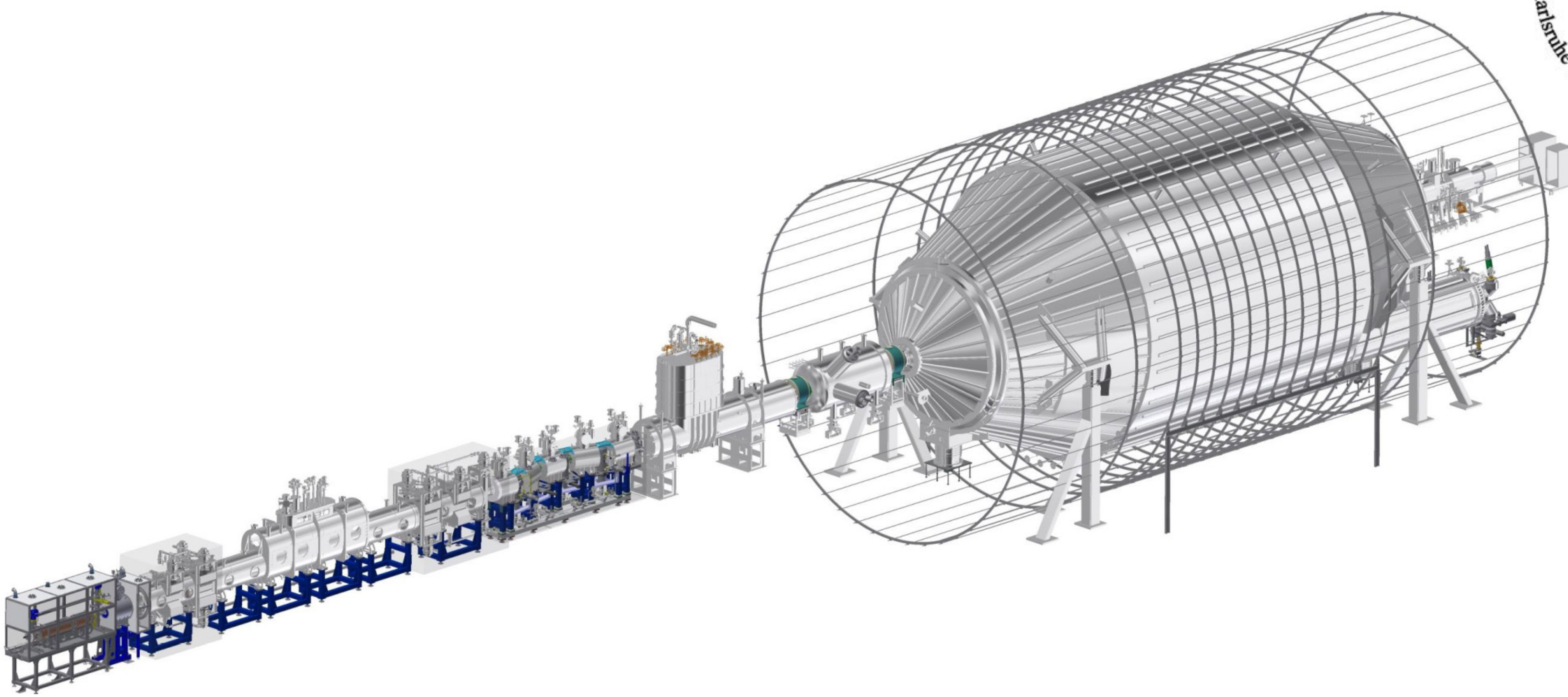

Main ideas:

- high activity source 10^{11} e^-/s
- high resolution MAC-E* filter to select electrons close to the end point
- count electrons as function of retarding potential
  → integral spectrum

*MAC-E: Magnetic Adiabatic Collimation with Electrostatic Filter

The KATRIN experiment

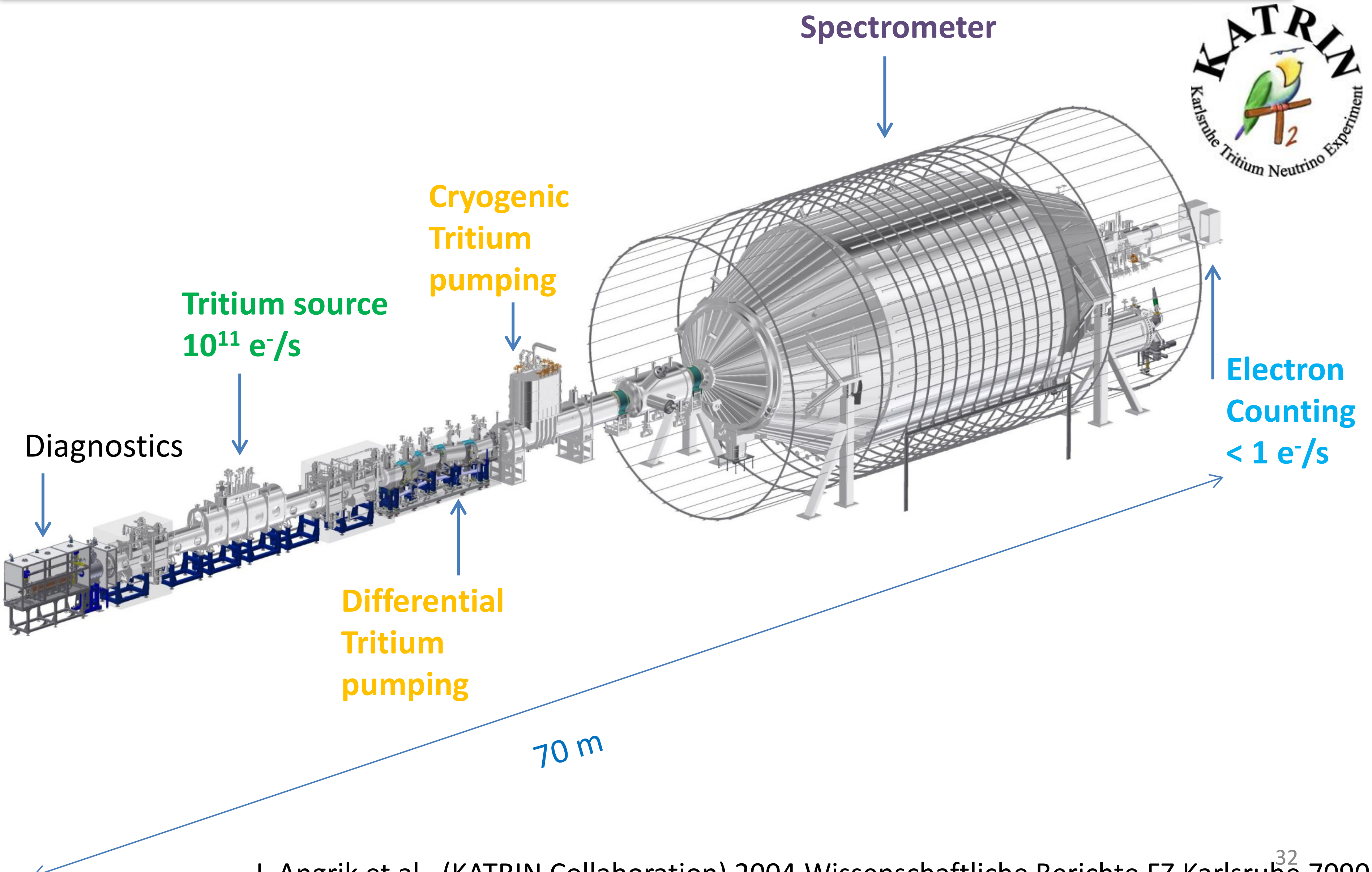

J. Angrik et al., (KATRIN Collaboration) 2004 Wissenschaftliche Berichte FZ Karlsruhe 7090

The KATRIN experiment: present status

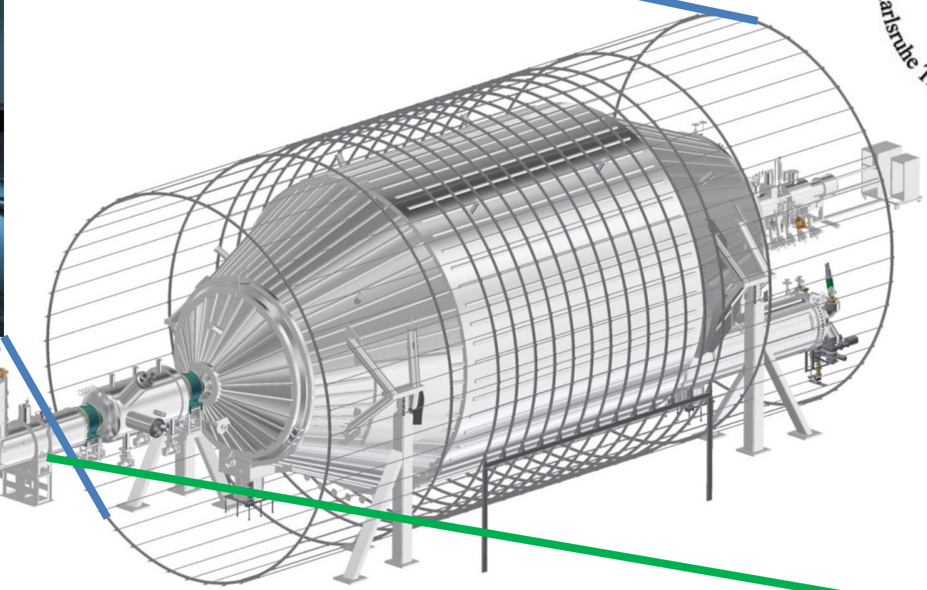

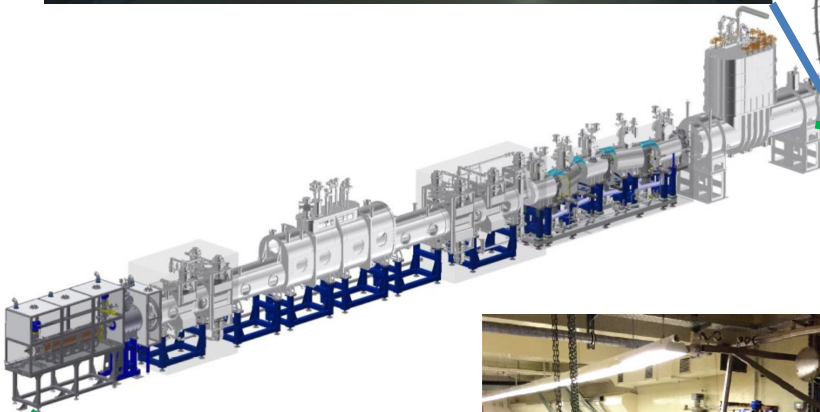

Photo K. Valerius

The KATRIN experiment: present status

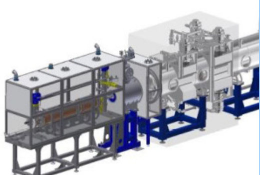

First light 14th October 2016

Photo Patrick Langer

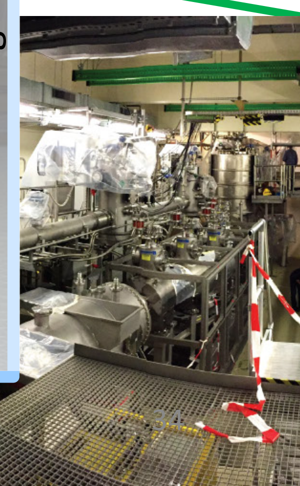

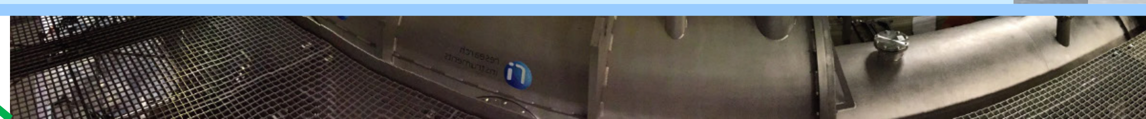

Photo K. Valerius

^{3}H based experiments

❖ KATRIN - Karlsruhe Tritium Neutrino Experiment

Main ideas:
- high activity source: 10^{11} e^-/s
- high resolution MAC-E filter to select electrons close to the end point
- count electrons as function of retarding potential
  → integral spectrum

❖ Project8

Main ideas:
- Source = detector: 10^{11} – 10^{13} $^3H_2$ molecules /cm^3
- Use cyclotron frequency to extract electron energy
- Differential spectrum

❖ PTOLEMY - Princeton Tritium Observatory for Light, Early-Universe, Massive-Neutrino Yield

Main ideas:
- large area tritium source: 100 g atomic ^{3}H
- MAC-E lter to select electrons close to the end point
- RF tracking and time-of-flight systems
- cryogenic calorimetry → differential spectrum

Beta decay and electron capture

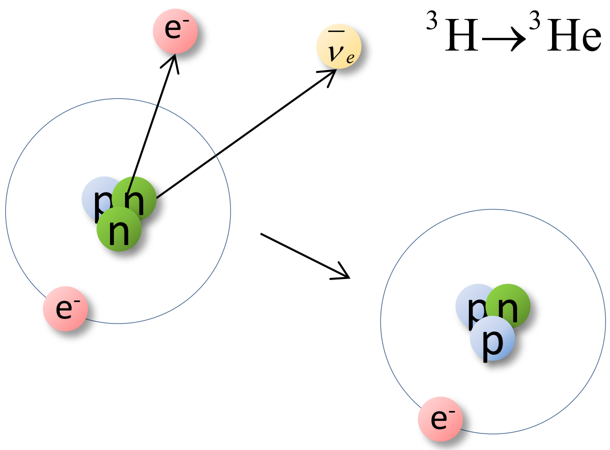

$$^{3}\mathrm{H} \rightarrow {}^{3}\mathrm{He} + e^{-} + \bar{\nu}_e$$

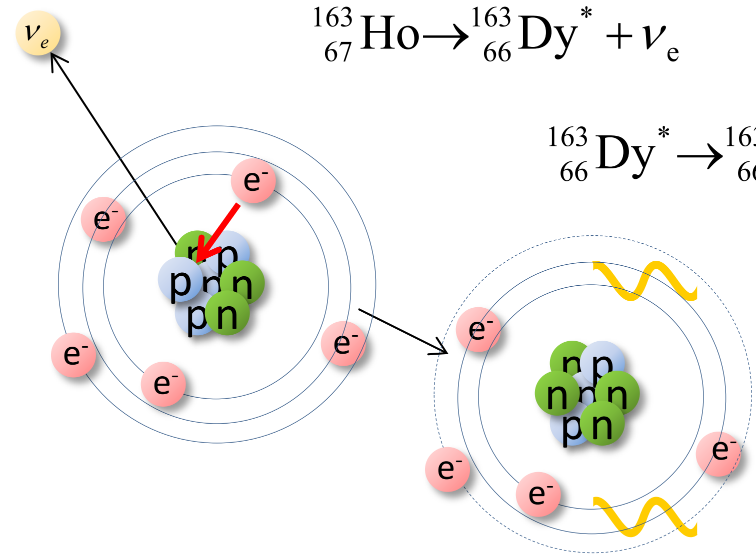

$$^{163}_{67}\mathrm{Ho} \rightarrow {}^{163}_{66}\mathrm{Dy}^{*} + \nu_{\mathrm{e}}$$

$$^{163}_{66}\mathrm{Dy}^{*} \rightarrow {}^{163}_{66}\mathrm{Dy} + E_{\mathrm{C}}$$

- $\tau_{1/2} \cong 12.3$ years (4*10^8 atoms for 1 Bq)
- Q_{EC} = 18 592.01(7) eV

E.G. Myers et al., *Phys. Rev. Lett.* **114** (2015) 013003

- $\tau_{1/2} \cong 4570$ years (2*10^{11} atoms for 1 Bq)
- Q_{EC} = $(2.833 \pm 0.030^{stat} \pm 0.015^{syst})$ keV

S. Eliseev et al., *Phys. Rev. Lett.* **115** (2015) 062501

Electron capture in ^{163}Ho: spectrum

Atomic de-excitation:

- X-ray emission
- Auger electrons
- Coster-Kronig transitions

$$^{163}_{67}\text{Ho} \rightarrow ^{163}_{66}\text{Dy}^* + \nu_e$$

$$^{163}_{66}\text{Dy}^* \rightarrow ^{163}_{66}\text{Dy} + E_C$$

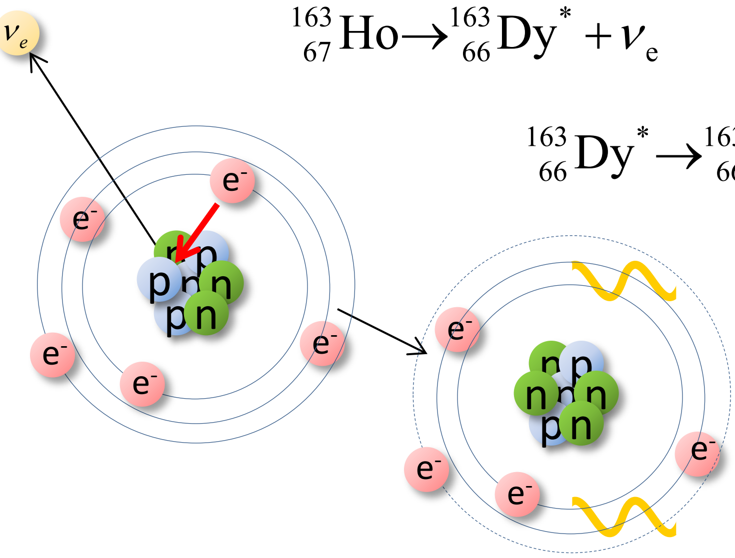

- $\tau_{1/2} \cong 4570$ years (2*10^{11} atoms for 1 Bq)
- Q_{EC} = $(2.833 \pm 0.030^{stat} \pm 0.015^{syst})$ keV

S. Eliseev et al., *Phys. Rev. Lett.* **115** (2015) 062501

Electron capture in ^{163}Ho: spectrum

Atomic de-excitation:

- **X-ray emission**
- Auger electrons
- Coster-Kronig transitions

$$^{163}_{67}\mathrm{Ho} \rightarrow ^{163}_{66}\mathrm{Dy}^{*} + \nu_{e}$$

$$^{163}_{66}\mathrm{Dy}^{*} \rightarrow ^{163}_{66}\mathrm{Dy} + E_{C}$$

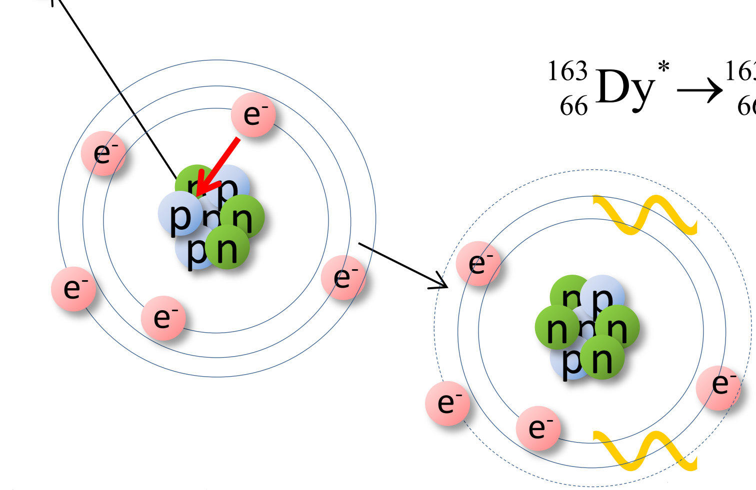

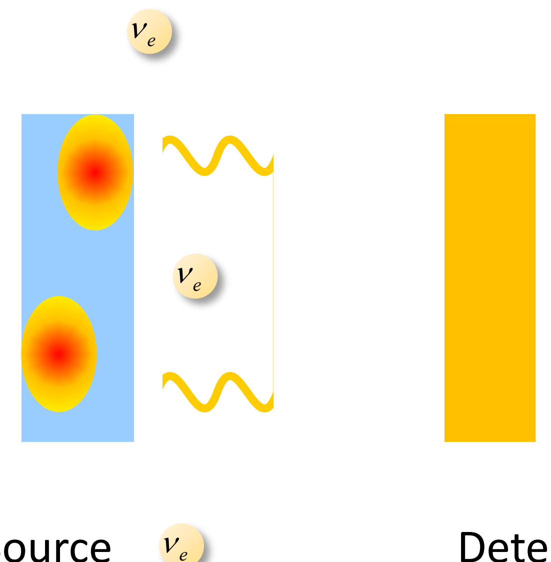

Source

Detector

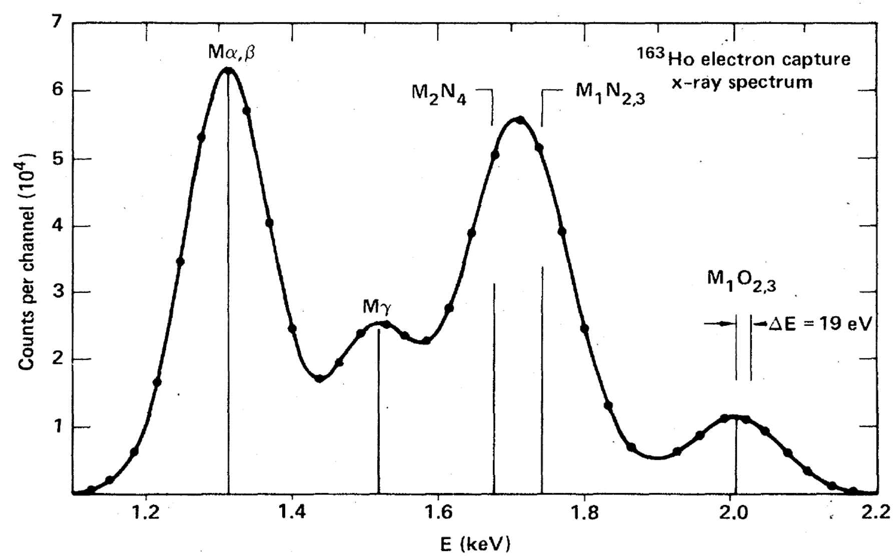

P. T. Springer, C. L. Bennett, and P. A. Baisden Phys. Rev. A 35 (1987) 679

Electron capture in ^{163}Ho: spectrum

$$^{163}_{67}\mathrm{Ho} \rightarrow ^{163}_{66}\mathrm{Dy}^{*} + \nu_e$$

$$^{163}_{66}\mathrm{Dy}^{*} \rightarrow ^{163}_{66}\mathrm{Dy} + E_C$$

Atomic de-excitation:

- **X-ray emission**
- **Auger electrons**
- **Coster-Kronig transitions**

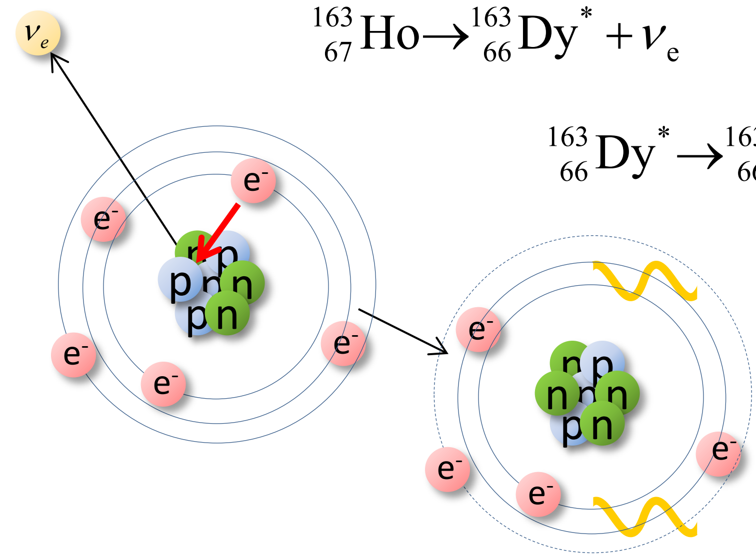

Calorimetric measurement

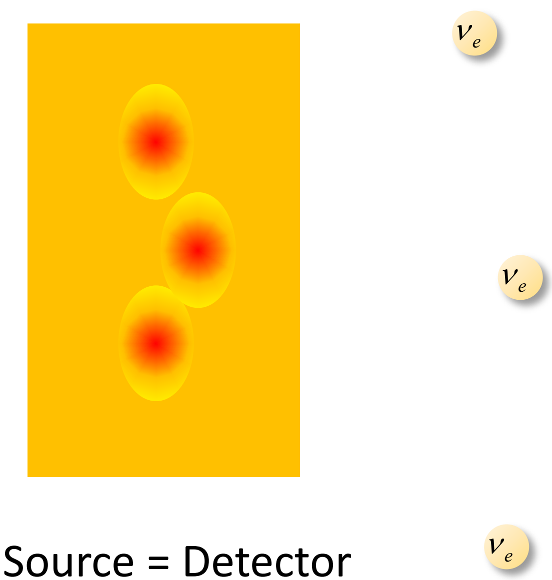

Source = Detector

Electron capture in ^{163}Ho: spectrum

Atomic de-excitation:

- **X-ray emission**
- **Auger electrons**
- **Coster-Kronig transitions**

$$^{163}_{67}\mathrm{Ho} \rightarrow ^{163}_{66}\mathrm{Dy}^{*} + \nu_{\mathrm{e}}$$

$$^{163}_{66}\mathrm{Dy}^{*} \rightarrow ^{163}_{66}\mathrm{Dy} + E_{\mathrm{C}}$$

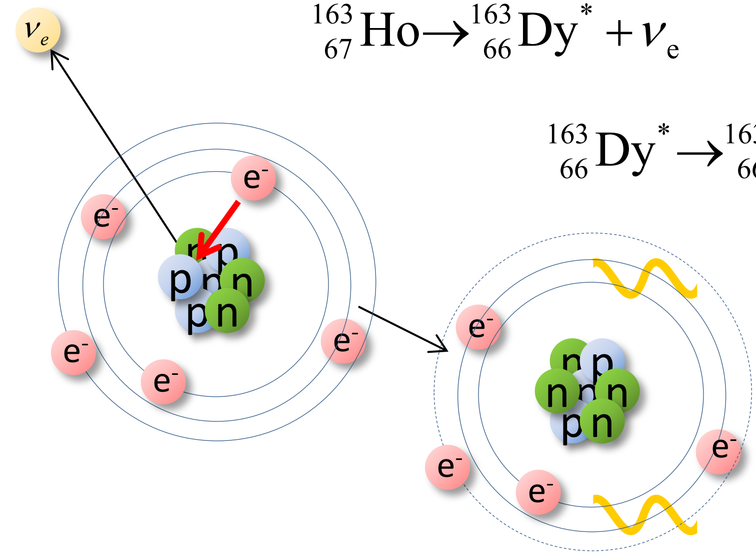

Calorimetric measurement

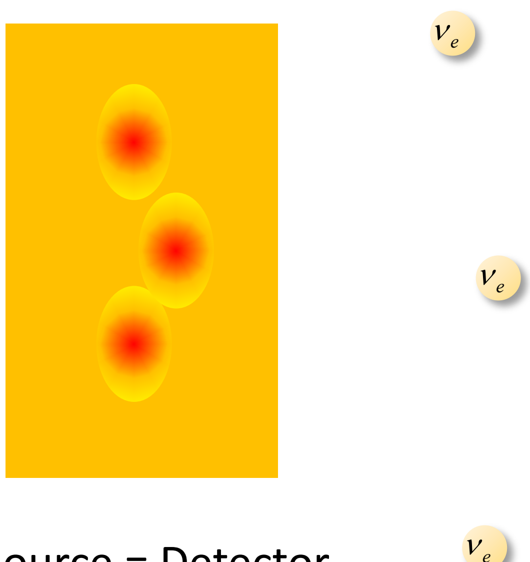

Source = Detector

Electron capture in ^{163}Ho: spectrum

Atomic de-excitation:

- **X-ray emission**
- **Auger electrons**
- **Coster-Kronig transitions**

$$^{163}_{67}\mathrm{Ho} \rightarrow ^{163}_{66}\mathrm{Dy}^{*} + \nu_e$$

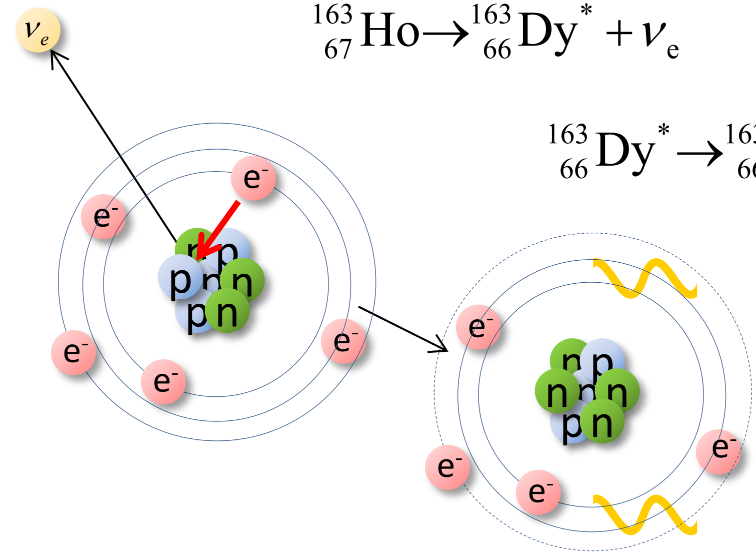

$$^{163}_{66}\mathrm{Dy}^{*} \rightarrow ^{163}_{66}\mathrm{Dy} + E_C$$

Calorimetric measurement

Volume 118B, number 4, 5, 6 PHYSICS LETTERS 9 December 1982

CALORIMETRIC MEASUREMENTS OF ^{163}HOLMIUM DECAY AS TOOLS TO DETERMINE THE ELECTRON NEUTRINO MASS

A. DE RÚJULA and M. LUSIGNOLI [1]
CERN, Geneva, Switzerland

Electron capture in ^{163}Ho: spectrum

Atomic de-excitation:

- **X-ray emission**
- **Auger electrons**
- **Coster-Kronig transitions**

$$^{163}_{67}\mathrm{Ho} \rightarrow {}^{163}_{66}\mathrm{Dy}^{*} + \nu_{e}$$

$$^{163}_{66}\mathrm{Dy}^{*} \rightarrow {}^{163}_{66}\mathrm{Dy} + E_{C}$$

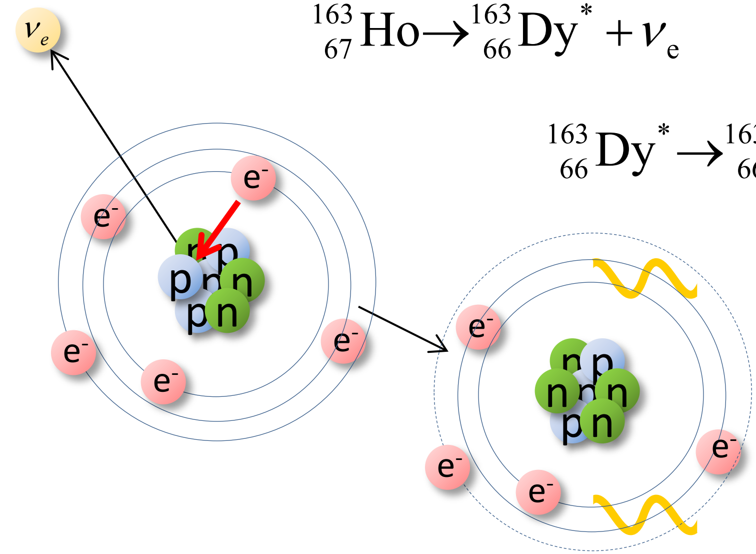

Calorimetric measurement

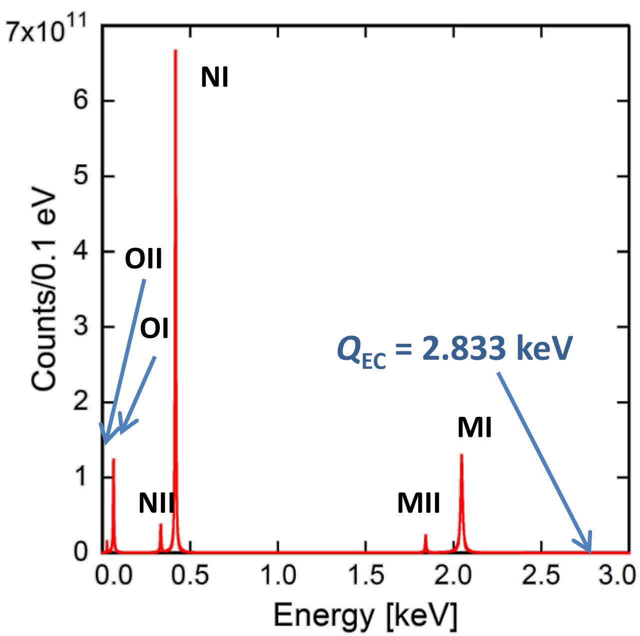

$$\frac{dW}{dE_C} = A(Q_{EC} - E_C)^2 \sqrt{1 - \frac{m_\nu^{\;2}}{(Q_{EC} - E_C)^2}} \sum_{H} B_H \varphi_H^{\;2}(0) \frac{\frac{\Gamma_H}{2\pi}}{(E_C - E_H)^2 + \frac{\Gamma_H^{\;2}}{4}}$$

Electron capture in ^{163}Ho: spectrum

Atomic de-excitation:

- **X-ray emission**
- **Auger electrons**
- **Coster-Kronig transitions**

$$^{163}_{67}\mathrm{Ho} \rightarrow ^{163}_{66}\mathrm{Dy}^* + \nu_e$$

$$^{163}_{66}\mathrm{Dy}^* \rightarrow ^{163}_{66}\mathrm{Dy} + E_C$$

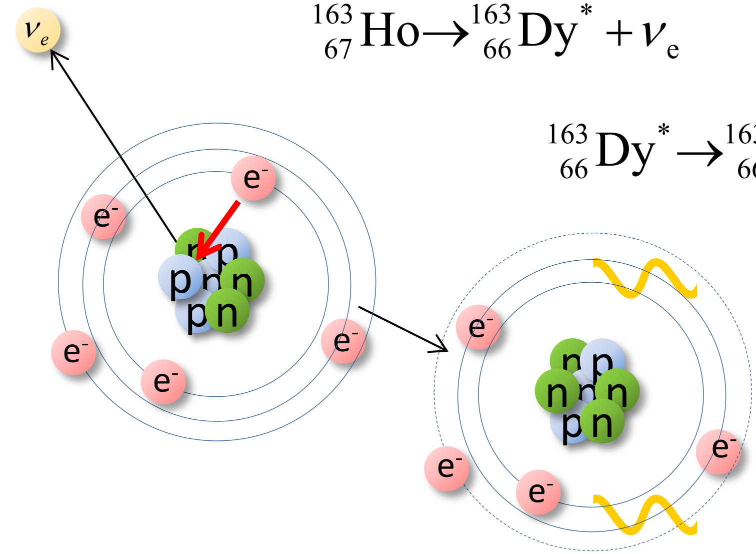

Calorimetric measurement

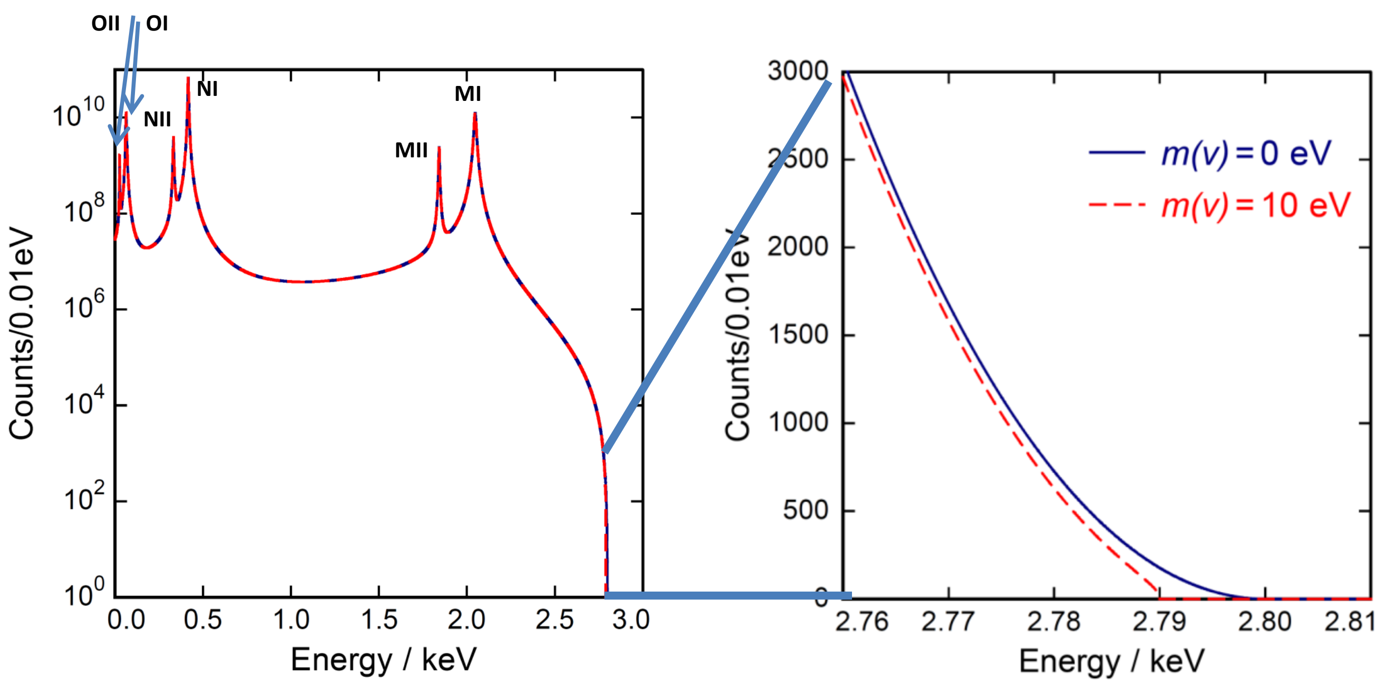

Electron capture in ^{163}Ho: history

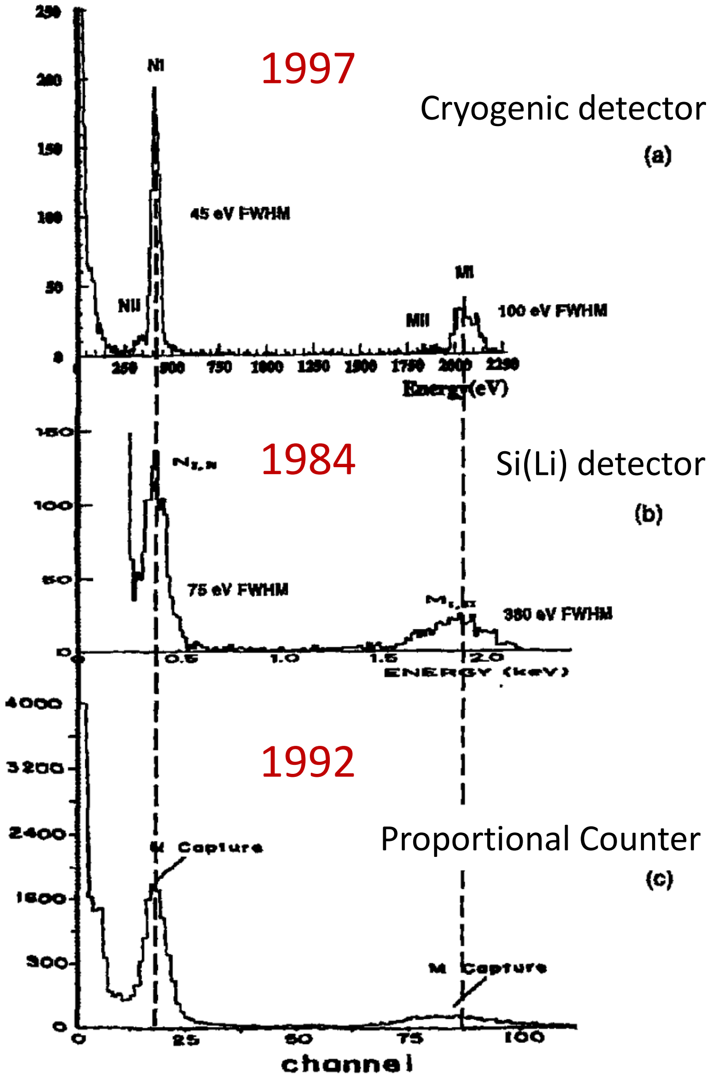

F. Gatti et al., Physics Letters B 398 (1997) 415-419

(a) F. Gatti et al., Physics Letters B 398 (1997) 415-419
(b) E. Laesgaard et al., Proceeding of 7th International Conference on Atomic Masses and Fundamental Constants (AMCO-7), (1984).
(c) F.X. Hartmann and R.A. Naumann, Nucl. Instr. Meth. A 3 13 (1992) 237.

Electron capture in ^{163}Ho: history

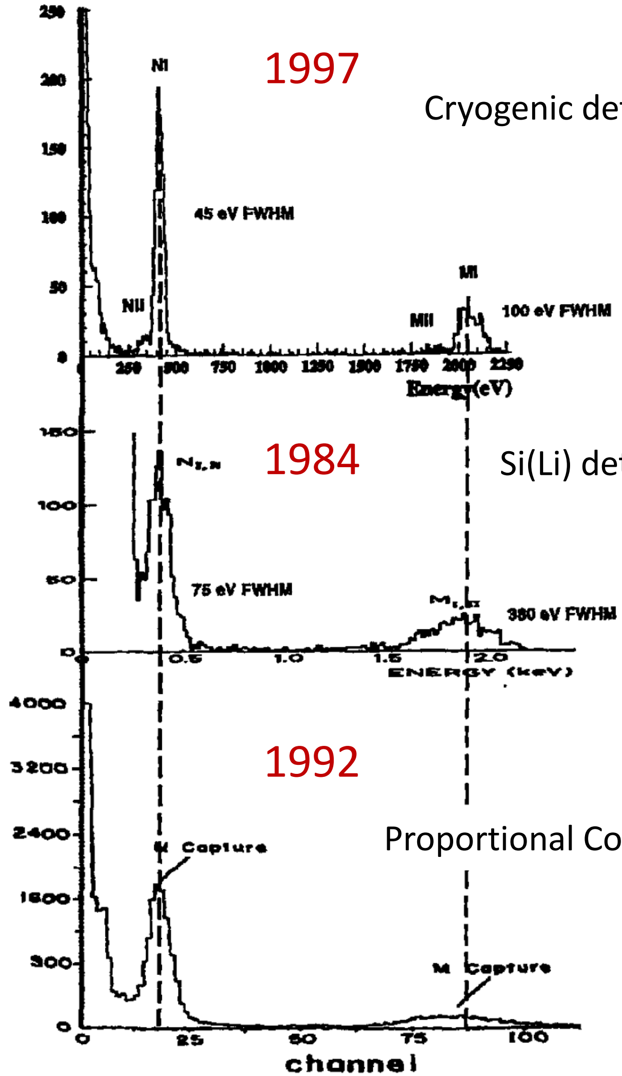

F. Gatti et al., Physics Letters B 398 (1997) 415-419

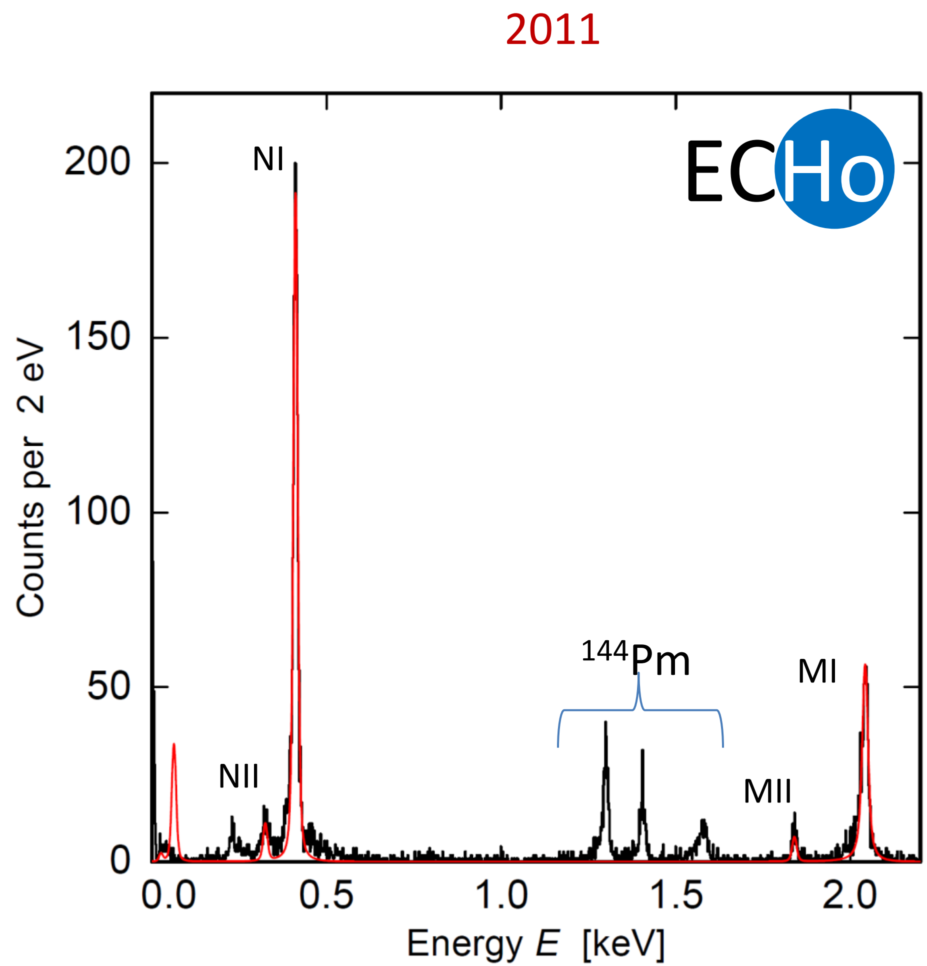

P. C.-O. Ranitzsch et al., J. Low Temp. Phys. 167, 1004 (2012)

(a) F. Gatti et al., Physics Letters B 398 (1997) 415-419
(b) E. Laesgaard et al., Proceeding of 7th International Conference on Atomic Masses and Fundamental Constants (AMCO-7), (1984).
(c) F.X. Hartmann and R.A. Naumann, Nucl. Instr. Meth. A 3 13 (1992) 237.

Electron capture in ^{163}Ho: history

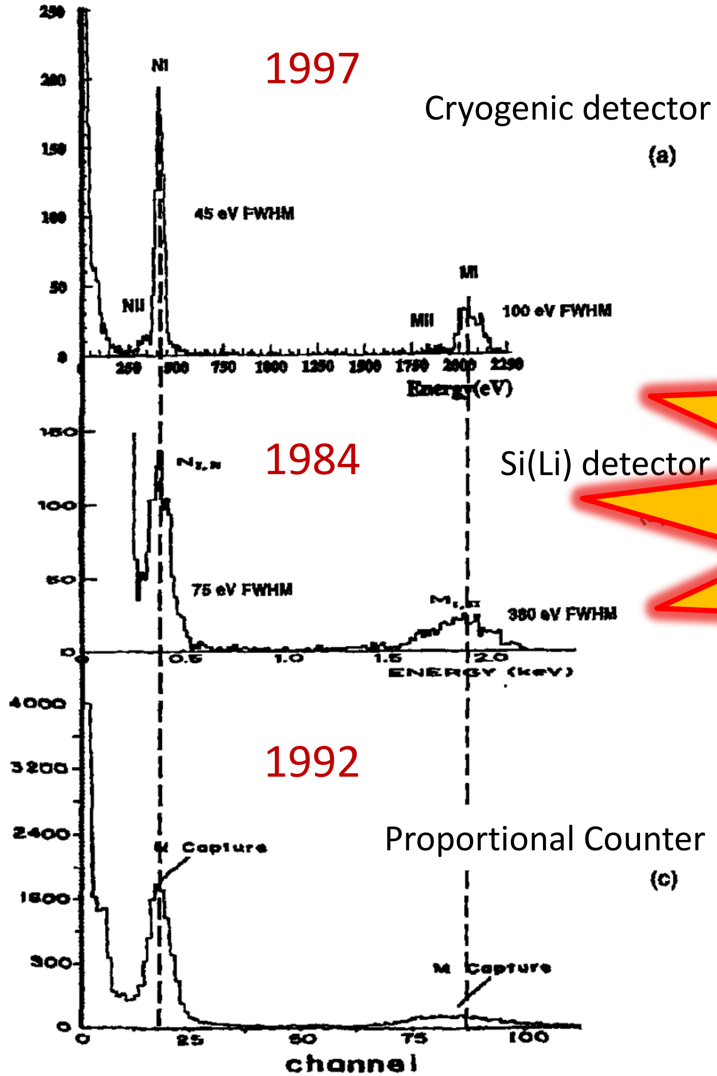

F. Gatti et al., Physics Letters B 398 (1997) 415-419

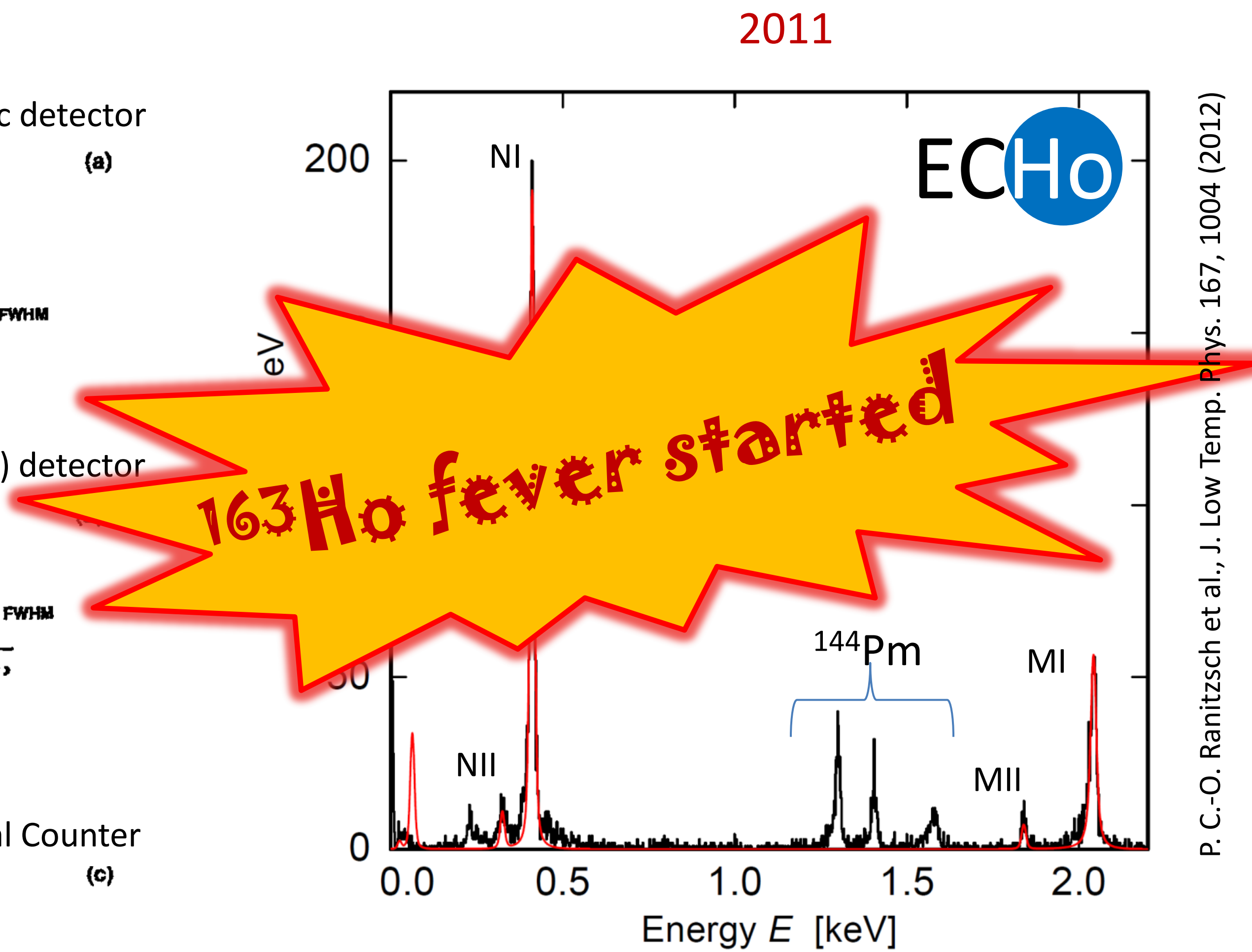

(a) F. Gatti et al., Physics Letters B 398 (1997) 415-419
(b) E. Laesgaard et al., Proceeding of 7th International Conference on Atomic Masses and Fundamental Constants (AMCO-7), (1984).
(c) F.X. Hartmann and R.A. Naumann, Nucl. Instr. Meth. A 3 13 (1992) 237.

Electron capture in ^{163}Ho: present

- Calorimetric measurement of the ^{163}Ho spectrum

2011

- Three internaltional collaborations

ECHo (1)

HOLMES (2)

NuMECS (3)

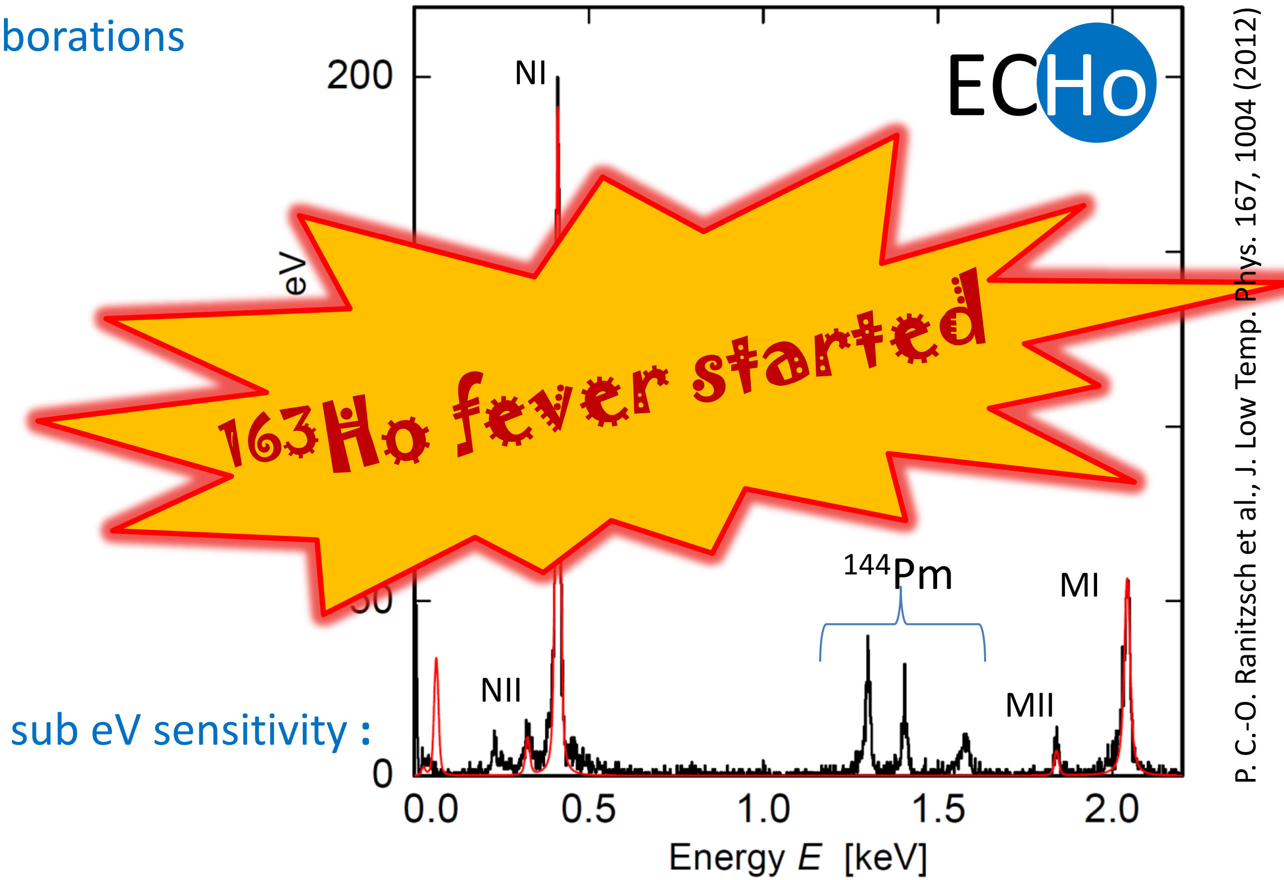

P. C.-O. Ranitzsch et al., J. Low Temp. Phys. 167, 1004 (2012)

Common challenges to reach sub eV sensitivity :

- Detector performance
- High purity ^{163}Ho source
- Background reduction
- Description of the ^{163}Ho EC spectrum

(1) The ECHo Collaboration EPJ-ST 226 8 (2017) 1623

(2) B. Alpert et al, Eur. Phys. J. C (2015) 75:112

(3) M. Croce et al., arXiv:1510.03874

Requirements for sub-eV sensitivity in ECHo

Statistics in the end point region

- $N_{ev} > 10^{14}$ → **A ≈ 1 MBq**

Fraction of events at endpoint regions

- In the interval 2.832 -2.833 keV only 6×10^{-13}

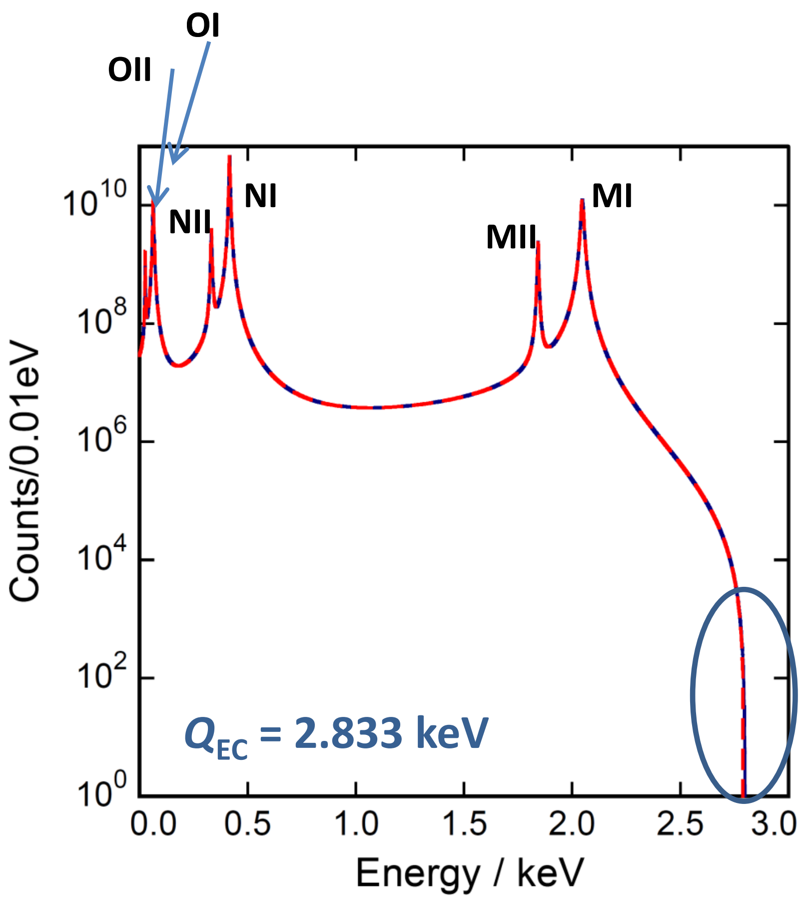

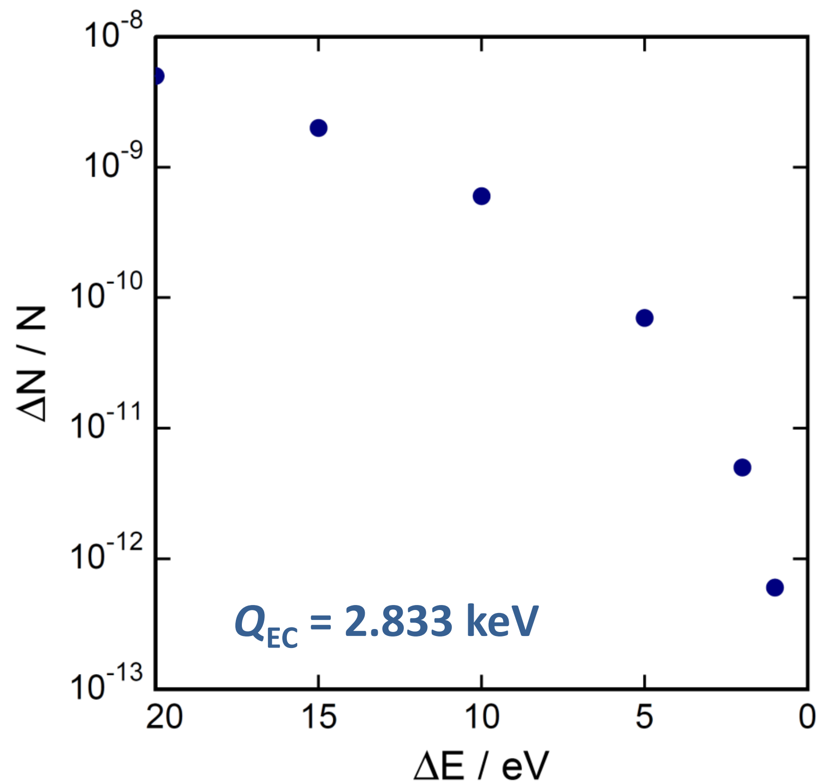

Requirements for sub-eV sensitivity in ECHo

Statistics in the end point region

- $N_{ev} > 10^{14}$ → **A ≈ 1 MBq**

Unresolved pile-up ($f_{pu} \sim a \cdot \tau_r$)

- $\boldsymbol{f_{pu} < 10^{-5}}$
- $\tau_r < 1$ µs → a ~ 10 Bq
- 10^5 pixels

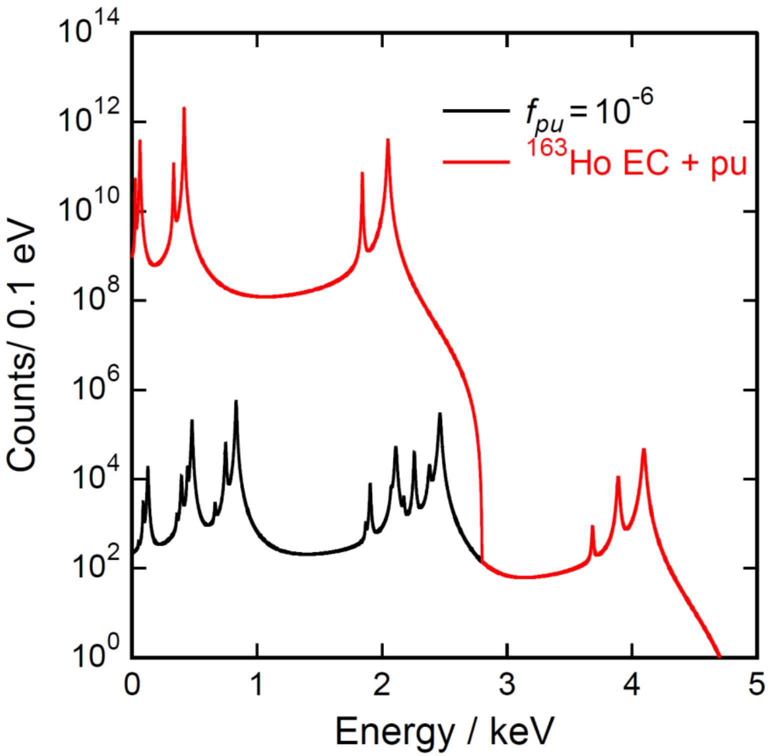

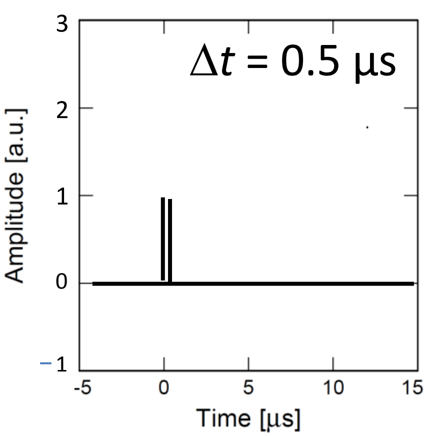

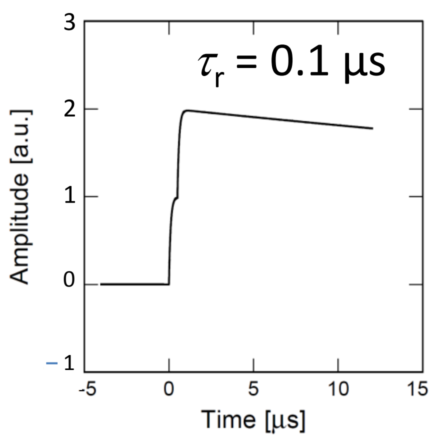

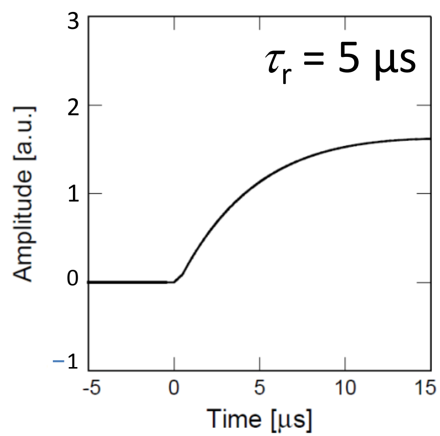

Requirements for sub-eV sensitivity in ECHo

Statistics in the end point region

- $N_{ev} > 10^{14}$ → **A ≈ 1 MBq**

Unresolved pile-up ($f_{pu} \sim a \cdot \tau_r$)

- $\boldsymbol{f_{pu} < 10^{-5}}$
- $\tau_r < 1\ \mu s$ → a ~ 10 Bq
- 10^5 pixels → **multiplexing**

Precision characterization of the endpoint region

- $\boldsymbol{\Delta E_{FWHM} < 3\ eV}$

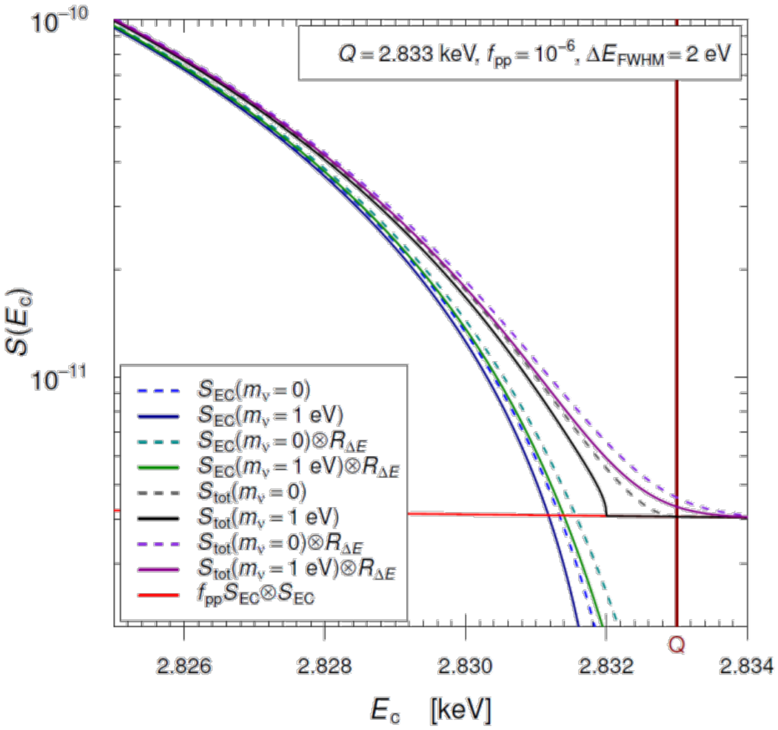

Requirements for sub-eV sensitivity in ECHo

Statistics in the end point region

- $N_{ev} > 10^{14}$ → **A ≈ 1 MBq**

Unresolved pile-up ($f_{pu} \sim a \cdot \tau_r$)

- f_{pu} **< 10^{-5}**
- τ_r < 1 µs → a ~ 10 Bq
- 10^5 pixels → **multiplexing**

Precision characterization of the endpoint region

- ΔE_{FWHM} **< 3 eV**

Background level

- **< 10^{-6} events/eV/det/day**

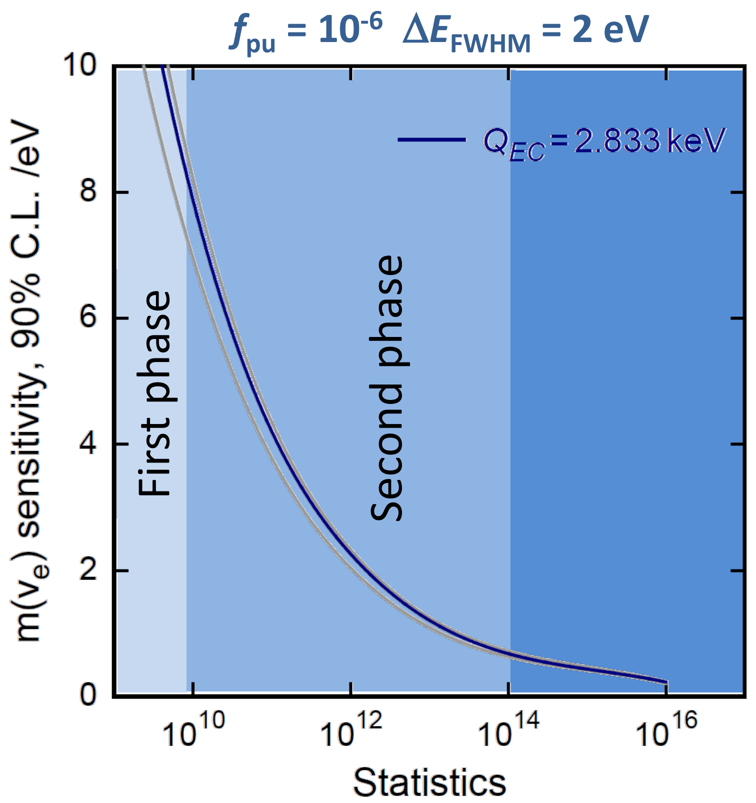

First detector prototype for ^{163}Ho

- Absorber for calorimetric measurement
  → ion implantation @ ISOLDE-CERN in 2009
  on-line process
- About 0.01 Bq per pixel
- Operated over more than 4 years

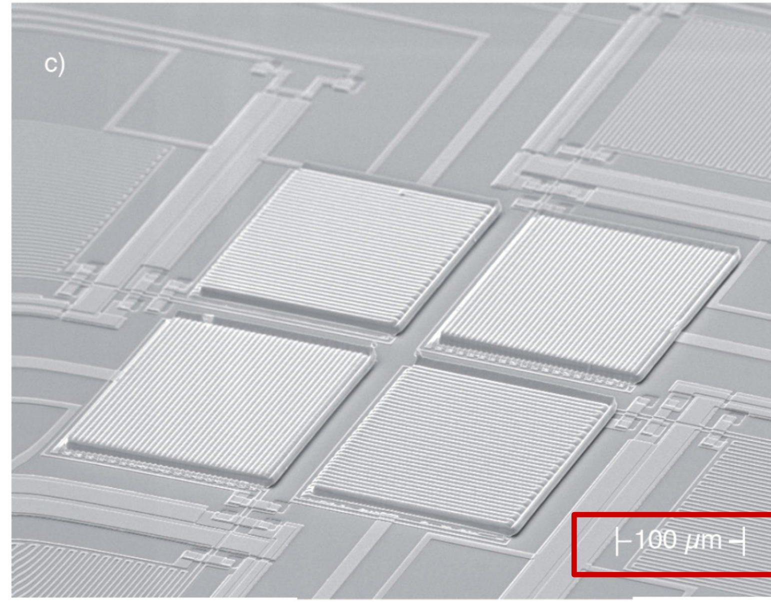

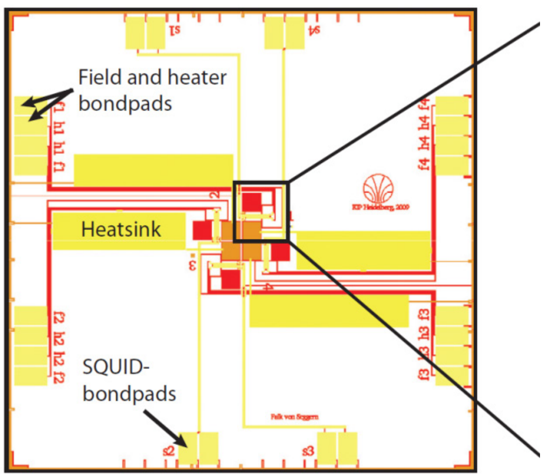

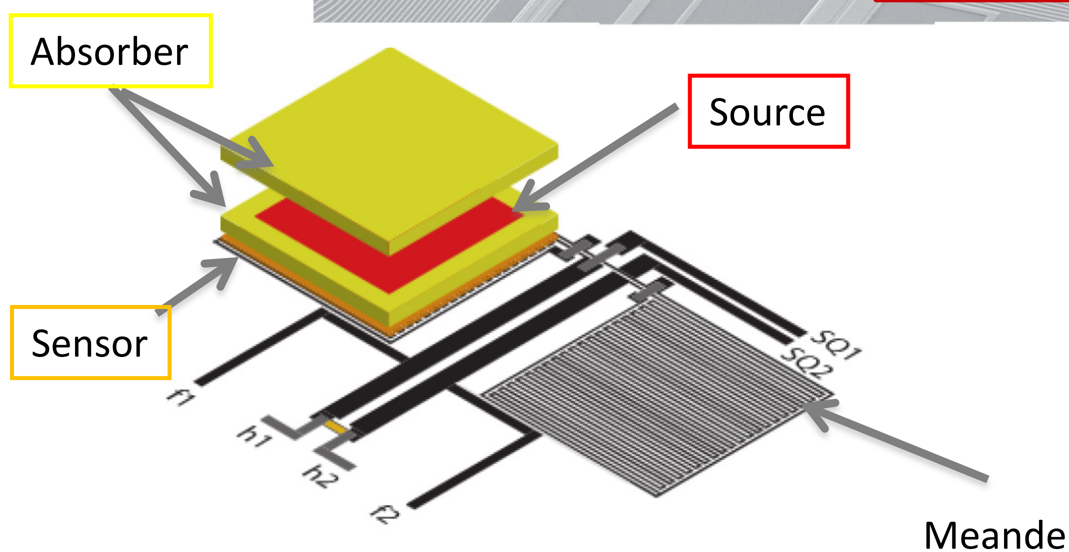

L. Gastaldo et al.,
Nucl. Inst. Meth. A, 711 (2013) 150

P. C.-O. Ranitzsch et al.,
http://arxiv.org/abs/1409.0071v1

Calorimetric spectrum

- Rise Time ~ 130 ns
- ΔE_{FWHM} = 7.6 eV @ 6 keV (2013)
- Non-Linearity < 1% @ 6keV

	E_H bind.	E_H exp.	Γ_H lit.	Γ_H exp
MI	2.047	2.040	13.2	13.7
MII	1.845	1.836	6.0	7.2
NI	0.420	0.411	5.4	5.3
NII	0.340	0.333	5.3	8.0
OI	0.050	0.048	5.0	4.3

First calorimetric measurement of the OI-line

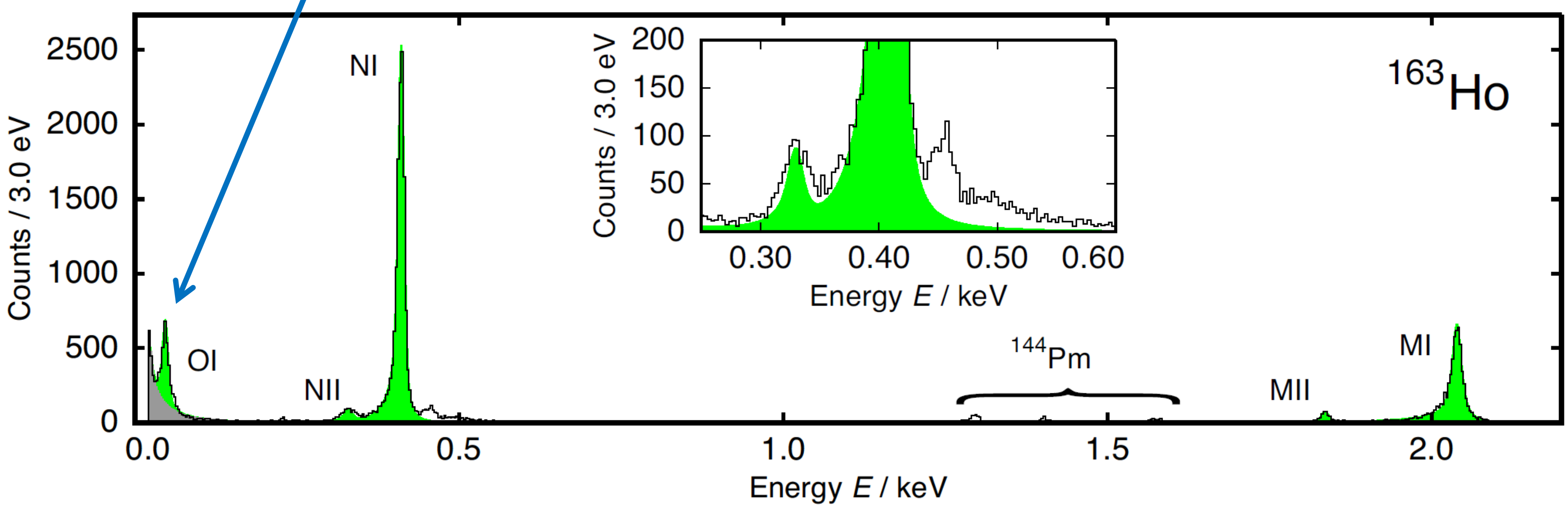

P. C.-O. Ranitzsch et al ., accepted for publication in PRL (2017)

Q_{EC} determination

$$\Phi_H(E) = \sqrt{\frac{n_H}{\varphi_H^2(0) B_H}} = \sqrt{C}\left(Q_{EC} - E_H\right)$$

Line amplitudes are affected by the phase space factor

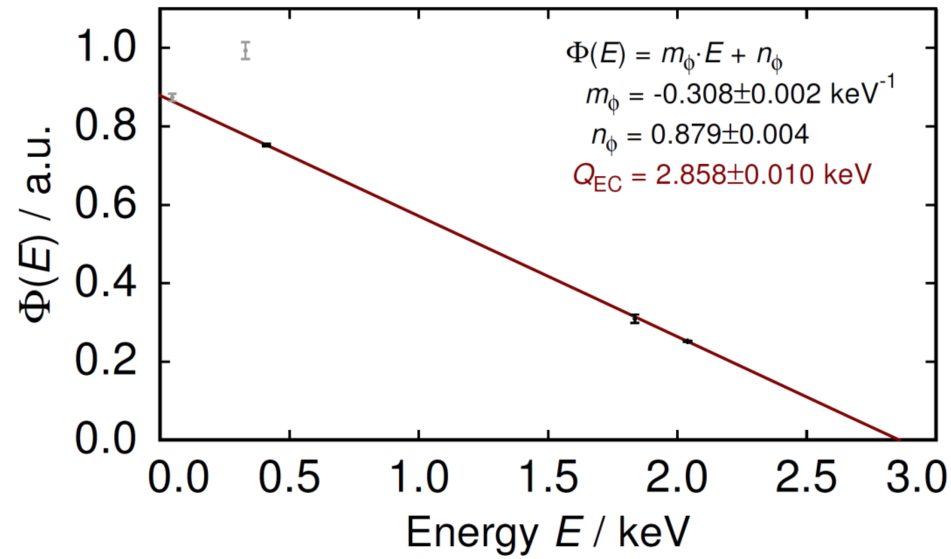

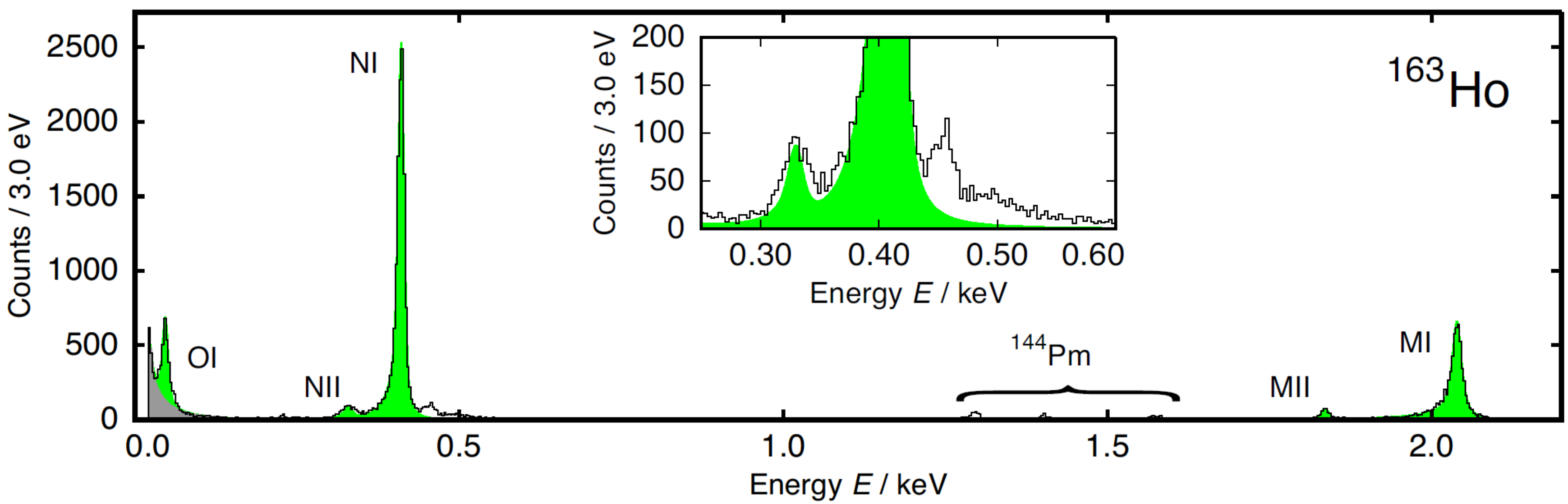

P. C.-O. Ranitzsch et al ., accepted for publication in PRL (2017)

Q_{EC} determination

$$\Phi_H(E) = \sqrt{\frac{n_H}{\varphi_H^2(0) B_H}} = \sqrt{C}(Q_{EC} - E_H)$$

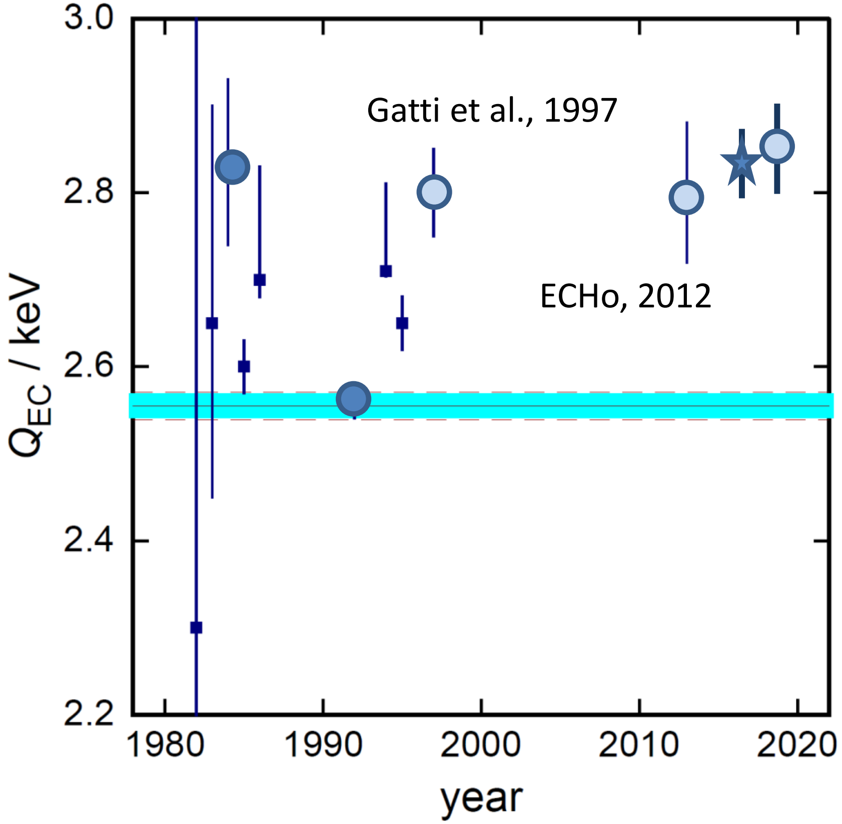

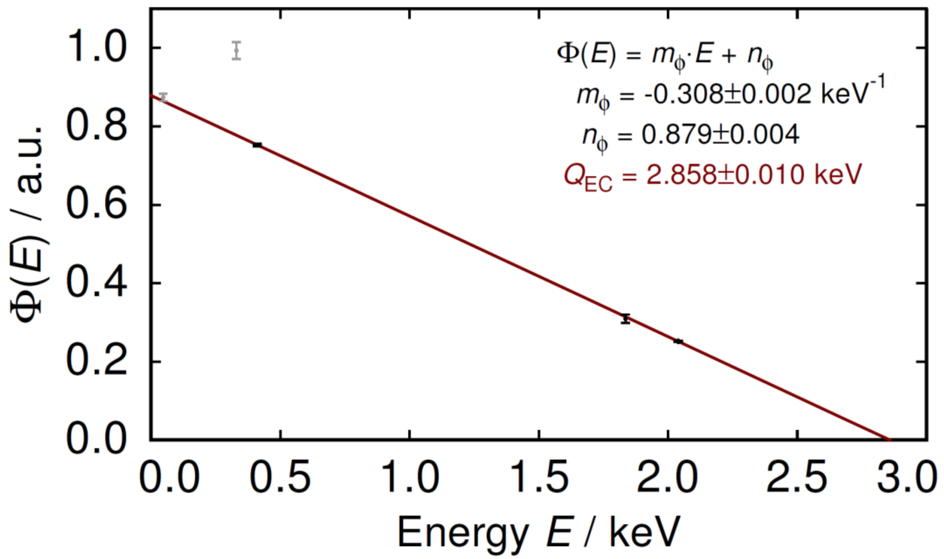

Our result:

$Q_{EC} = (2.858 \pm 0.010^{stat} \pm 0.05^{syst})$ keV

Penning Trap Mass Spectrometry result:

$Q_{EC} = (2.833 \pm 0.030^{stat} \pm 0.015^{syst})$ keV

P. C.-O. Ranitzsch et al ., accepted for publication in PRL (2017)

Scaling up

^{163}Ho high purity source

Required activity in the detectors: Final experiment → $>10^{6}$ Bq → $>10^{17}$ atoms

- Neutron irradiation

  (n,γ)-reaction on ^{162}Er

  High cross-section

  Radioactive contaminants

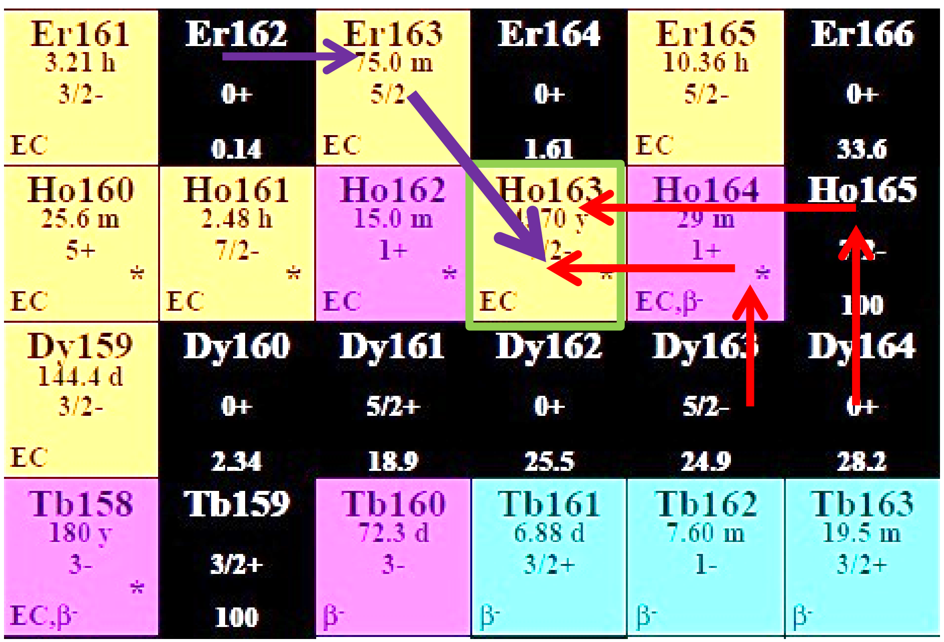

- Charged particle activation

  ^{nat}Dy(p,xn) ^{163}Ho

  ^{nat}Dy(α, xn) ^{163}Er (ε) ^{163}Ho

  ^{159}Tb(^{7}Li, 3n) ^{163}Er (ε) ^{163}Ho

  Small cross-section

  Few radioactive contaminants

^{163}Ho high purity source

Required activity in the detectors: Final experiment → >10^6 Bq → >10^{17} atoms

- Neutron irradiation

  (n,γ)-reaction on ^{162}Er

  High cross-section

  Radioactive contaminants

ECHo HOLMES

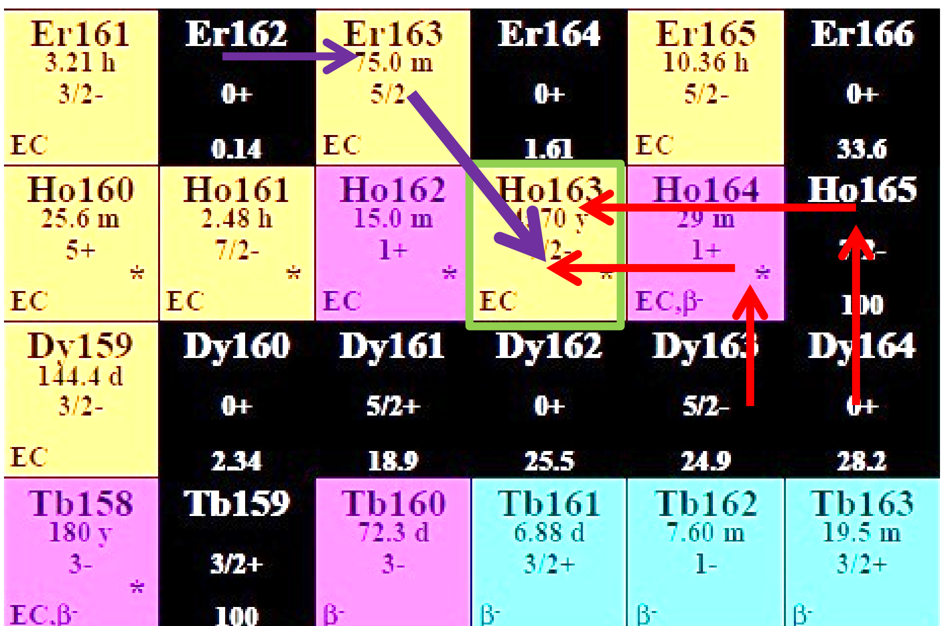

- Charged particle activation

  ^{nat}Dy(p,xn) ^{163}Ho

  ^{nat}Dy(α, xn) ^{163}Er (ε) ^{163}Ho

  ^{159}Tb(^{7}Li, 3n) ^{163}Er (ε) ^{163}Ho

  Small cross-section

  Few radioactive contaminants

NuMECS

Mass separation and ^{163}Ho ion-implantation

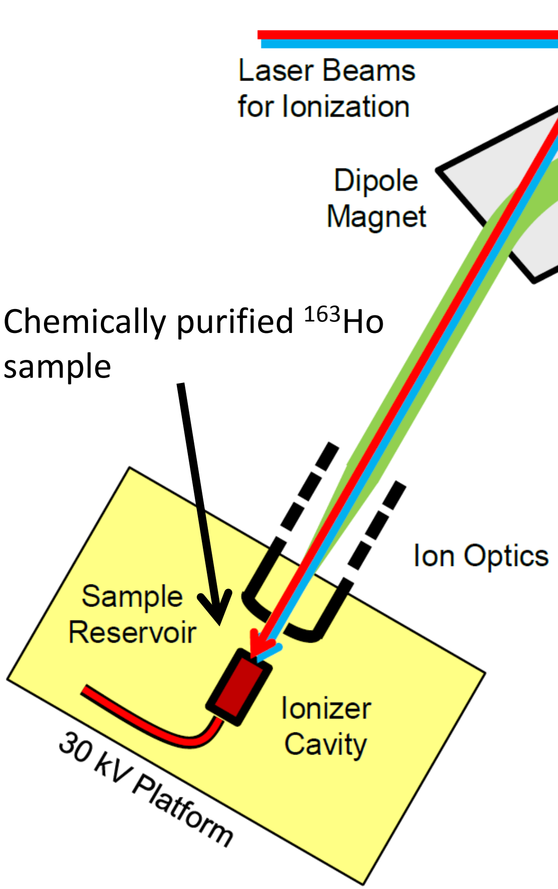

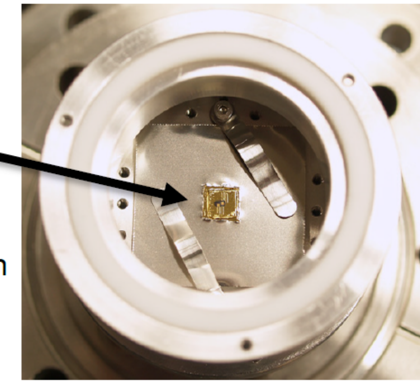

RISIKO @ Physics Institute, Mainz University

- Resonant laser ion source efficiency **42%**
- Suppression of neighboring masses > 700

  → $^{166m}Ho/^{163}Ho < 10^{-5}$

- Optimization of beam focalization

F. Schneider et al ., *NIM B* **376** (2016) 388

Fabrication 4π absorber

Stems between absorber and sensor prevent athermal phonon loss to the substrate

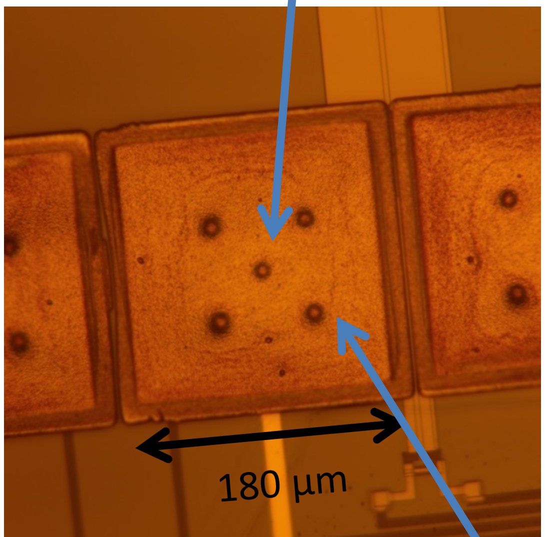

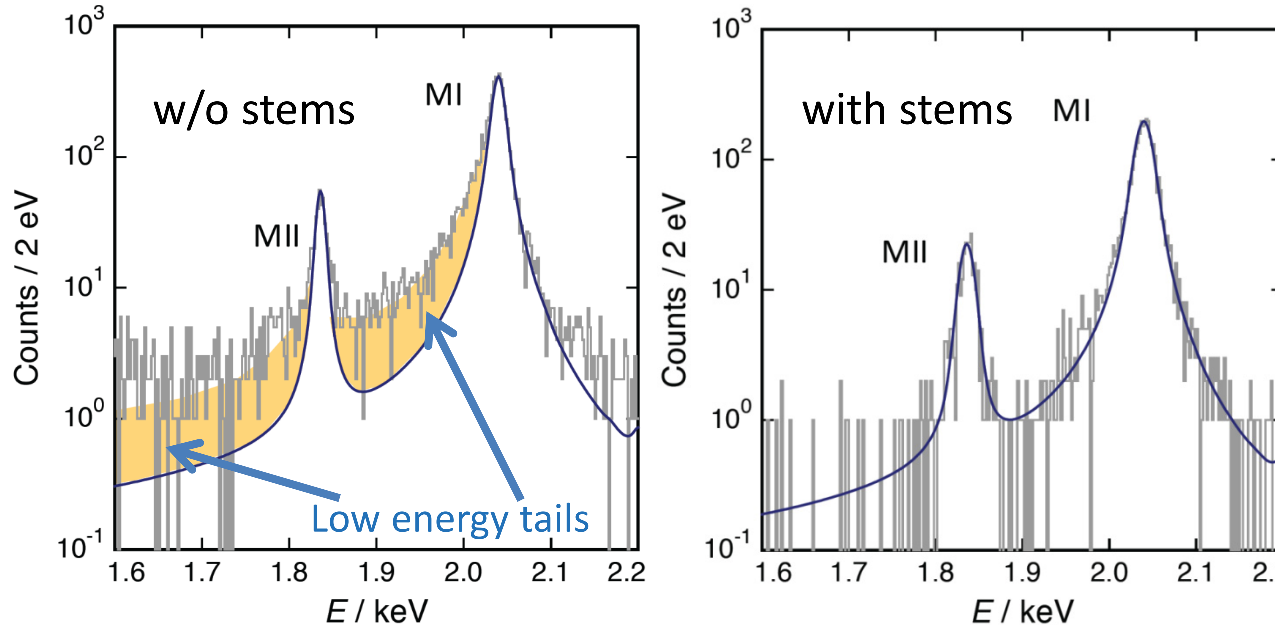

Definition of the implantation area by microstructuring a photoresist layer

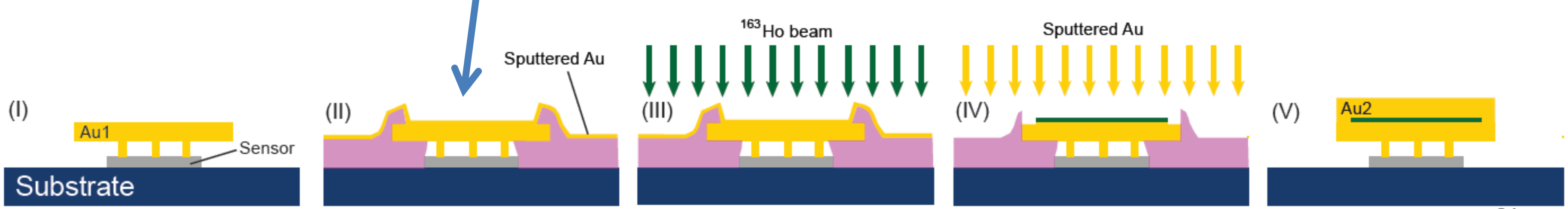

ECHo-1k array

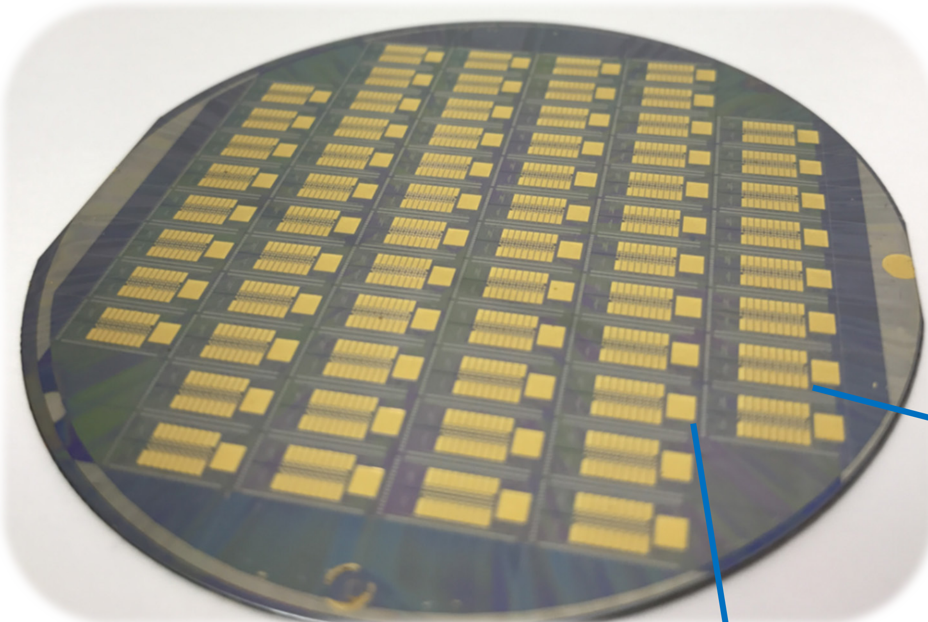

3“ wafer with 64 ECHo-1k chip

Suitable for
parallel and multiplexed readout

64 pixels which can be loaded with ^{163}Ho
+ 4 detectors for diagnostics

Design performance:
ΔE_{FWHM} ~ 5 eV
τ_r ~ 90 ns (single channel readout)
τ_r ~ 300 ns (multiplexed read-out)

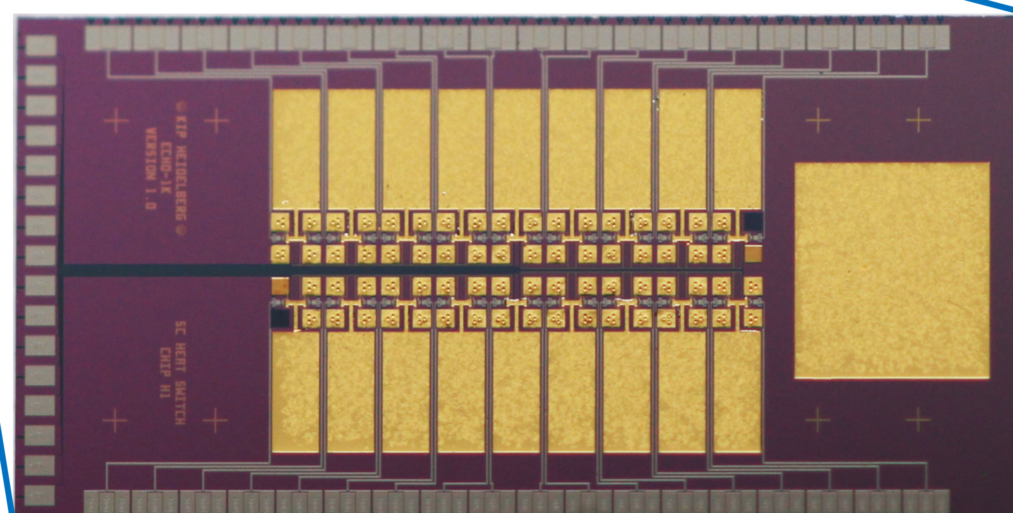

S.Kempf *et al.*, *J. Low. Temp. Phys*. **176** (2014) 426

ECHo-1k array

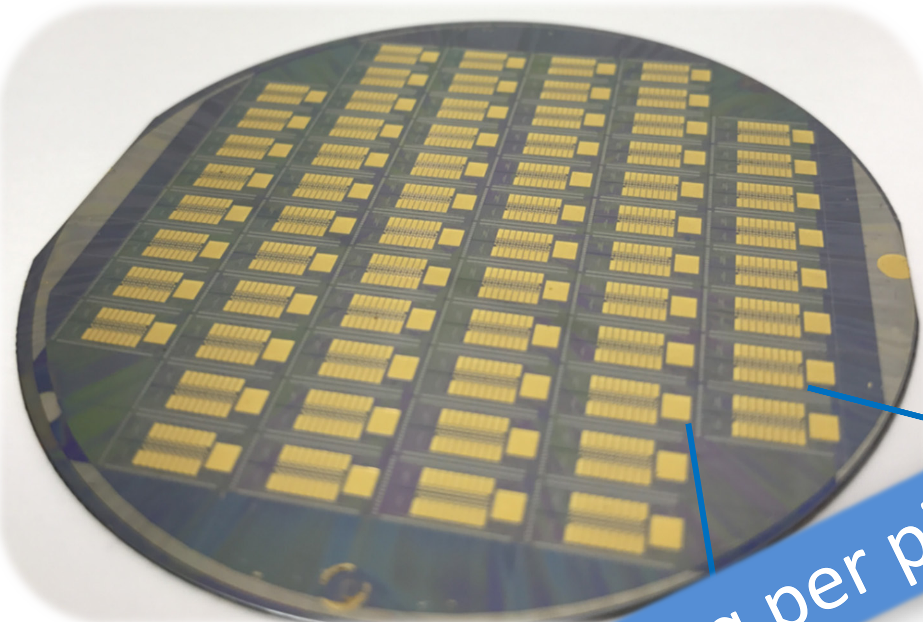

3“ wafer with 64 ECHo-1k chip

Suitable for
parallel and mu... ...dout

4 chips with a few Bq per pixel ready to be measured

64 pixels which ... ...d with ^{163}Ho
+ 4 detect... ...ostics

Desig... ...ormance:
ΔE_{FWHM} ~ 5 eV
τ_r ~ 90 ns (single channel readout)
τ_r ~ 300 ns (multiplexed read-out)

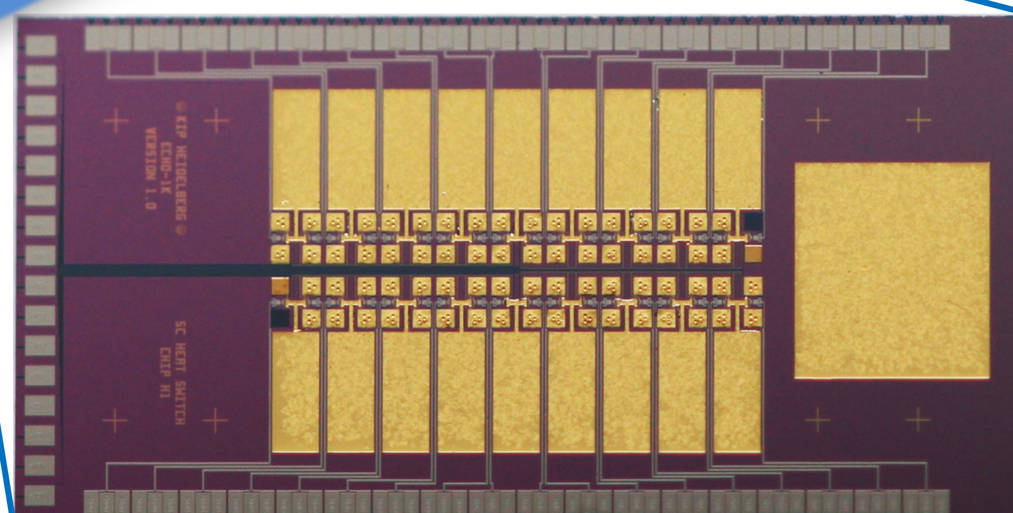

S.Kempf *et al., J. Low. Temp. Phys.* **176** (2014) 426

Characterisation of spectral shape

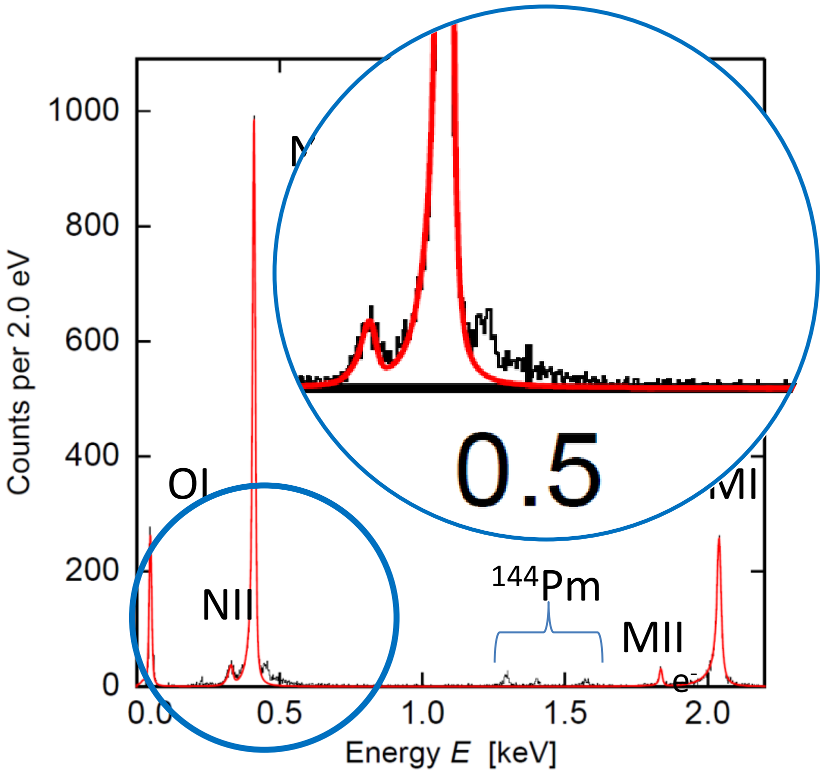

- A. Faessler et al.
  J. Phys. G **42** (2015) 015108
- R. G. H. Robertson
  Phys. Rev. C **91**, 035504 (2015)
- A. Faessler and F. Simkovic
  Phys. Rev. C **91**, 045505 (2015)
- A. Faessler et al.
  Phys. Rev. C **91**, 064302 (2015)
- A. De Rujula and M. Lusignoli
  JHEP 05 (2016) 015, arXiv:1601.04990v1
- A. Faessler et al.
  Phys. Rev. C **95**, (2017) 045502

Two-holes excited states: shake-up
shake-off

ECHo-1k (2015 - 2018)

^{163}Ho activity: **A_t = 1 kBq**

Detectors: Metallic Magnetic Calorimeters

→ Energy resolution **$\Delta E_{FWHM} \leq 5$ eV**

→ Time resolution **$\tau \leq 1$ µs**

Unresolved pile-up fraction $f_{pu} \leq 10^{-5}$

→activity per pixel: **A = 10 Bq**

→number of detectors **N = 100**

Read-out : Microwave SQUID Multiplexing

→ 2 arrays with ~50 single pixels

Background **$b < 10^{-5}$ /eV/det/day**

Measuring time **t = 1 year**

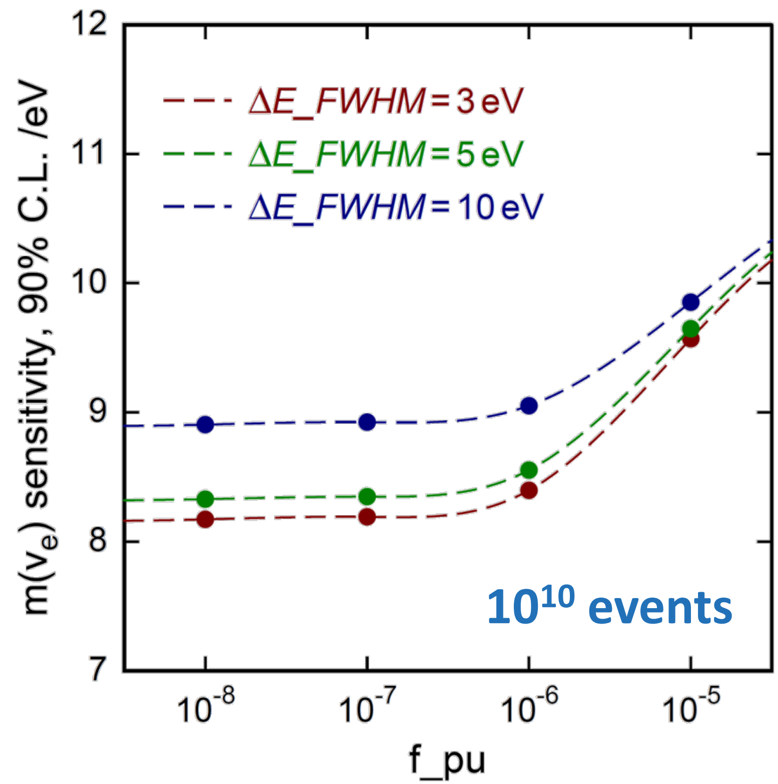

$m(\nu_e) < 10$ eV 90% C.L.

The ECHo Collaboration EPJ-ST 226 8 (2017) 1623

ECHo cryogenic platform

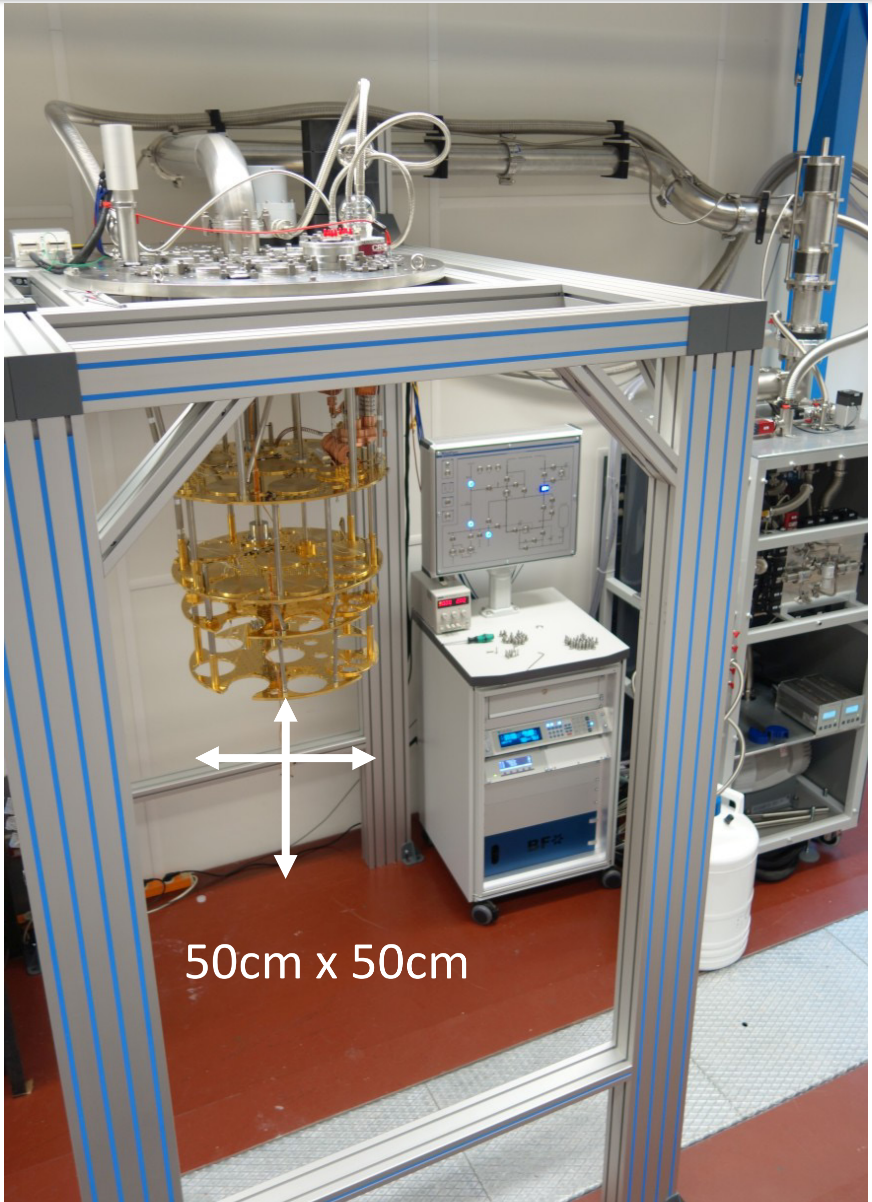

- Large space at MXC enough for several ECHo phases
- cooling power: 15µW @ 20 mK
- Possibility to load 200kg for passive shielding

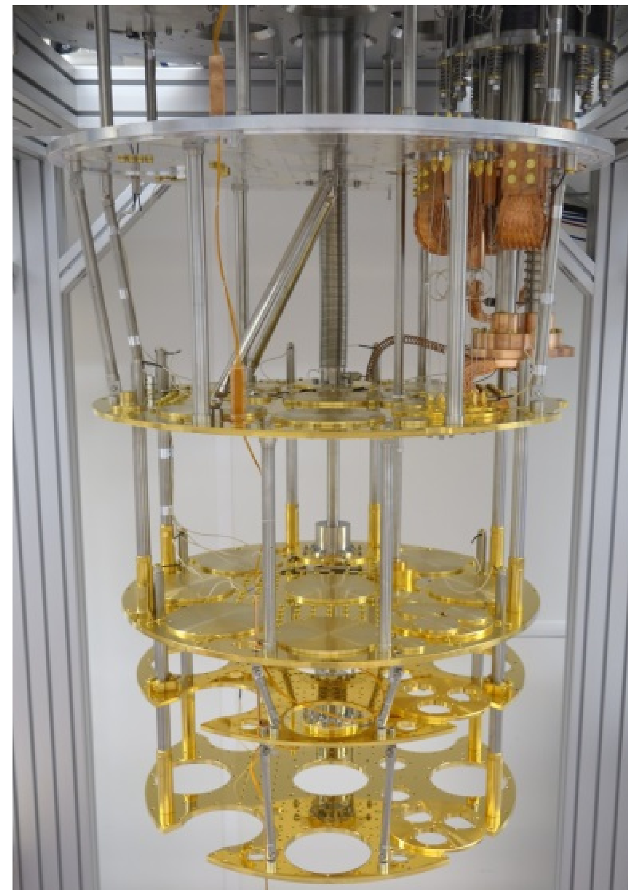

ECHo cryogenic platform

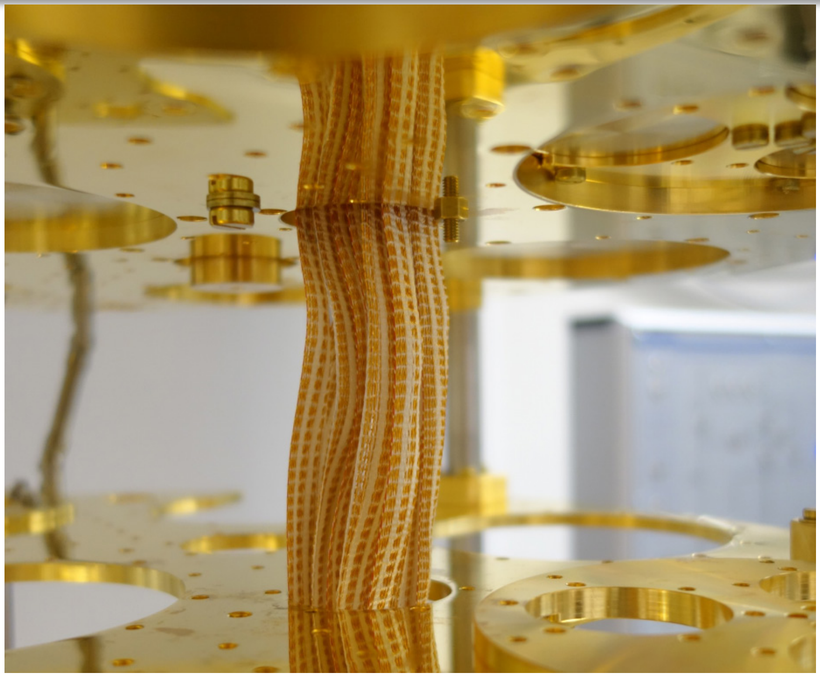

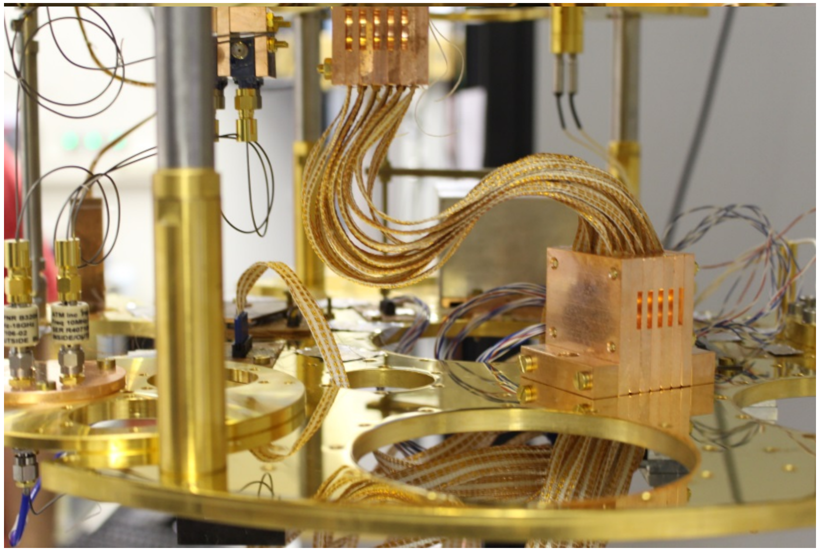

- Large space at MXC enough for several ECHo phases
- cooling power: 15µW @ 20 mK
- Possibility to load 200kg for passive shielding
- Presently equipped with:

  2 RF lines for microwave multiplexing readour of 2 MMC arrays

  12 ribbons each with 30 Cu98Ni2 0.2 mm, 1.56 Ohm/m, cables from RT to mK
  → allows for parallel readout of 36 two-stage SQUID set-up

ECHo-1M (next future)

^{163}Ho activity: A_t = 1 MBq

Detectors: Metallic Magnetic Calorimeters

→ Energy resolution $\Delta E_{FWHM} \leq 3$ eV

→ Time resolution $\tau \leq 0.1$ μs

Unresolved pile-up fraction $f_{pu} \leq 10^{-6}$

→activity per pixel: A = 10 Bq

→number of detectors $N = 10^5$

Read-out : Microwave SQUID Multiplexing

→ 100 arrays with ~1000 single pixels

Background $b < 10^{-6}$ /eV/det/day

Measuring time t = 1 – 3 year

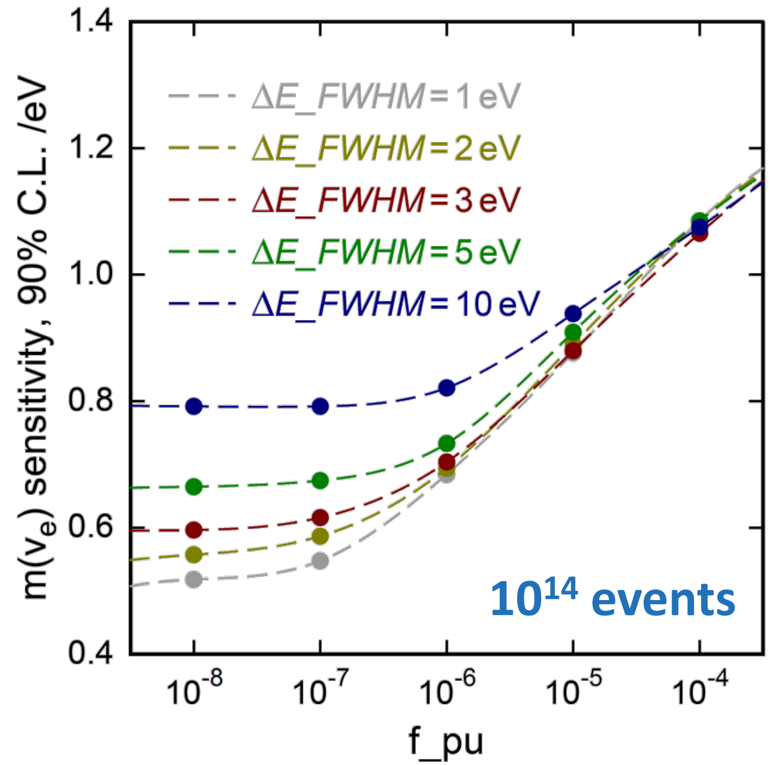

$m(\nu_e) < 1$ eV 90% C.L.

The ECHo Collaboration EPJ-ST 226 8 (2017) 1623

How does
the existence of sterile neutrino
affect the EC spectrum?

Sterile Neutrino and ^{163}Ho

$$\frac{dW}{dE_C} = A(Q_{EC} - E_C)^2 \sqrt{1 - \frac{m_\nu^{\,2}}{(Q_{EC} - E_C)^2}} \sum_H B_H \varphi_H^{\,2}(0) \frac{\frac{\Gamma_H}{2\pi}}{(E_C - E_H)^2 + \frac{\Gamma_H^{\,2}}{4}}$$

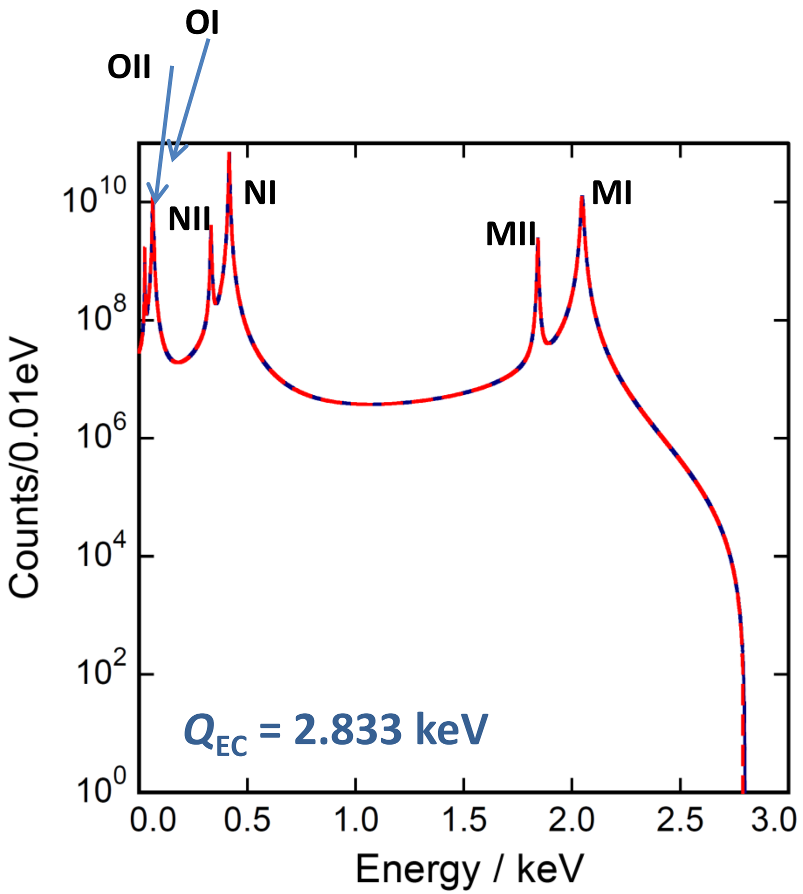

Sterile Neutrino and ^{163}Ho

$$\frac{dW}{dE_C} = A(Q_{EC} - E_C)^2 \sum_i |U_{ei}|^2 \sqrt{1 - \frac{m_i^2}{(Q_{EC} - E_C)^2}} \sum_H B_H \varphi_H^2(0) \frac{\frac{\Gamma_H}{2\pi}}{(E_C - E_H)^2 + \frac{\Gamma_H^2}{4}}$$

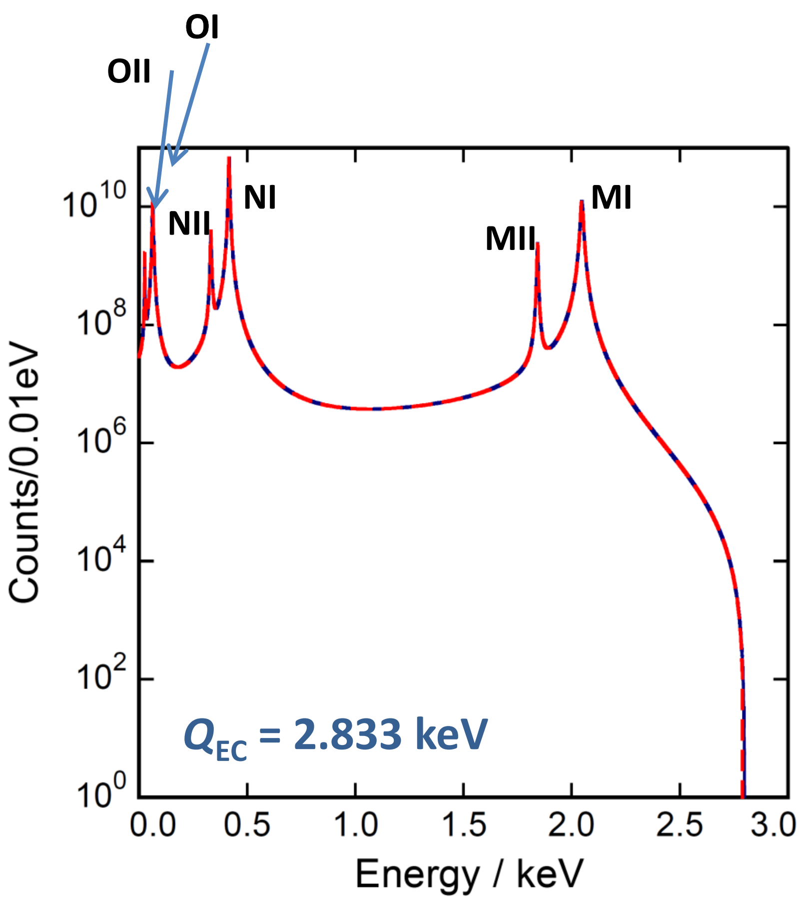

- Electron neutrino as superposition of mass eigenstates

Sterile Neutrino and ^{163}Ho

$$\frac{dW}{dE_C} = A(Q_{EC} - E_C)^2 \left[\left(1 - |U_{e4}|^2\right) + |U_{e4}|^2 \sqrt{1 - \frac{m_4^{\ 2}}{(Q_{EC} - E_C)^2}} H(Q_{EC} - E_c - m_4) \right] \sum_H B_H \varphi_H^{\ 2}(0) \frac{\frac{\Gamma_H}{2\pi}}{(E_C - E_H)^2 + \frac{\Gamma_H^{\ 2}}{4}}$$

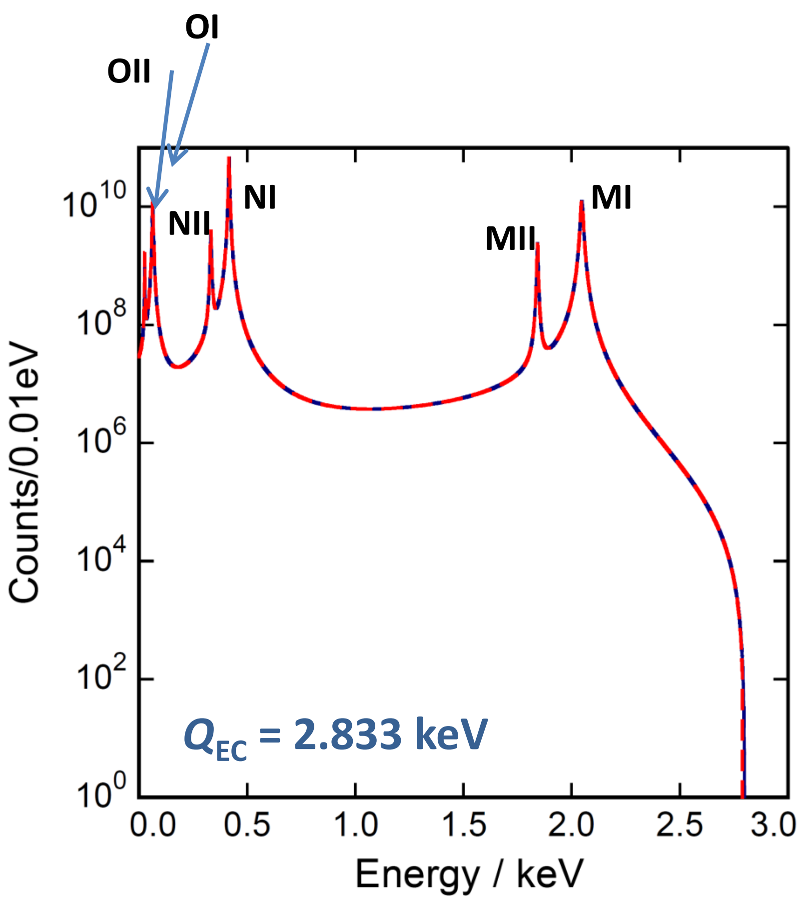

- Electron neutrino as superposition of mass eigenstates
- $m_{i=1,2,3} << m_4$ → $m_{i=1,2,3} \sim 0$ eV

Sterile Neutrino and ^{163}Ho

$$\frac{dW}{dE_C} = A(Q_{EC} - E_C)^2 \left[\left(1 - |U_{e4}|^2\right) + |U_{e4}|^2 \sqrt{1 - \frac{m_4^2}{(Q_{EC} - E_C)^2}} H(Q_{EC} - E_c - m_4) \right] \sum_H B_H \varphi_H^2(0) \frac{\frac{\Gamma_H}{2\pi}}{(E_C - E_H)^2 + \frac{\Gamma_H^2}{4}}$$

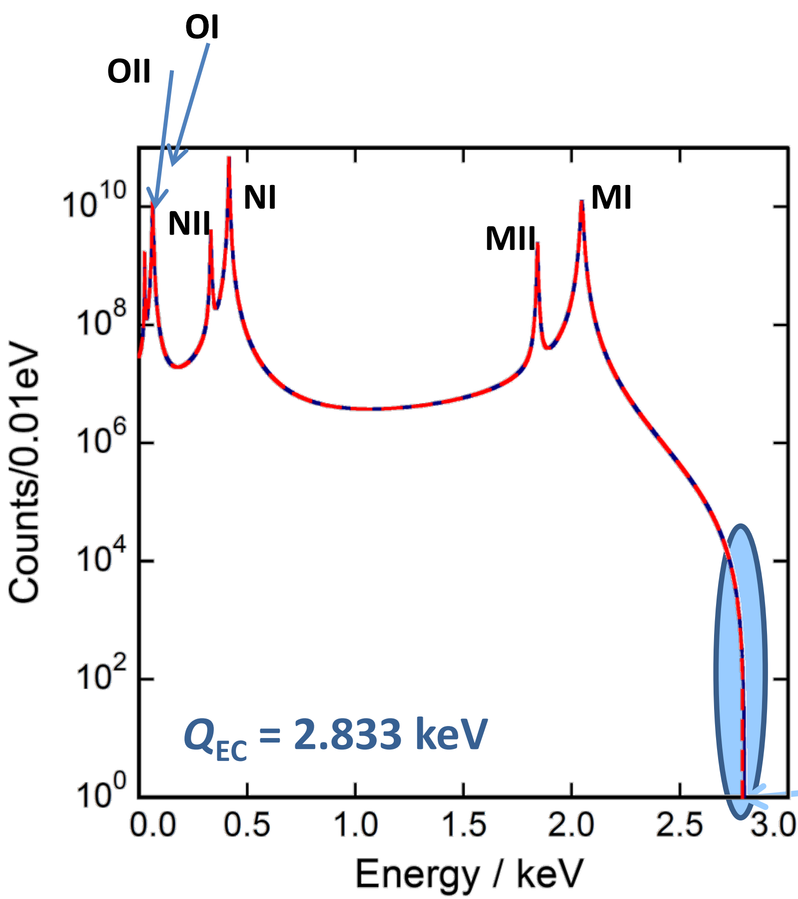

- Electron neutrino as superposition of mass eigenstates
- $m_{i=1,2,3} << m_4$ → $m_{i=1,2,3}$ ~ 0 eV

eV-scale sterile neutrinos

eV-scale sterile neutrino

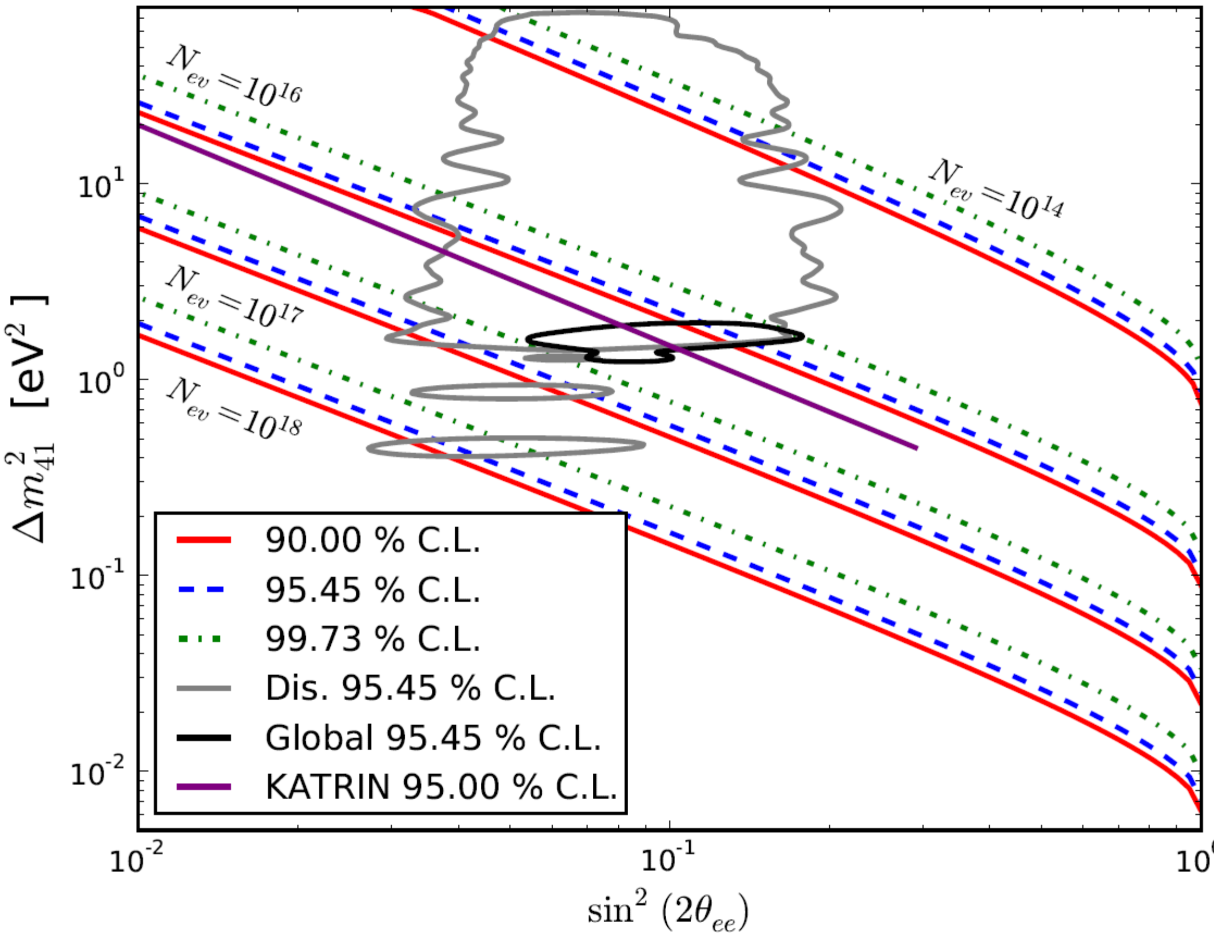

L. Gastaldo, C. Giunti, E. Zavanin.,
High Energ. Phys. **06** (2016) 61.

keV-scale sterile neutrino

$$\frac{dW}{dE_C} = A(Q_{EC} - E_C)^2 \left[\left(1 - |U_{e4}|^2\right) + |U_{e4}|^2 \sqrt{1 - \frac{m_4^{\ 2}}{(Q_{EC} - E_C)^2}} H(Q_{EC} - E_c - m_4) \right] \sum_H B_H \varphi_H^{\ 2}(0) \frac{\frac{\Gamma_H}{2\pi}}{(E_C - E_H)^2 + \frac{\Gamma_H^{\ 2}}{4}}$$

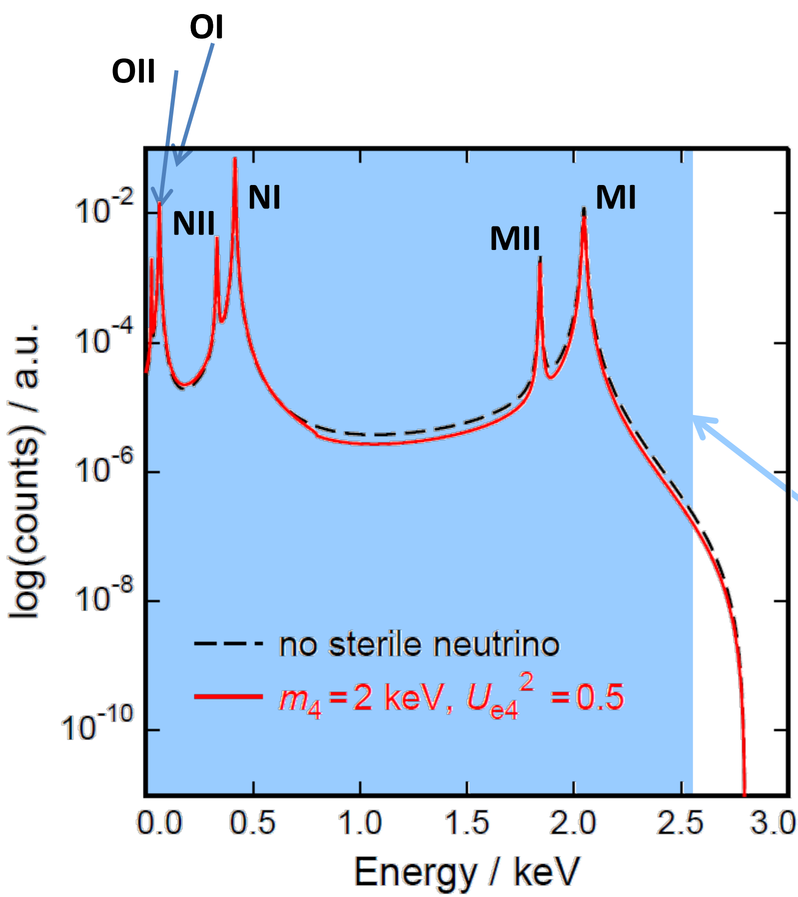

- Electron neutrino as superposition of mass eigenstates
- $m_{i=1,2,3} << m_4$ → $m_{i=1,2,3} \sim 0$ eV

keV-scale sterile neutrinos

keV-scale sterile neutrino

m_4=2 keV, $U_{e4}{}^2$=0.5

no sterile neutrino

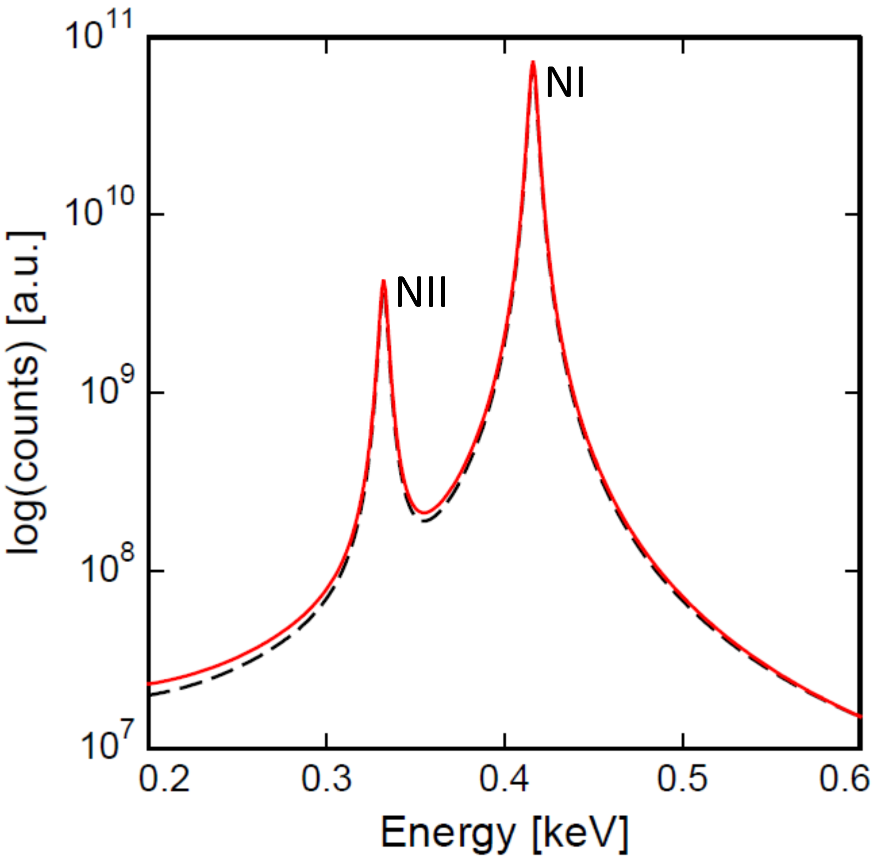

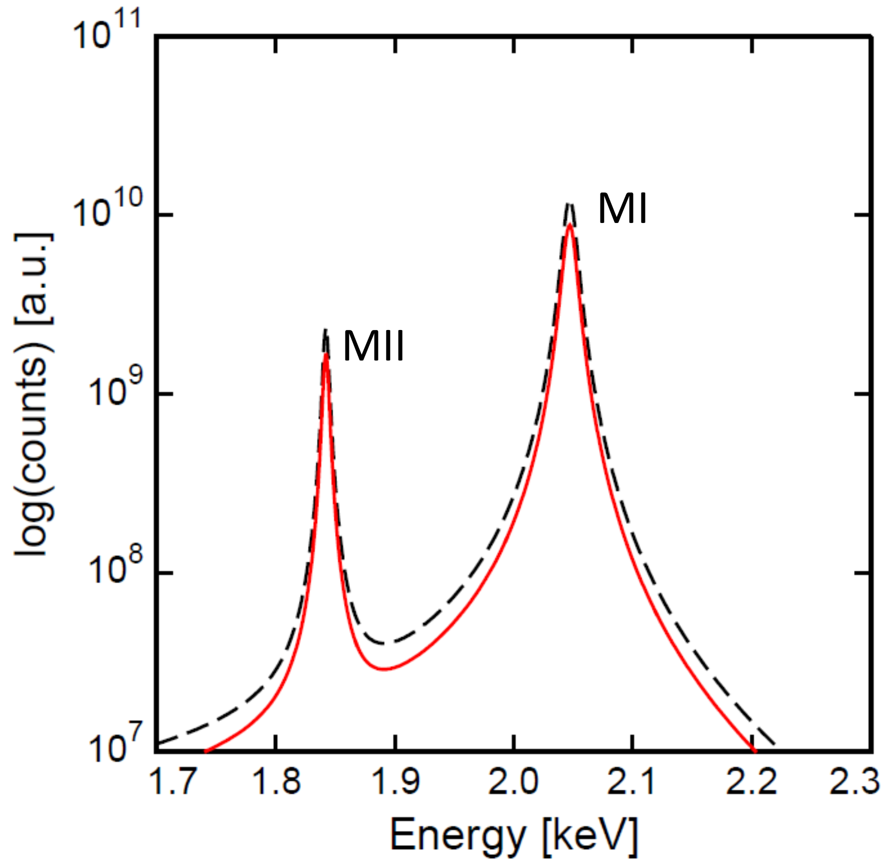

keV-scale sterile neutrino

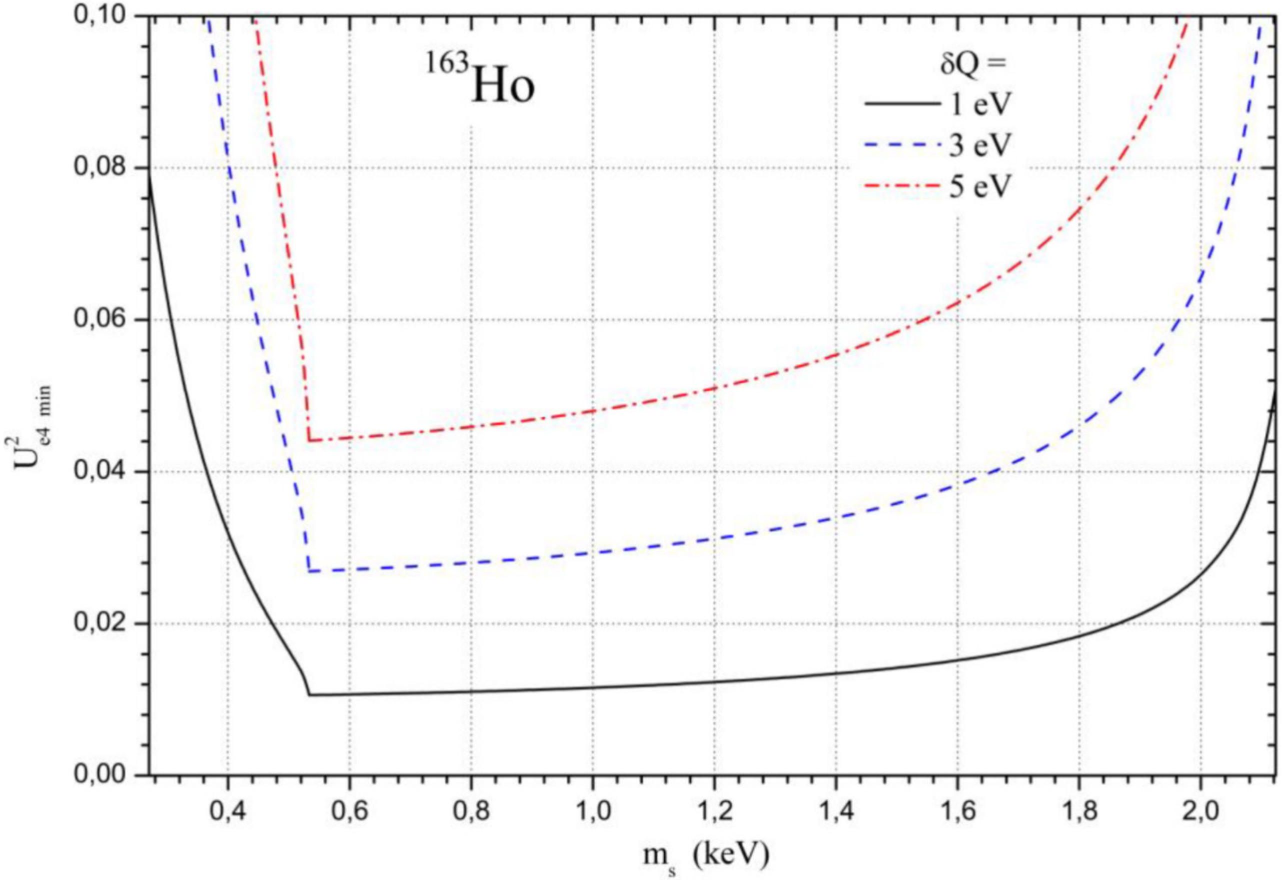

Sensitivity to the mixing matrix element at 90% CL as a function of the sterile neutrino mass achievable with about 10^{10} events in the full EC spectrum.

P. Filianin et al., *J. Phys. G: Nucl. Part. Phys.* **41** (2014) 095004

keV-scale sterile neutrino

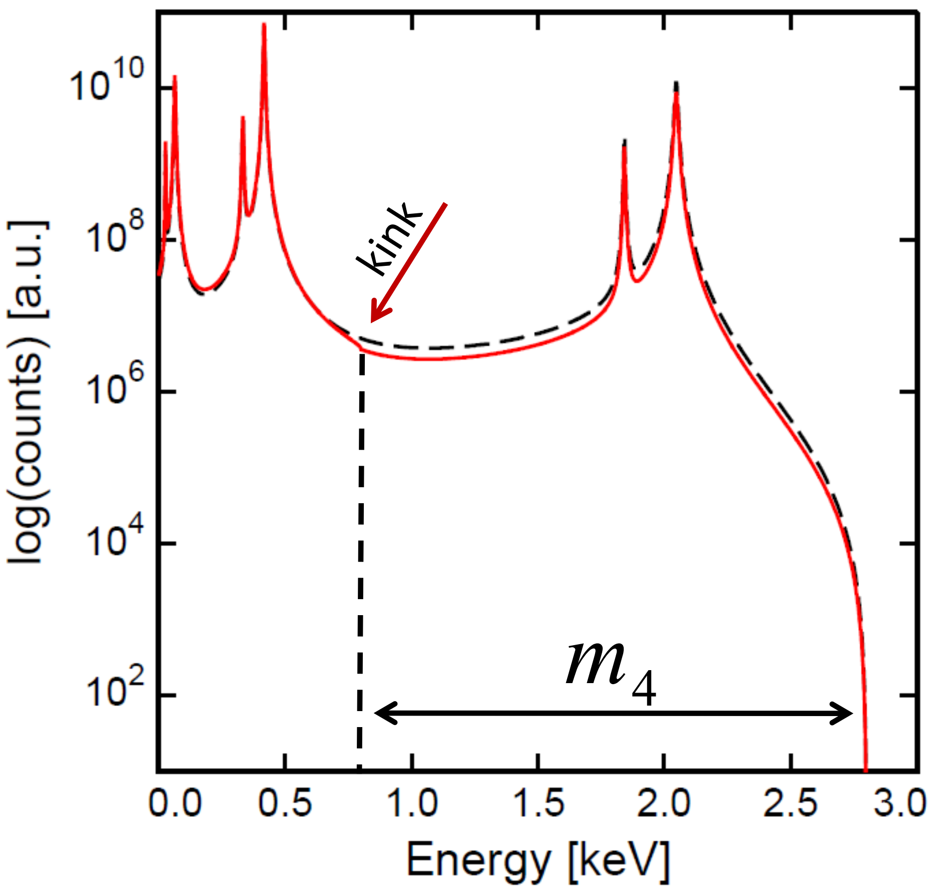

m_4=2 keV, U_{e4}^2=0.5

no sterile neutrino

- postion of kink => m_4
- depth of kink => $|U_{e4}|^2$

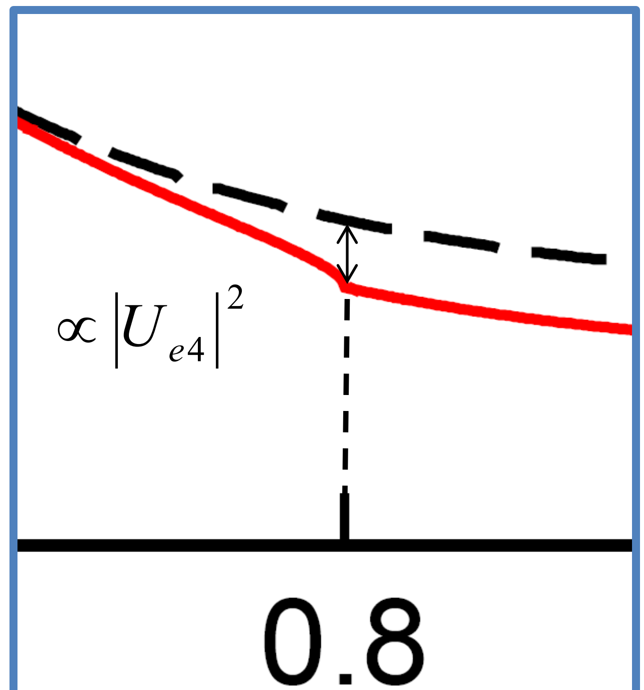

keV-scale sterile neutrino

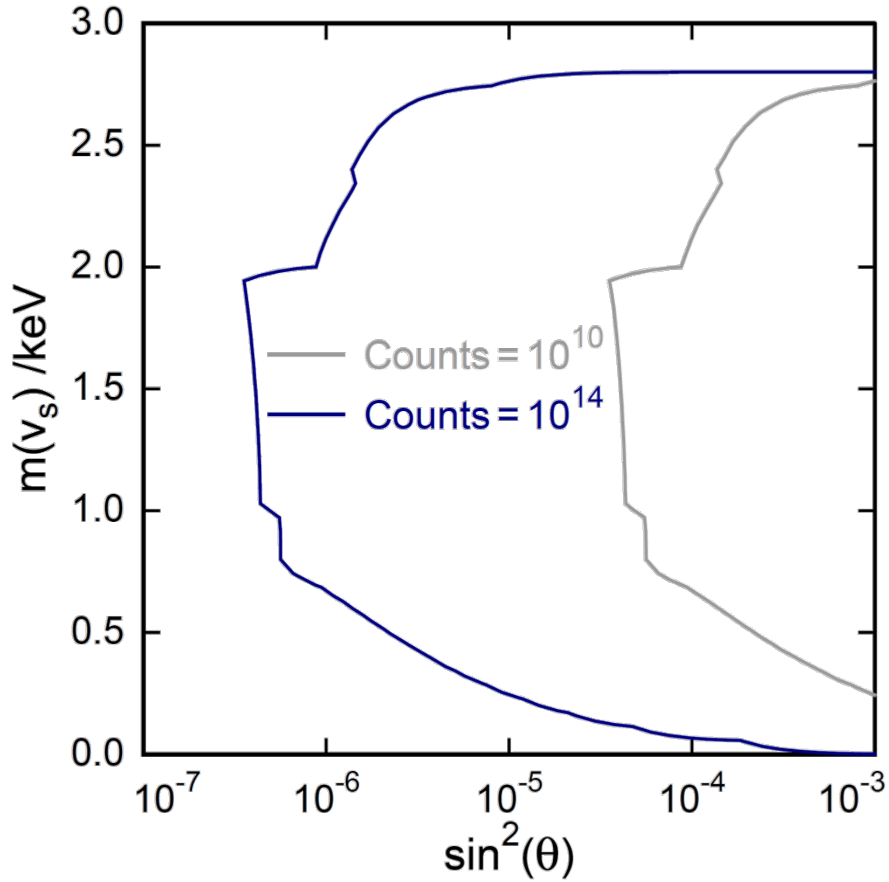

- Statistical Fluctuation
- No Pile Up
- Theoretical Spectrum supposed to be perfectly known

A White Paper on keV Sterile Neutrino Dark Matter arXiv:1602.04816v1

Sterile Neutrino (keV) and Electron Capture

Other condidates in the EC branch:

- Q_{EC} < 100 keV
- Reasonable halflife

Nuclide	$T_{1/2}$	EC-transition	Q (keV) [22]	B_i (keV) [23]	B_j (keV) [23]	$\lvert\psi_i\rvert^2/\lvert\psi_j\rvert^2$	$Q-B_i$ (keV)
^{123}Te	$>2\cdot10^{15}$ y	?	52.7(16)	K: 30.4912(3)	L_I: 4.9392(3)	7.833	22.2
^{157}Tb	71 y	$3/2^+\to3/2^-$	60.04(30)	K: 50.2391(5)	L_I: 8.3756(5)	7.124	9.76
^{163}Ho	4570 y	$7/2^-\to5/2^-$	2.555(16)	M_I: 2.0468(5)	N_I: 0.4163(5)	4.151	0.51
^{179}Ta	1.82 y	$7/2^+\to9/2^+$	105.6(4)	K: 65.3508(6)	L_I: 11.2707(4)	6.711	40.2
^{193}Pt	50 y	$1/2^-\to3/2^+$	56.63(30)	L_I: 13.4185(3)	M_I: 3.1737(17)	4.077	43.2
^{202}Pb	52 ky	$0^+\to2^-$	46(14)	L_I: 15.3467(4)	M_I: 3.7041(4)	4.036	30.7
^{205}Pb	13 My	$5/2^-\to1/2^+$	50.6(5)	L_I: 15.3467(4)	M_I: 3.7041(4)	4.036	35.3
^{235}Np	396 d	$5/2^+\to7/2^-$	124.2(9)	K: 115.6061(16)	L_I: 21.7574(3)	5.587	8.6

P. Filianin et al., *J. Phys. G: Nucl. Part. Phys.* **41** (2014) 095004

Sterile Neutrino (keV) and Electron Capture

Other condidates in the EC branch:

- Q_{EC} < 100 keV
- Reasonable halflife

Nuclide	$T_{1/2}$	EC-transition	Q (keV) [22]	B_i (keV) [23]	B_j (keV) [23]	$\lvert\psi_i\rvert^2/\lvert\psi_j\rvert^2$	$Q-B_i$ (keV)
^{123}Te	$>2\cdot10^{15}$ y	?	52.7(16)	K: 30.4912(3)	L_I: 4.9392(3)	7.833	22.2
^{157}Tb	71 y	$3/2^+\to3/2^-$	60.04(30)	K: 50.2391(5)	L_I: 8.3756(5)	7.124	9.76
^{163}Ho	4570 y	$7/2^-\to5/2^-$	2.555(16)	M_I: 2.0468(5)	N_I: 0.4163(5)	4.151	0.51
^{179}Ta	1.82 y	$7/2^+\to9/2^+$	105.6(4)	K: 65.3508(6)	L_I: 11.2707(4)	6.711	40.2
^{193}Pt	50 y	$1/2^-\to3/2^+$	56.63(30)	L_I: 13.4185(3)	M_I: 3.1737(17)	4.077	43.2
^{202}Pb	52 ky	$0^+\to2^-$	46(14)	L_I: 15.3467(4)	M_I: 3.7041(4)	4.036	30.7
^{205}Pb	13 My	$5/2^-\to1/2^+$	50.6(5)	L_I: 15.3467(4)	M_I: 3.7041(4)	4.036	35.3
^{235}Np	396 d	$5/2^+\to7/2^-$	124.2(9)	K: 115.6061(16)	L_I: 21.7574(3)	5.587	8.6

P. Filianin et al., *J. Phys. G: Nucl. Part. Phys.* **41** (2014) 095004

Sterile Neutrino (keV) and Electron Capture

Other condidates in the EC branch:

- Q_{EC} < 100 keV
- Reasonable halflife

Nuclide	$T_{1/2}$	EC-transition	Q (keV) [22]	B_i (keV) [23]	B_j (keV) [23]	$\lvert\psi_i\rvert^2/\lvert\psi_j\rvert^2$	Q–B_i (keV)
^{123}Te	$>2\cdot10^{15}$ y	?	52.7(16)	K: 30.4912(3)	L_I: 4.9392(3)	7.833	22.2
^{157}Tb	71 y	$3/2^+\rightarrow3/2^-$	60.04(30)	K: 50.2391(5)	L_I: 8.3756(5)	7.124	9.76
^{163}Ho	4570 y	$7/2^-\rightarrow5/2^-$	2.555(16)	M_I: 2.0468(5)	N_I: 0.4163(5)	4.151	0.51
^{179}Ta	1.82 y	$7/2^+\rightarrow9/2^+$	105.6(4)	K: 65.3508(6)	L_I: 11.2707(4)	6.711	40.2
^{193}Pt	50 y	$1/2^-\rightarrow3/2^+$	56.63(30)	L_I: 13.4185(3)	M_I: 3.1737(17)	4.077	43.2
^{202}Pb	52 ky	$0^+\rightarrow2^-$	46(14)	L_I: 15.3467(4)	M_I: 3.7041(4)	4.036	30.7
^{205}Pb	13 My	$5/2^-\rightarrow1/2^+$	50.6(5)	L_I: 15.3467(4)	M_I: 3.7041(4)	4.036	35.3
^{235}Np	396 d	$5/2^+\rightarrow7/2^-$	124.2(9)	K: 115.6061(16)	L_I: 21.7574(3)	5.587	8.6

P. Filianin et al., *J. Phys. G: Nucl. Part. Phys.* **41** (2014) 095004

Sterile Neutrino (keV) and Electron Capture

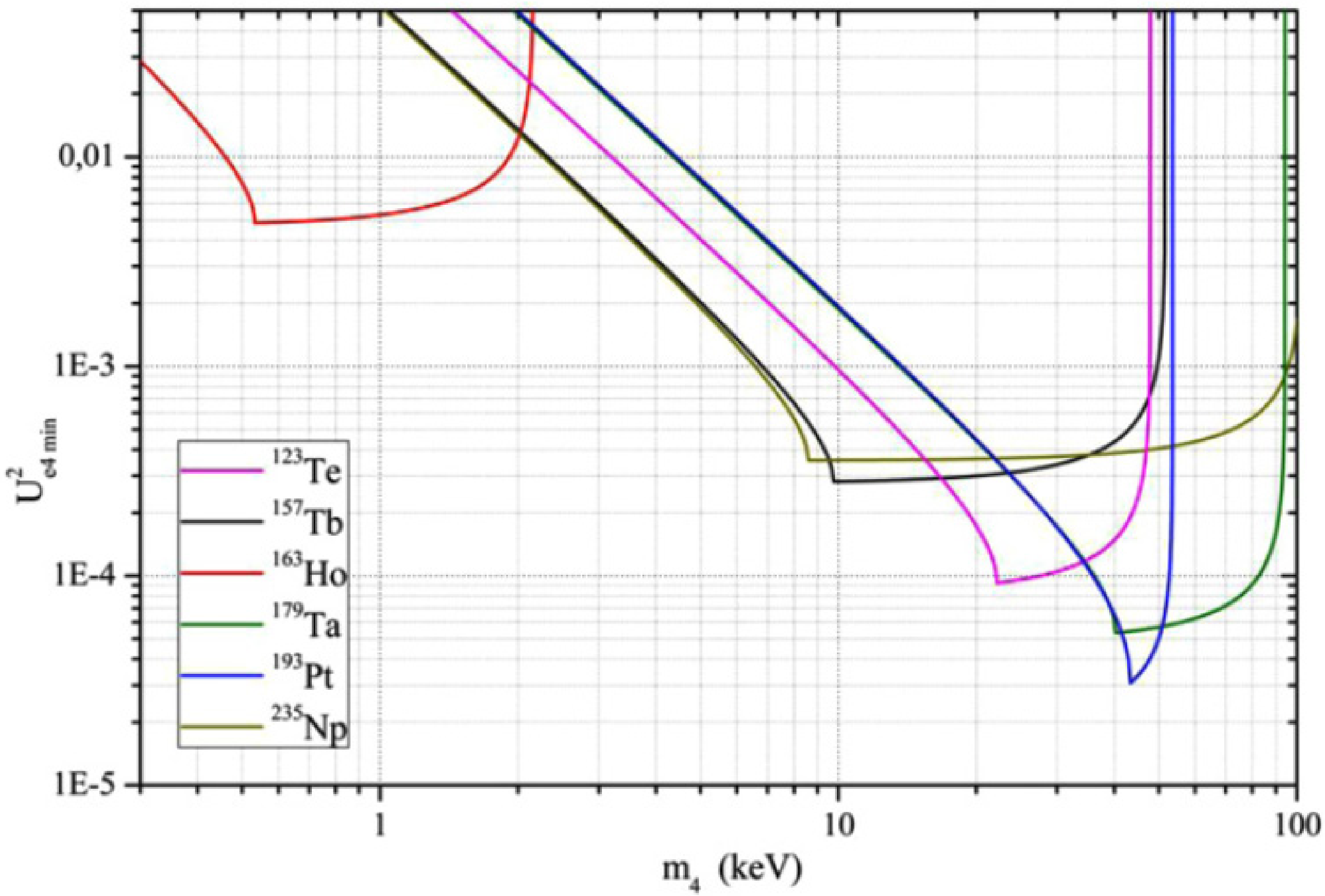

Same statistics + including errors : ($\delta\ \psi_{i,j} = 0$) $\delta Q_{EC} = 1$ eV $\delta E_{i,j} = 0.1$ eV.

P. Filianin et al., *J. Phys. G: Nucl. Part. Phys.* **41** (2014) 095004

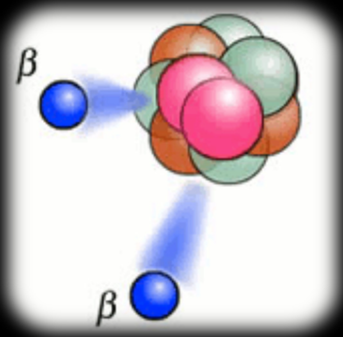

Neutrinoless double beta decay

Neutrinoless double beta decay

If conservation rules don´t allow simple beta decay:

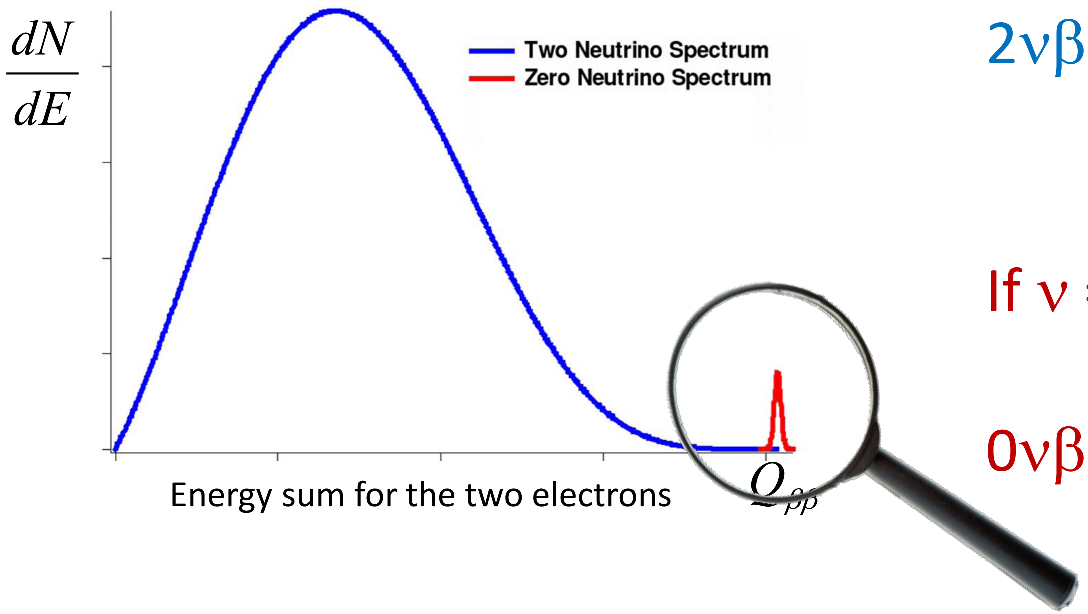

$2\nu\beta\beta$: (A,Z) → (A, Z+2) + $2e^-$ + $2\overline{\nu}_e$

$\tau_{1/2} \approx 10^{20}$ years

If $\nu = \overline{\nu}$:

$0\nu\beta\beta$: (A,Z) → (A, Z+2) + $2e^-$

$\tau_{1/2} > 10^{25}$ years

Neutrinoless double beta decay

If conservation rules don´t allow simple beta decay:

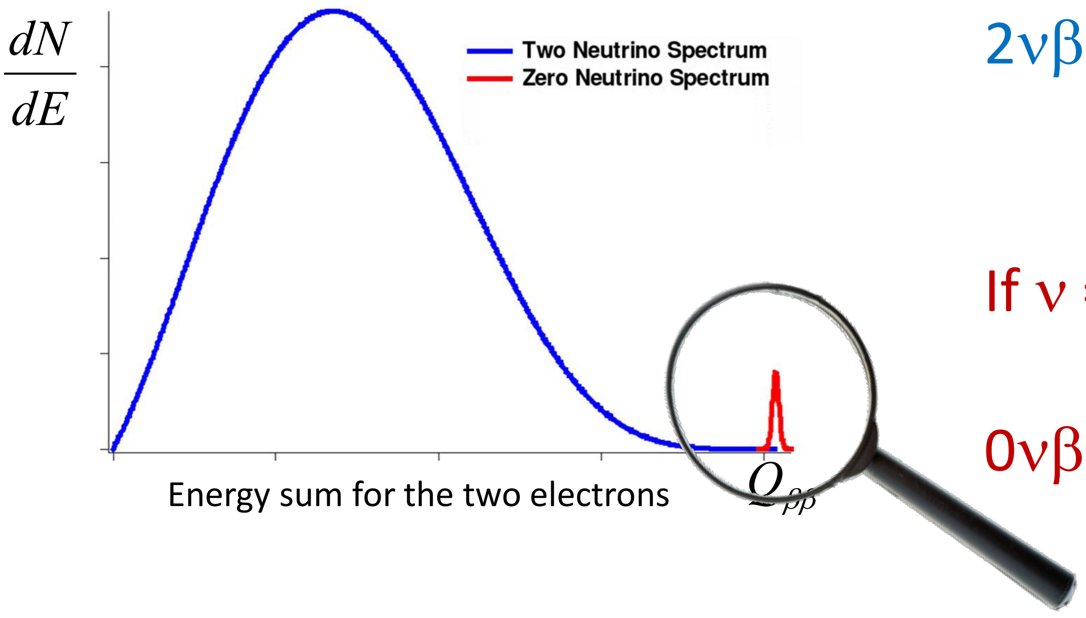

$2\nu\beta\beta$: (A,Z) → (A, Z+2) + $2e^-$ + $2\overline{\nu}_e$

$\tau_{1/2} \approx 10^{20}$ years

If $\nu = \overline{\nu}$:

$0\nu\beta\beta$: (A,Z) → (A, Z+2) + $2e^-$

$\tau_{1/2} > 10^{25}$ years

Very rare events!

Neutrinoless double beta decay - ν mass

The halflife for 0ν2β decay depends on the neutrino mass

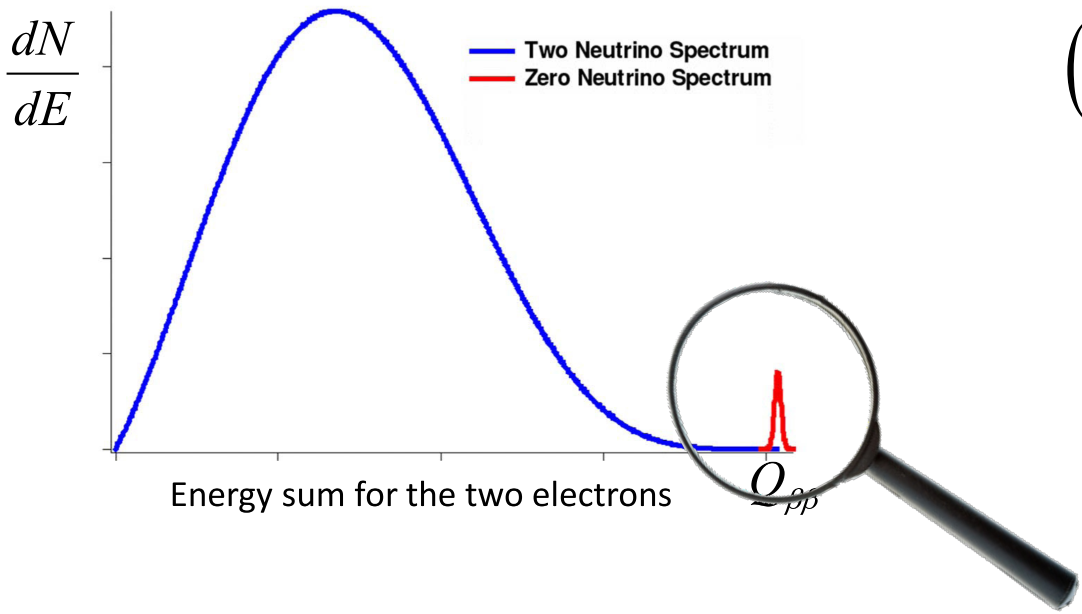

Nuclear matrix element

Phase space term

$$\left(\tau_{1/2}^{0\nu}\right)^{-1} = \left|\frac{m_{\beta\beta}}{m_e}\right|^2 \left|M_\nu^{0\nu}\right|^2 G^{0\nu}$$

$$m_{\beta\beta}^2 = \left|\sum U_{ei}^2 m(\nu_i)\right|^2$$

Neutrinoless double beta decay - ν mass

The halflife for 0ν2β decay depends on the neutrino mass

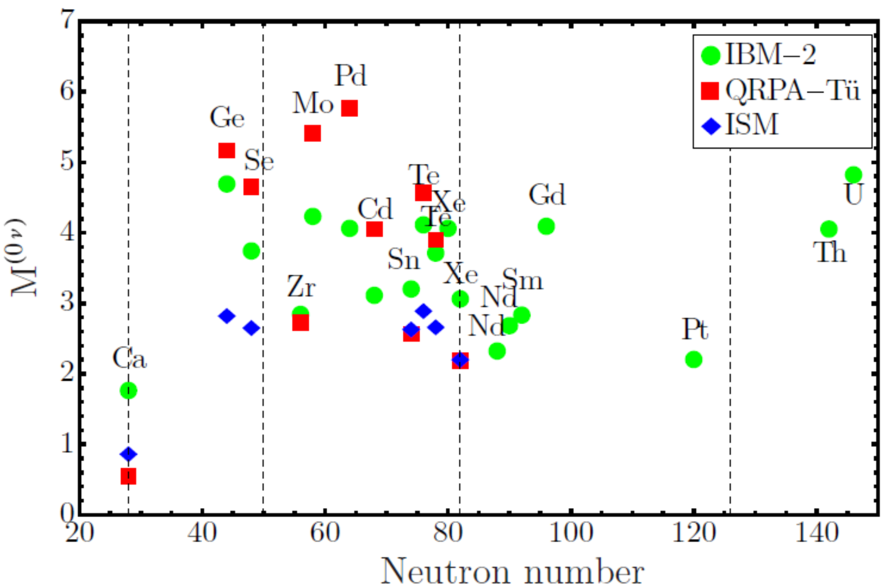

F. Iachello et al., PoS(NEUTEL2015)047

Phase space term

Nuclear matrix element

$$\left(\tau_{1/2}^{0\nu}\right)^{-1} = \left|\frac{m_{\beta\beta}}{m_e}\right|^2 \left|M_\nu^{0\nu}\right|^2 G^{0\nu}$$

$$m_{\beta\beta}^2 = \left|\sum U_{ei}^2 m(\nu_i)\right|^2$$

Uncertainties to evaluate the effective Majorana mass due to:

- Nuclear matrix element

QRPA-Tu: F. Simkovic *et al.*, **Phys. Rev. C 87, 045501 (2013)**
pnQRPA: J. Hyvarinen *et al.*, **Phys. Rev. C 91, 024613 (2015)**
IBM-2: J. Barea *et al.*, **Phys. Rev. C 91, 034304 (2015)**
ISM: J. Menendez *et al.*, **Nucl. Phys. A 818, 139 (2009)**

Present status

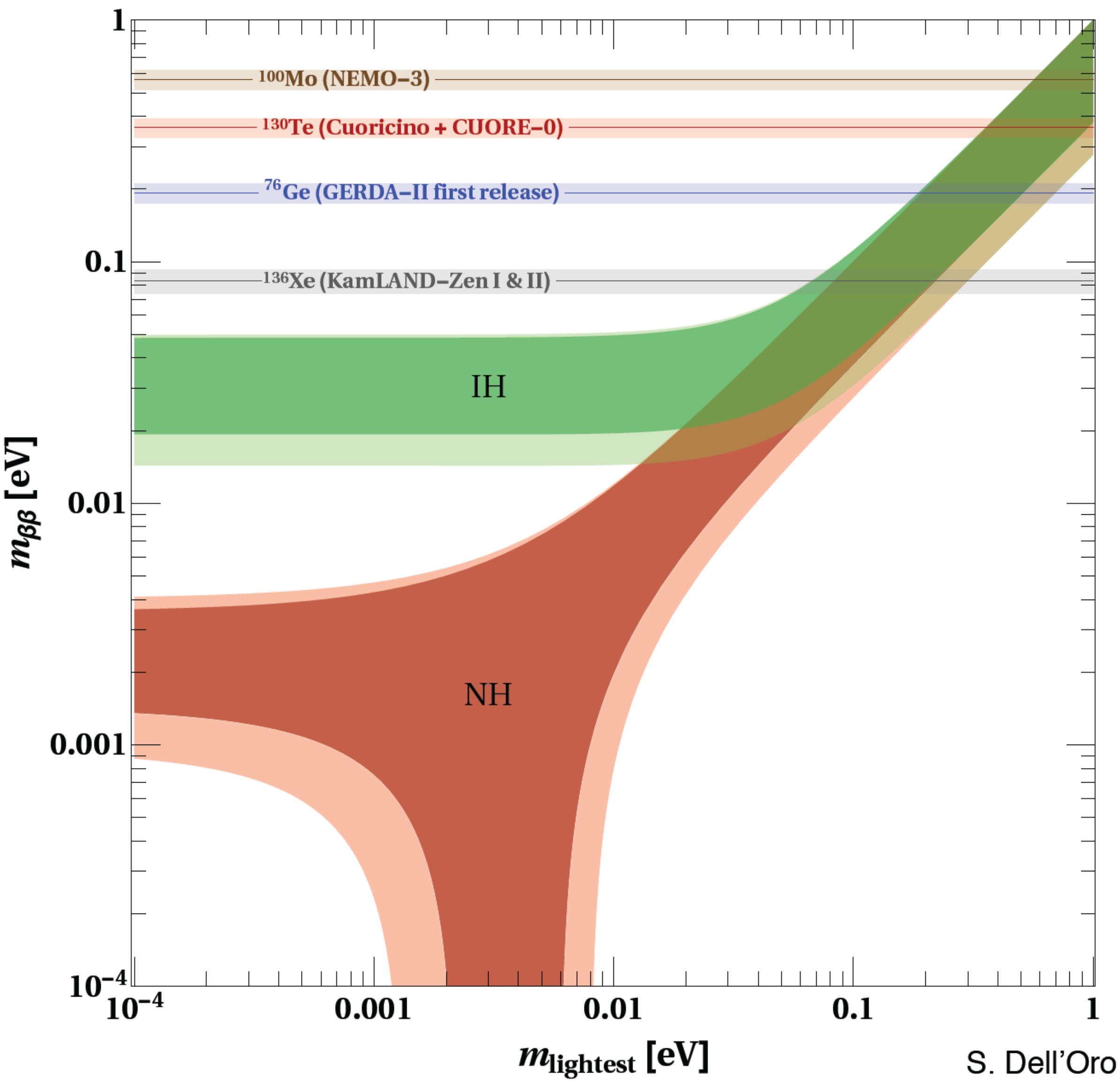

S. Dell'Oro,

Neutrinoless double beta decay - sensitivity

Typically an excess of events is not found…

A limit on the halflife for 0ν2e decay can be defined as function of:

Mass of the isotope	***M***	[kg]	Exposure $M \times T$	[kg × year]
Measuring time	***T***	[year]		
Energy resolution	***ΔE***	[keV]		
Background index	***b***	[$keV^{-1}ton^{-1}year^{-1}$]		

Two limits defined by the background index

> 1 background events in ROI

$$\left(\tau_{1/2}^{\exp}\right)^{-1} = (\ln 2) N_a \frac{a}{A} \varepsilon \sqrt{\frac{MT}{b \Delta E}}$$

<1 background events in ROI

$$\left(\tau_{1/2}^{\exp}\right)^{-1} = (\ln 2) N_a \frac{a}{A} \varepsilon \frac{MT}{n_{CL}}$$

Neutrinoless double beta decay - nuclides

Is there a prefered nuclide?

$$\left(\tau_{1/2}^{\exp}\right)^{-1} = (\ln 2) N_a \frac{a}{A} \varepsilon \sqrt{\frac{MT}{b \Delta E}}$$

transition	$G^{01}(E_0, Z)$ $\times 10^{14} y$	$Q_{\beta\beta}$ [MeV]	Abund. (%)
$^{150}Nd \to {}^{150}Sm$	26.9	3.667	6
$^{48}Ca \to {}^{48}Ti$	8.04	4.271	0.2
$^{96}Zr \to {}^{96}Mo$	7.37	3.350	3
$^{116}Cd \to {}^{116}Sn$	6.24	2.802	7
$^{136}Xe \to {}^{136}Ba$	5.92	2.479	9
$^{100}Mo \to {}^{100}Ru$	5.74	3.034	10
$^{130}Te \to {}^{130}Xe$	5.55	2.533	34
$^{82}Se \to {}^{82}Kr$	3.53	2.995	9
$^{76}Ge \to {}^{76}Se$	0.79	2.040	8

Neutrinoless double beta decay - nuclides

Is there a prefered nuclide?

$$\left(\tau_{1/2}^{\exp}\right)^{-1} = (\ln 2) N_a \frac{a}{A} \varepsilon \sqrt{\frac{MT}{b \Delta E}}$$

transition	$G^{01}(E_0, Z)$ $\times 10^{14} y$	$Q_{\beta\beta}$ [MeV]	Abund. (%)
$^{150}Nd \rightarrow {}^{150}Sm$	26.9	3.667	6
$^{48}Ca \rightarrow {}^{48}Ti$	8.04	4.271	0.2
$^{96}Zr \rightarrow {}^{96}Mo$	7.37	3.350	3
$^{116}Cd \rightarrow {}^{116}Sn$	6.24	2.802	7
$^{136}Xe \rightarrow {}^{136}Ba$	5.92	2.479	9
$^{100}Mo \rightarrow {}^{100}Ru$	5.74	3.034	10
$^{130}Te \rightarrow {}^{130}Xe$	5.55	2.533	34
$^{82}Se \rightarrow {}^{82}Kr$	3.53	2.995	9
$^{76}Ge \rightarrow {}^{76}Se$	0.79	2.040	8

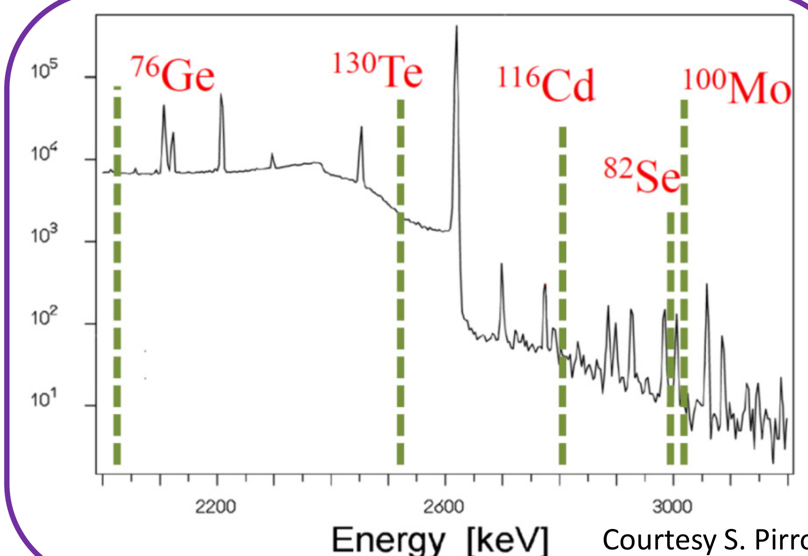

Courtesy S. Pirro

Neutrinoless double beta decay - nuclides

Is there a prefered nuclide?

$$\left(\tau_{1/2}^{\exp}\right)^{-1} = (\ln 2) N_a \frac{a}{A} \varepsilon \sqrt{\frac{MT}{b \Delta E}}$$

transition	$G^{01}(E_0, Z)$ $\times 10^{14} y$	$Q_{\beta\beta}$ [MeV]	Abund. (%)
$^{150}Nd \rightarrow {}^{150}Sm$	26.9	3.667	6
$^{48}Ca \rightarrow {}^{48}Ti$	8.04	4.271	0.2
$^{96}Zr \rightarrow {}^{96}Mo$	7.37	3.350	3
$^{116}Cd \rightarrow {}^{116}Sn$	6.24	2.802	7
$^{136}Xe \rightarrow {}^{136}Ba$	5.92	2.479	9
$^{100}Mo \rightarrow {}^{100}Ru$	5.74	3.034	10
$^{130}Te \rightarrow {}^{130}Xe$	5.55	2.533	34
$^{82}Se \rightarrow {}^{82}Kr$	3.53	2.995	9
$^{76}Ge \rightarrow {}^{76}Se$	0.79	2.040	8

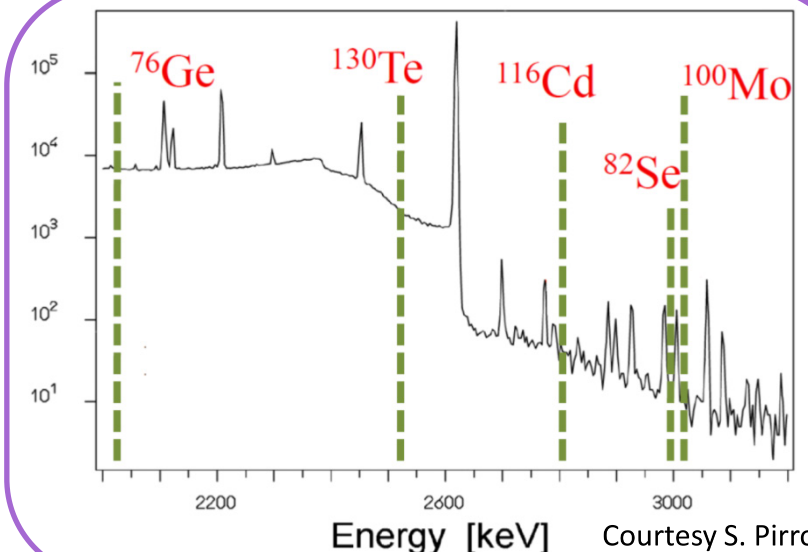

Courtesy S. Pirro

Detector Properties:
- **Efficiency**
- **Energy resolution**

Neutrinoless double beta decay - nuclides

Is there a prefered nuclide?

$$\left(\tau_{1/2}^{\exp}\right)^{-1} = (\ln 2) N_a \frac{a}{A} \varepsilon \sqrt{\frac{MT}{b \Delta E}}$$

No optimal nuclide

transition			
$^{150}Nd \rightarrow {}^{150}Sm$			
$^{48}Ca \rightarrow {}^{48}Ti$			
$^{96}Zr \rightarrow {}^{96}Mo$	7.[illegible]	3.350	3
$^{116}Cd \rightarrow {}^{116}Sn$	6.24	2.802	7
$^{136}Xe \rightarrow {}^{136}Ba$	5.92	2.479	9
$^{100}Mo \rightarrow {}^{100}Ru$	5.74	3.034	10
$^{130}Te \rightarrow {}^{130}Xe$	5.55	2.533	34
$^{82}Se \rightarrow {}^{82}Kr$	3.53	2.995	9
$^{76}Ge \rightarrow {}^{76}Se$	0.79	2.040	8

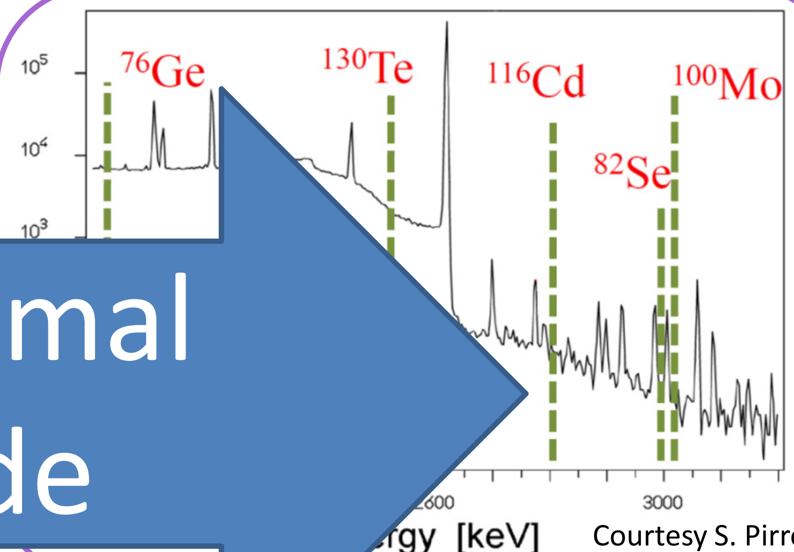

Courtesy S. Pirro

Detector Properties:

- **Efficiency**
- **Energy resolution**

Neutrinoless double beta decay - nuclides

Is there a prefered nuclide?

$$\left(\tau_{1/2}^{\exp}\right)^{-1} = (\ln 2) N_a \frac{a}{A} \varepsilon \sqrt{\frac{MT}{b \Delta E}}$$

transition	$G^{01}(E_0, Z)$ $\times 10^{14} y$	$Q_{\beta\beta}$ [MeV]	Abund. (%)
$^{150}Nd \rightarrow {}^{150}Sm$	26.9	3.667	6
$^{48}Ca \rightarrow {}^{48}Ti$	8.04	4.271	0.2
$^{96}Zr \rightarrow {}^{96}Mo$	7.37	3.350	3
$^{116}Cd \rightarrow {}^{116}Sn$	6.24	2.802	7
$^{136}Xe \rightarrow {}^{136}Ba$	5.92	2.479	9
$^{100}Mo \rightarrow {}^{100}Ru$	5.74	3.034	10
$^{130}Te \rightarrow {}^{130}Xe$	5.55	2.533	34
$^{82}Se \rightarrow {}^{82}Kr$	3.53	2.995	9
$^{76}Ge \rightarrow {}^{76}Se$	0.79	2.040	8

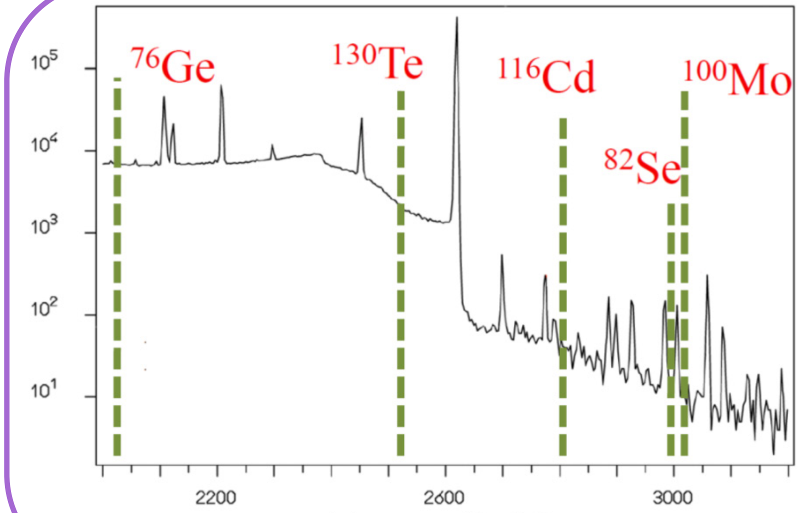

Courtesy S. Pirro

Detector Properties:

- **Efficiency**
- **Energy resolution**

Background

Many different experiments

Experiment	Isotope	Technique	Mass ββ(0v) isotope
CUORICINO	130Te	TeO2 Bolometer	10 kg
NEMO3	100Mo/82Se	Foils with tracking	6.9/0.9 kg
GERDA I	76Ge	Ge diodes in LAr	15 kg
EXO200	136Xe	Xe liquid TPC	160 kg
KamLAND-ZEN	136Xe	2.7% in liquid scint.	380 kg
CUORE-0	130Te	TeO2 Bolometer	11 kg
GERDA II	76Ge	Point contact Ge in LAr	30+35 kg
Majorana D	76Ge	Point contact Ge	30 kg
CUORE	130Te	TeO2 Bolometer	206 kg
SNO+	130Te	0.3% natTe suspended in Scint	55 kg
NEXT-100	136Xe	High pressure Xe TPC	80 kg
SuperNEMO D	82Se	Foils with tracking	7 kg
CANDLES	48Ca	305 kg of CaF2 crystals - liq. scint	0.3 kg
LUCIFER	82Se	ZnSe scint. bolometer	18 kg
1TGe (GERDA+MJ)	76Ge	Best technology from GERDA and MAJORANA	~ tonne
CUPID	-	Hybrid Bolometers	~ tonne
nEXO	136Xe	Xe liquid TPC	~ tonne
SuperNEMO	82Se	Foils with tracking	100 kg
AMoRE	100Mo	CaMoO4 scint. bolometer	50 kg
MOON	100Mo	Mo sheets	200 kg
COBRA	116Cd	CdZnTe detectors	10 kg/183 kg
CARVEL	48Ca	48CaWO4 crystal scint.	~ tonne
DCBA	150Nd	Nd foils & tracking chambers	20 kg

Best results

Promising technique

Promising technologies - Scintillating crystals

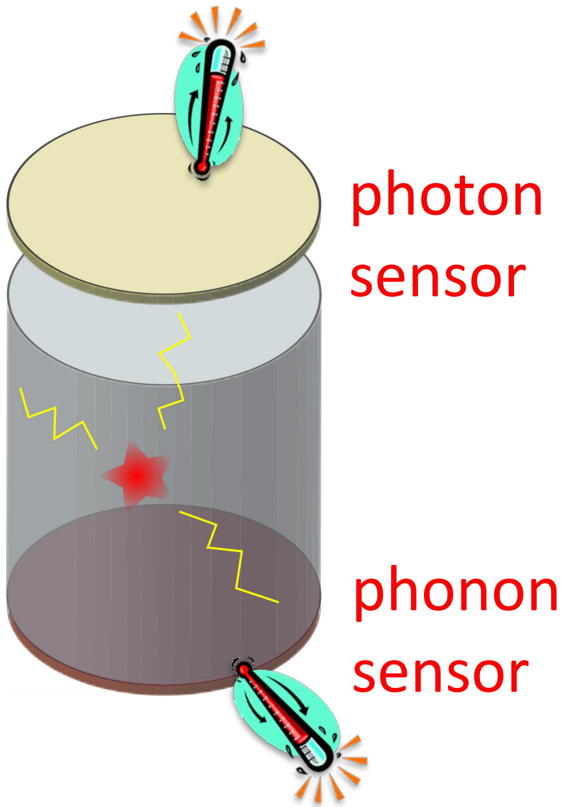

Above ground

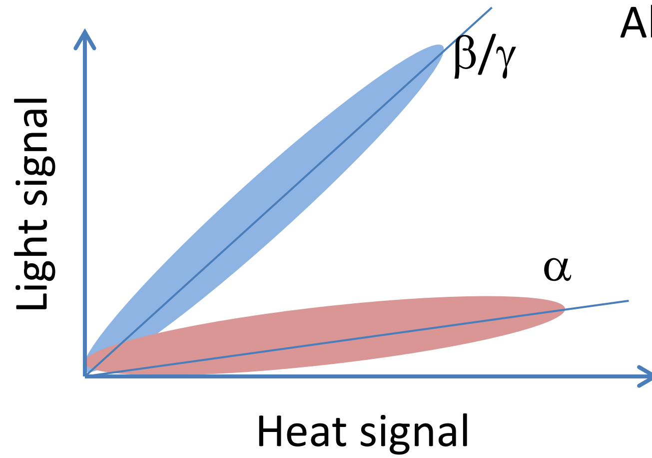

Promising technologies - Scintillating crystals

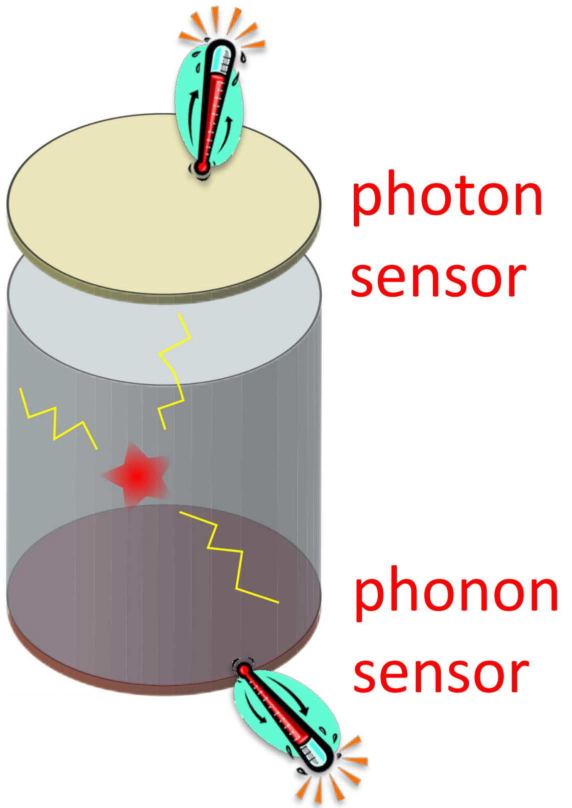

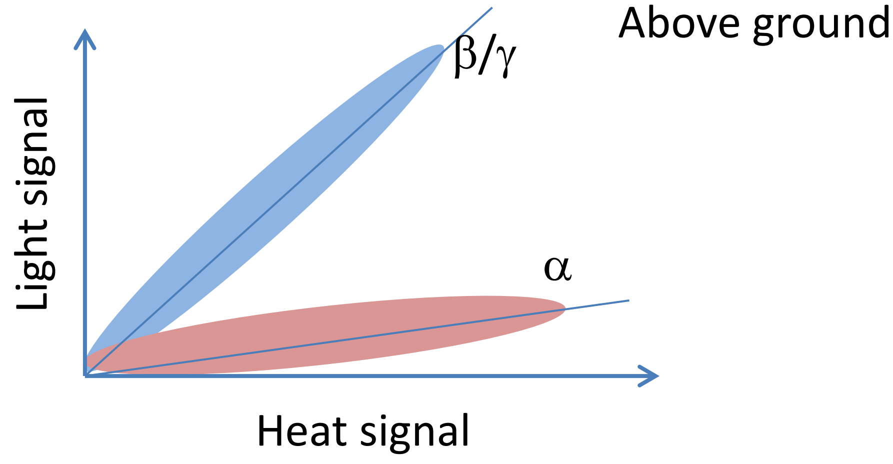

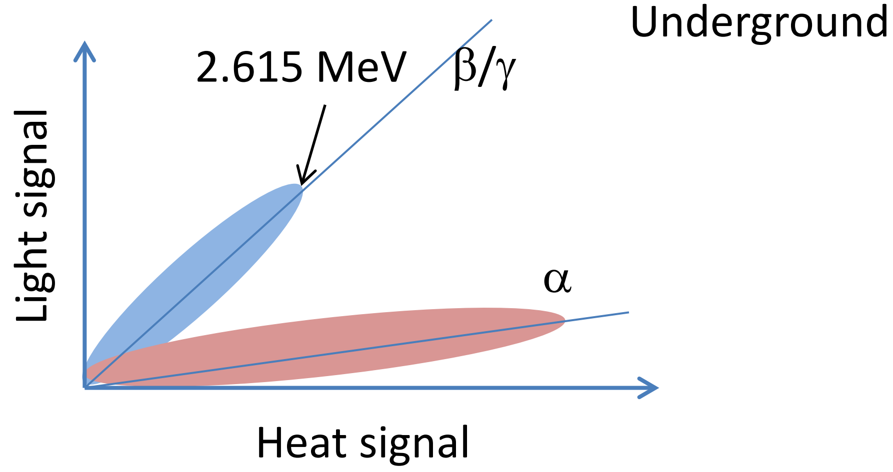

Background due to α particle can be removed

Promising technologies - Scintillating crystals

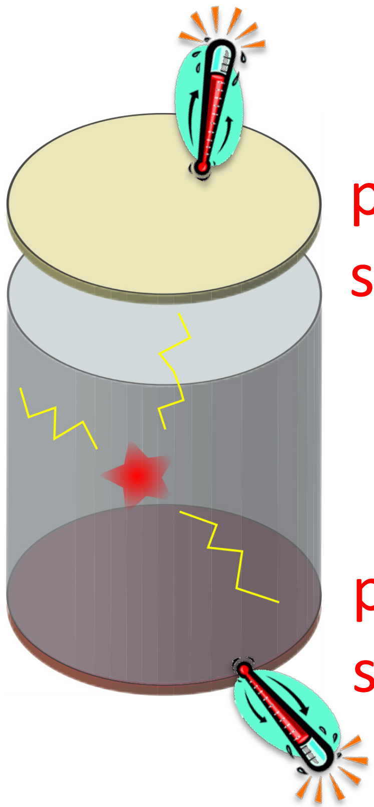

transition	$G^{01}(E_0, Z)$ $\times 10^{14} y$	$Q_{\beta\beta}$ [MeV]		Abund. (%)
$^{150}Nd \rightarrow {}^{150}Sm$	26.9	3.667	←	6
$^{48}Ca \rightarrow {}^{48}Ti$	8.04	4.271	←	0.2
$^{96}Zr \rightarrow {}^{96}Mo$	7.37	3.350	←	3
$^{116}Cd \rightarrow {}^{116}Sn$	6.24	2.802	←	7
$^{136}Xe \rightarrow {}^{136}Ba$	5.92	2.479		9
$^{100}Mo \rightarrow {}^{100}Ru$	5.74	3.034	←	10
$^{130}Te \rightarrow {}^{130}Xe$	5.55	2.533		34
$^{82}Se \rightarrow {}^{82}Kr$	3.53	2.995	←	9
$^{76}Ge \rightarrow {}^{76}Se$	0.79	2.040		8

Promising technologies - Scintillating crystals

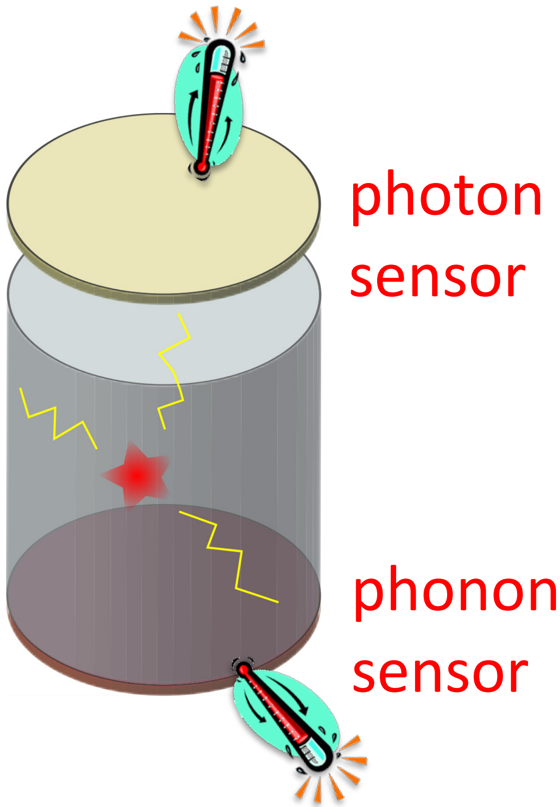

transition	$G^{01}(E_0, Z)$ $\times 10^{14} y$	$Q_{\beta\beta}$ [MeV]	Abund. (%)
$^{150}Nd \rightarrow {}^{150}Sm$	26.9	3.667	← 6
$^{48}Ca \rightarrow {}^{48}Ti$	8.04	4.271	← 0.2
$^{96}Zr \rightarrow {}^{96}Mo$	7.37	3.350	← 3
$^{116}Cd \rightarrow {}^{116}Sn$	6.24	2.802	← 7
$^{136}Xe \rightarrow {}^{136}Ba$	5.92	2.479	9
$^{100}Mo \rightarrow {}^{100}Ru$	5.74	3.034	← 10
$^{130}Te \rightarrow {}^{130}Xe$	5.55	2.533	34
$^{82}Se \rightarrow {}^{82}Kr$	3.53	2.995	← 9
$^{76}Ge \rightarrow {}^{76}Se$	0.79	2.040	8

Temperature signal: $\Delta T \cong \frac{\Delta E_{phonon}}{C}$

Light signal is also detected as $\Delta T \cong \frac{\Delta E_{photon}}{C}$ of a suitable photon detector

Promising technologies - Scintillating crystals

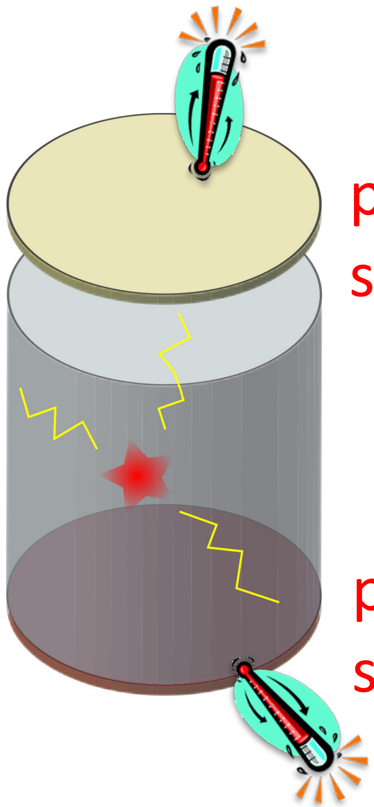

transition	$G^{01}(E_0, Z)$ $\times 10^{14} y$	$Q_{\beta\beta}$ [MeV]	Abund. (%)
$^{150}Nd \rightarrow {}^{150}Sm$	26.9	3.667 ←	6
$^{48}Ca \rightarrow {}^{48}Ti$	8.04	4.271 ←	0.2
$^{96}Zr \rightarrow {}^{96}Mo$	7.37	3.350 ←	3
$^{116}Cd \rightarrow {}^{116}Sn$	6.24	2.802 ←	7
$^{136}Xe \rightarrow {}^{136}Ba$	5.92	2.479	9
$^{100}Mo \rightarrow {}^{100}Ru$	5.74	3.034 ←	10
$^{130}Te \rightarrow {}^{130}Xe$	5.55	2.533	34
$^{82}Se \rightarrow {}^{82}Kr$	3.53	2.995 ←	9
$^{76}Ge \rightarrow {}^{76}Se$	0.79	2.040	8

Low T thermal detectors are the best candidate for these measurements

^{100}Mo-based experiments

$$^{100}Mo \rightarrow {}^{100}Ru + 2e^- + (2\nu_e) \quad T_{1/2} = [7.15 \pm 0.37\,(\mathrm{stat}) \pm 0.66\,(\mathrm{syst})] \times 10^{18}\ \mathrm{y}$$

$$Q_{\beta\beta} = 3034\ \mathrm{keV}$$

L. Cardani et al., J. Phys. G: Nucl. Part. Phys. 41 (2014) 075204

LUCIFER

Different scintillating crystals coupled to NTD_Ge

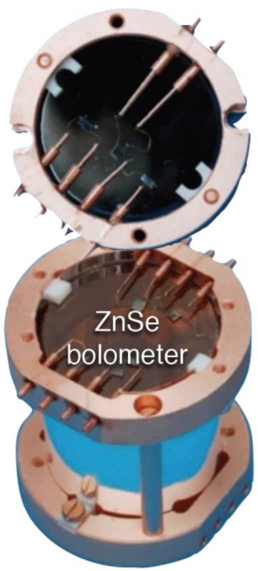

LUCIFER, http://arxiv.org/abs/1303.4080
JINST 8 (2013) P05021

LUMINEU

$ZnMoO_4$, $LiMoO_4$

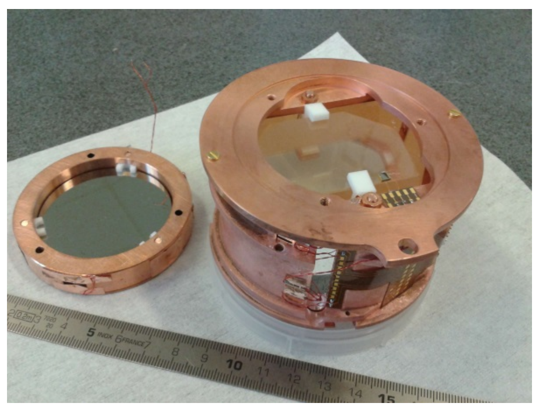

NTD-Ge baseline for photon and phonon channel
MMC R&D for photon channel

LUMINEU arXiv:1704.01758
Submitted to EPJC

AMoRE

$CaMoO_4$

- SB28 weight 196 g
- SB29 weight 390 g
- S35 weight ~300 g

MMC for photon and phonon channel

Technical Design Report for the AMoRE 0νββ Decay Search Experiment
arXiv:1512.05957 [physics.ins-det]

^{100}Mo-based experiments

$$^{100}Mo \rightarrow ^{100}Ru + 2e^- + (2\nu_e) \quad T_{1/2} = [7.15 \pm 0.37\,(\text{stat}) \pm 0.66\,(\text{syst})] \times 10^{18}\ \text{y}$$

$$Q_{\beta\beta} = 3034\ \text{keV}$$

L. Cardani et al., J. Phys. G: Nucl. Part. Phys. 41 (2014) 075204

R&D phases succesfully concluded
Starting of I phase experiments

LUCIFER

Different scintillating crystals coupled to NTD_Ge

LUCIFER, http://arxiv.org/abs/1303.4080
JINST 8 (2013) P05021

LUMINEU

$ZnMoO_4$, $LiMoO_4$

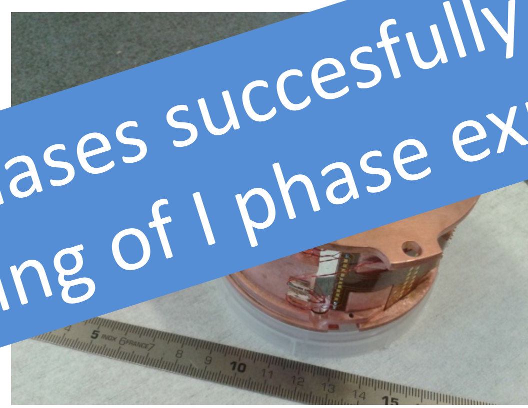

NTD-Ge baseline for photon and phonon channel
MMC R&D for photon channel

LUMINEU arXiv:1704.01758
Submitted to EPJC

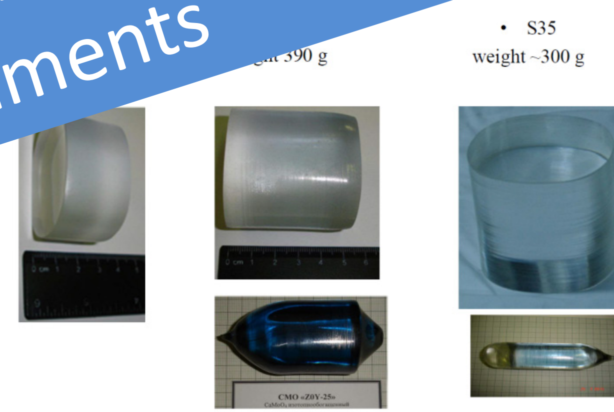

MMC for photon and phonon channel

Technical Design Report for the AMoRE 0νββ Decay Search Experiment
arXiv:1512.05957 [physics.ins-det]

Approach used in AMoRe

Technical Design Report for the
AMoRE $0\nu\beta\beta$ Decay Search Experiment
arXiv:1512.05957 [physics.ins-det]

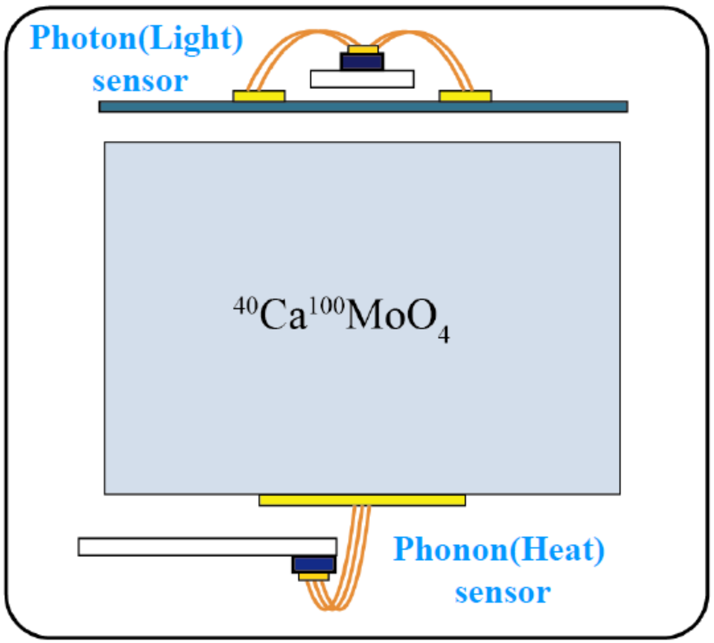

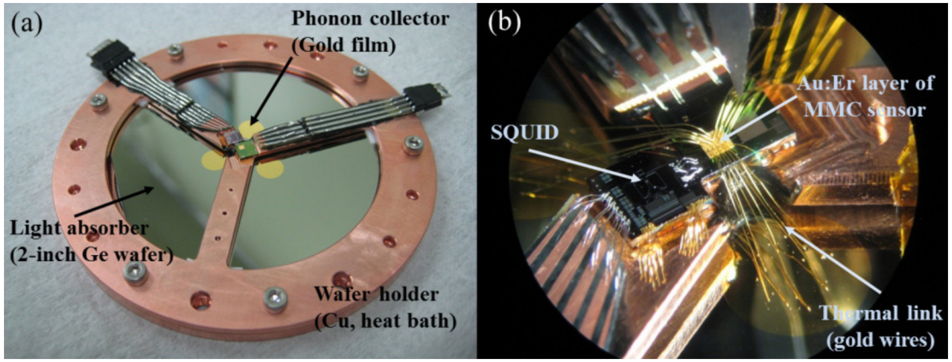

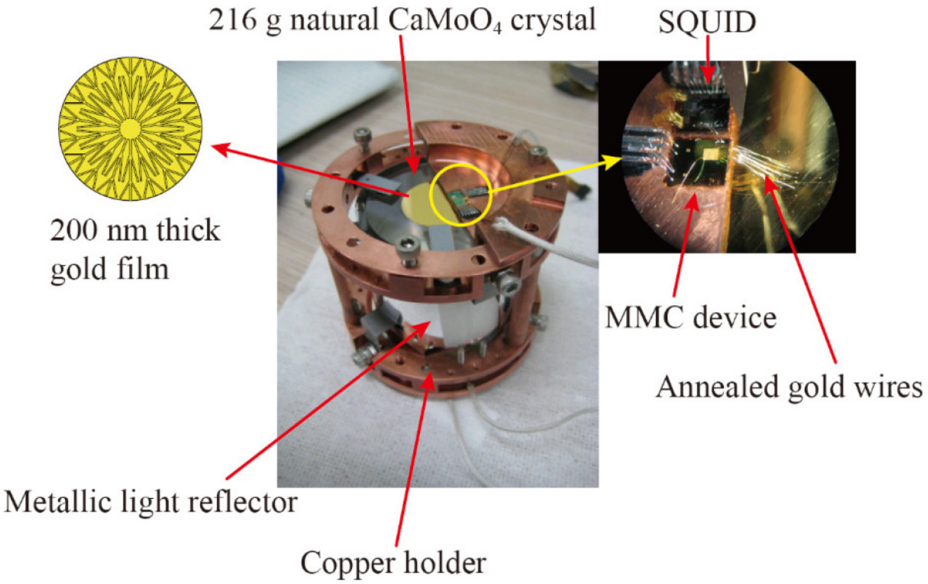

Approach used in AMoRe

Technical Design Report for the
AMoRE 0νββ Decay Search Experiment
arXiv:1512.05957 [physics.ins-det]

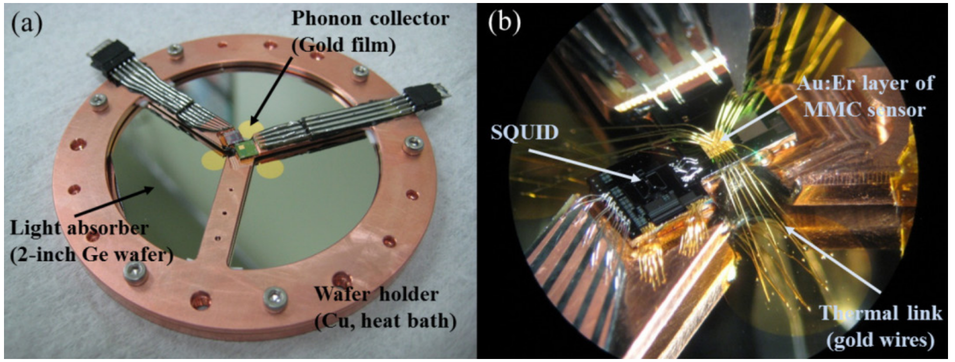

545 eV @ 6 keV

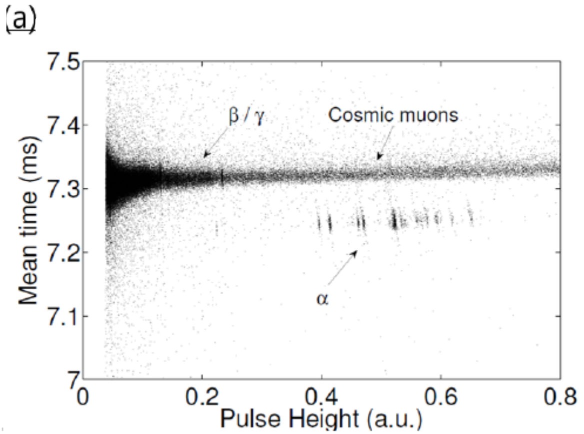

11 keV @ 2615 keV
6.5 keV @ 583 keV

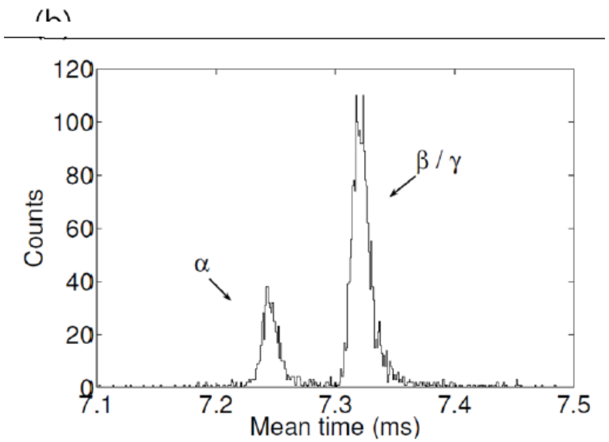

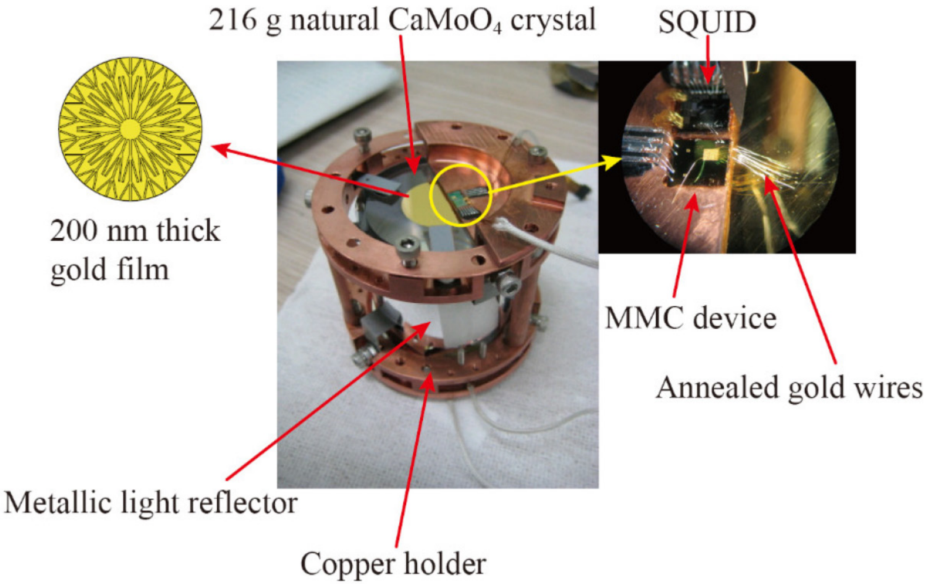

Combined Photon and Phonon Detector: P2

- Phonon detector:
  - energy resolution $\Delta E_{FWHM} < 100$ eV
  - rise time $\tau < 200$ µs
- Photon detector:
  - energy resolution $\Delta E_{FWHM} < 10$ eV
  - rise time $\tau < 50$ µs

Substrate: Ge or Si 3'' wafer

- A minimum of (contaminated?) parts
- Position sensitivity possible

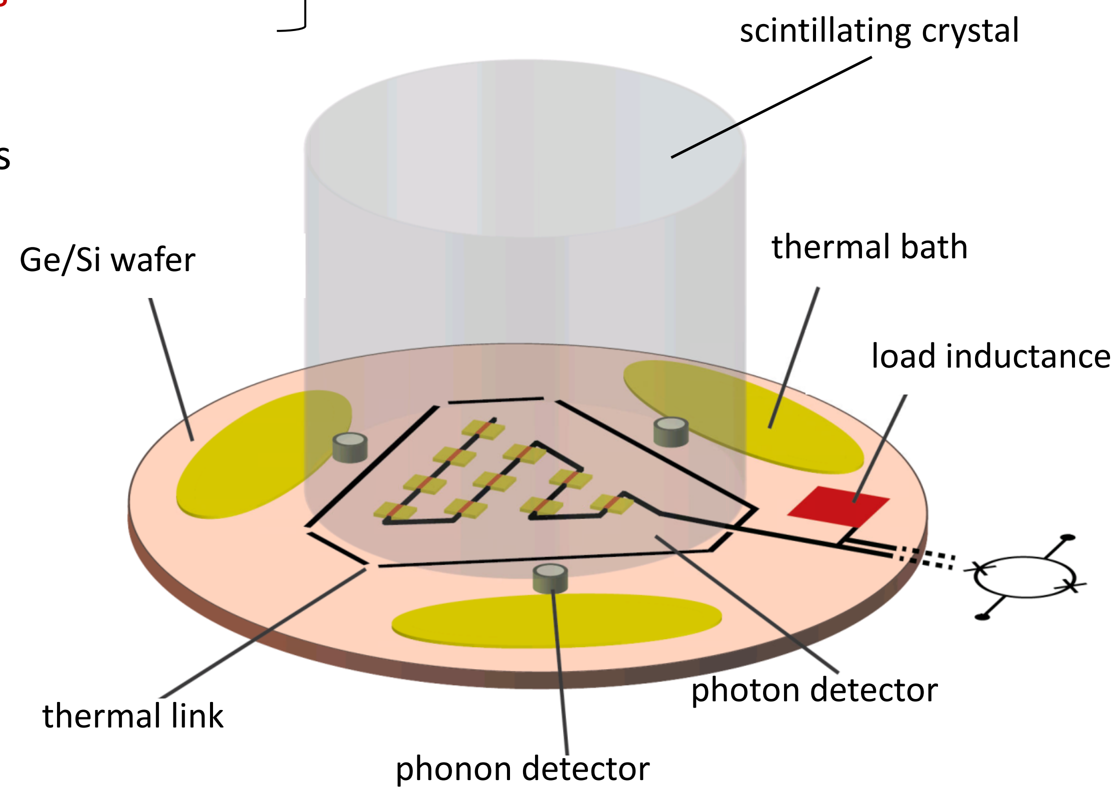

Combined photon and phonon detector: P2

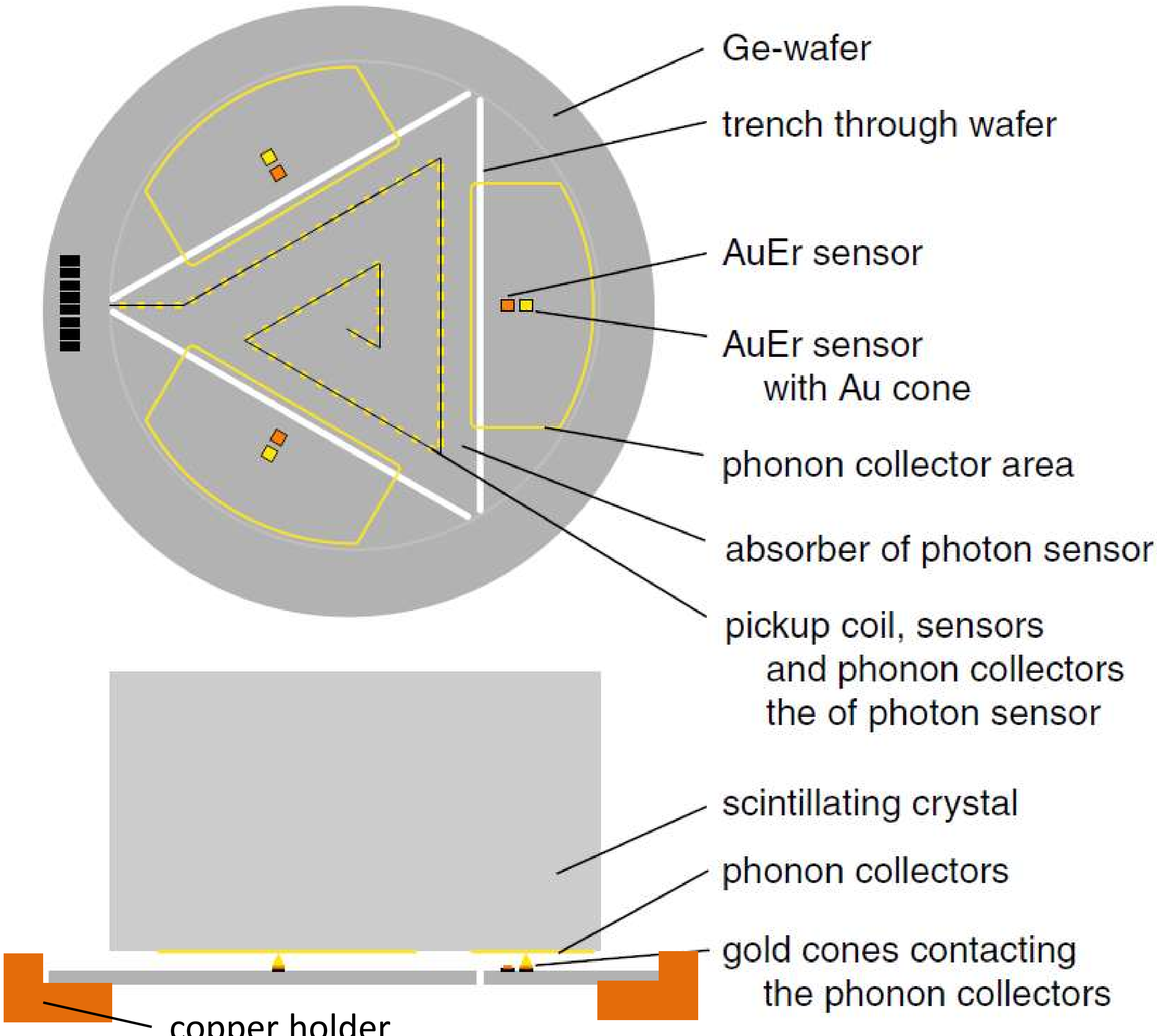

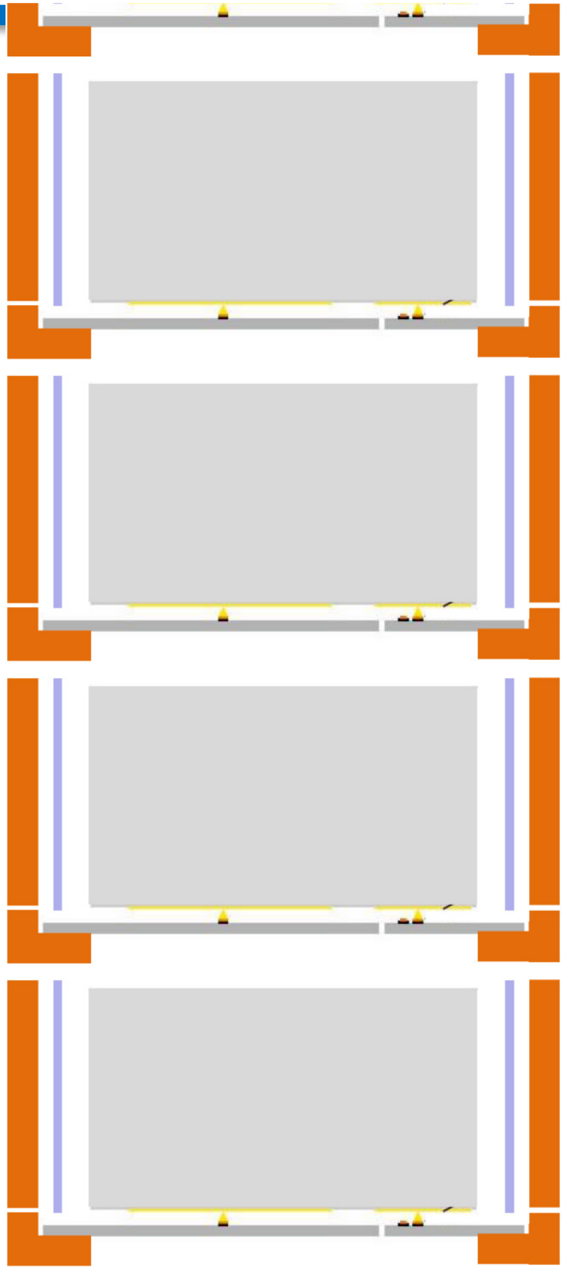

Integrated light and heat detectors P2

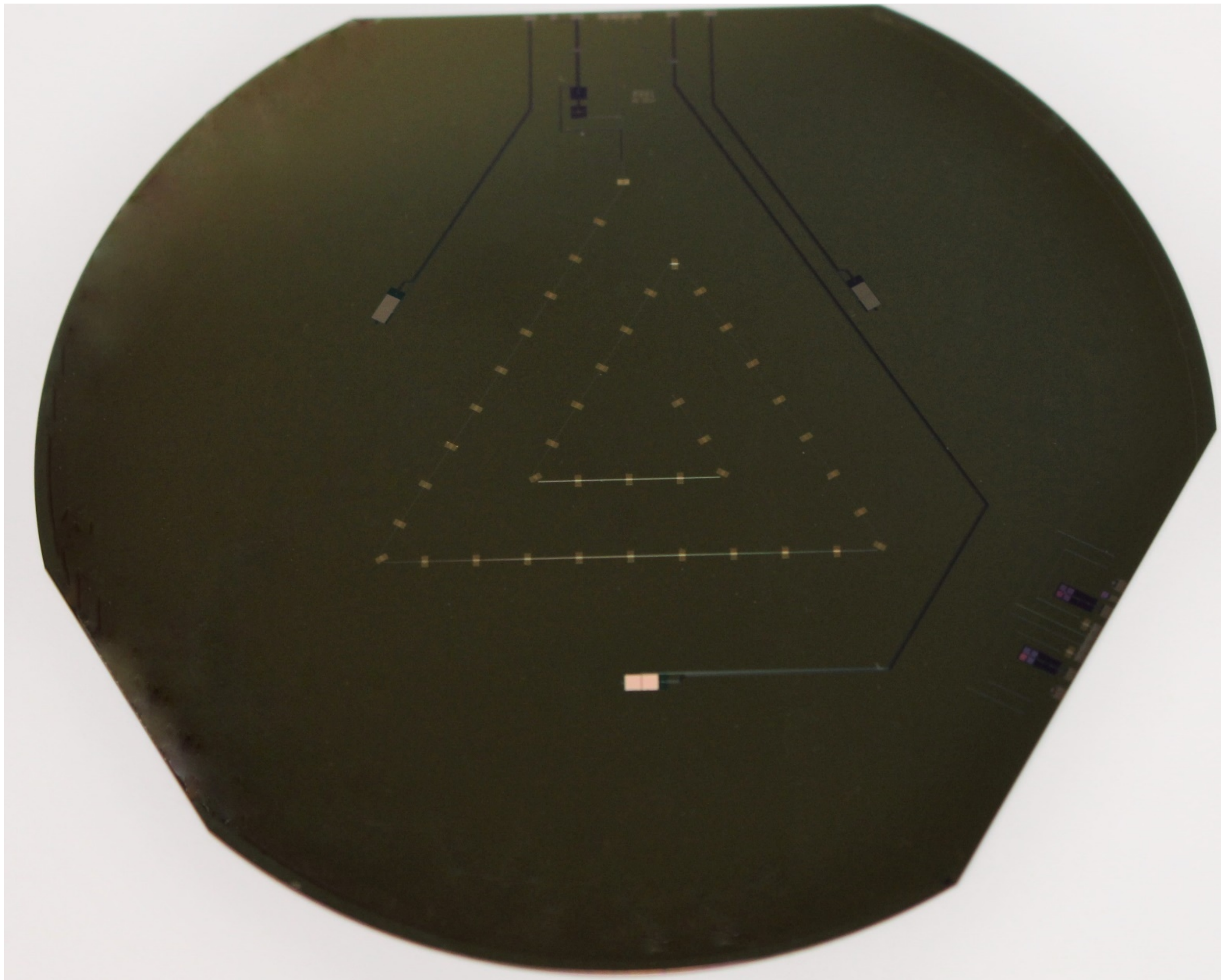

Integrated light and heat detectors P2

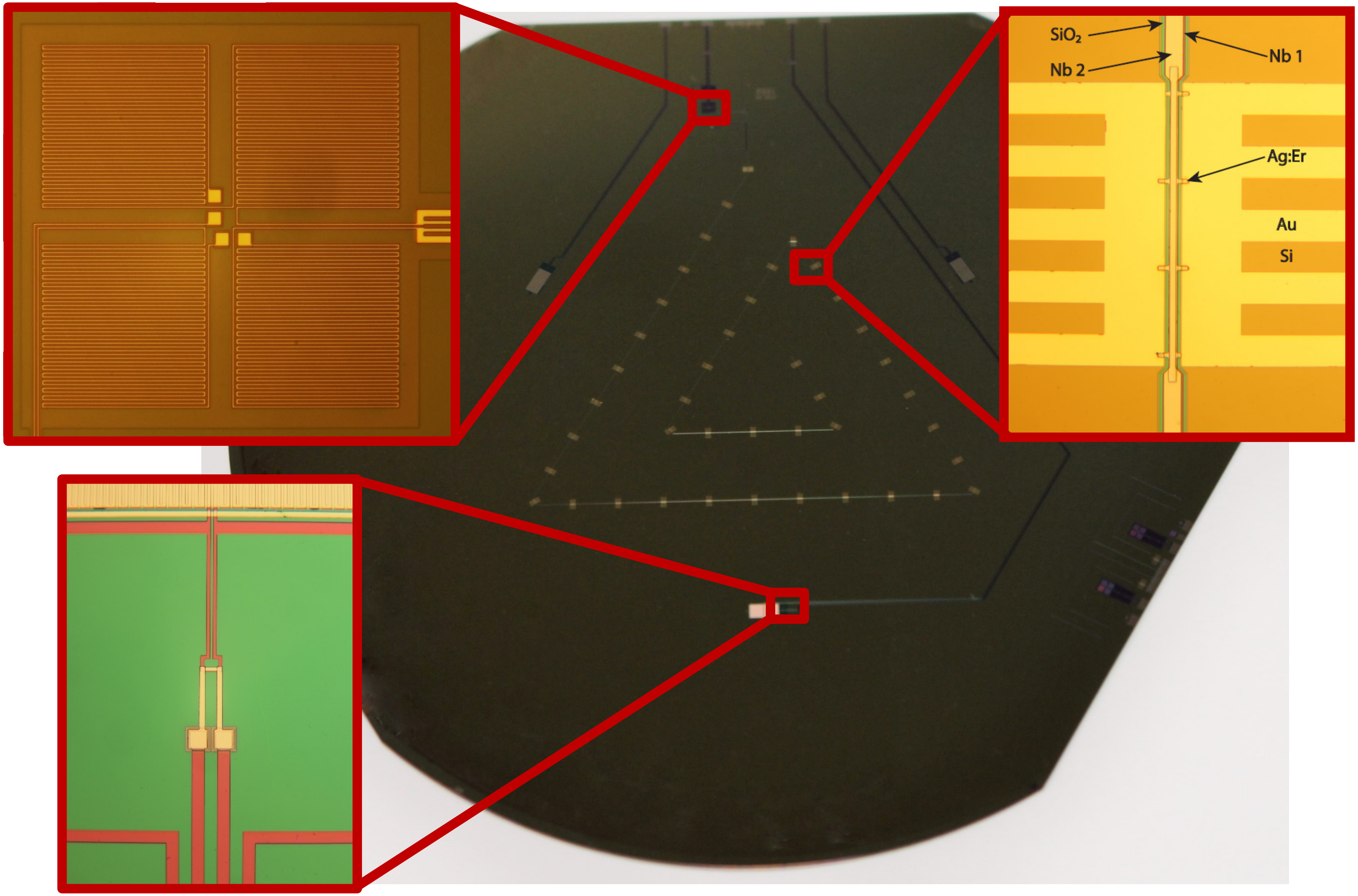

Experimental set-up for P2

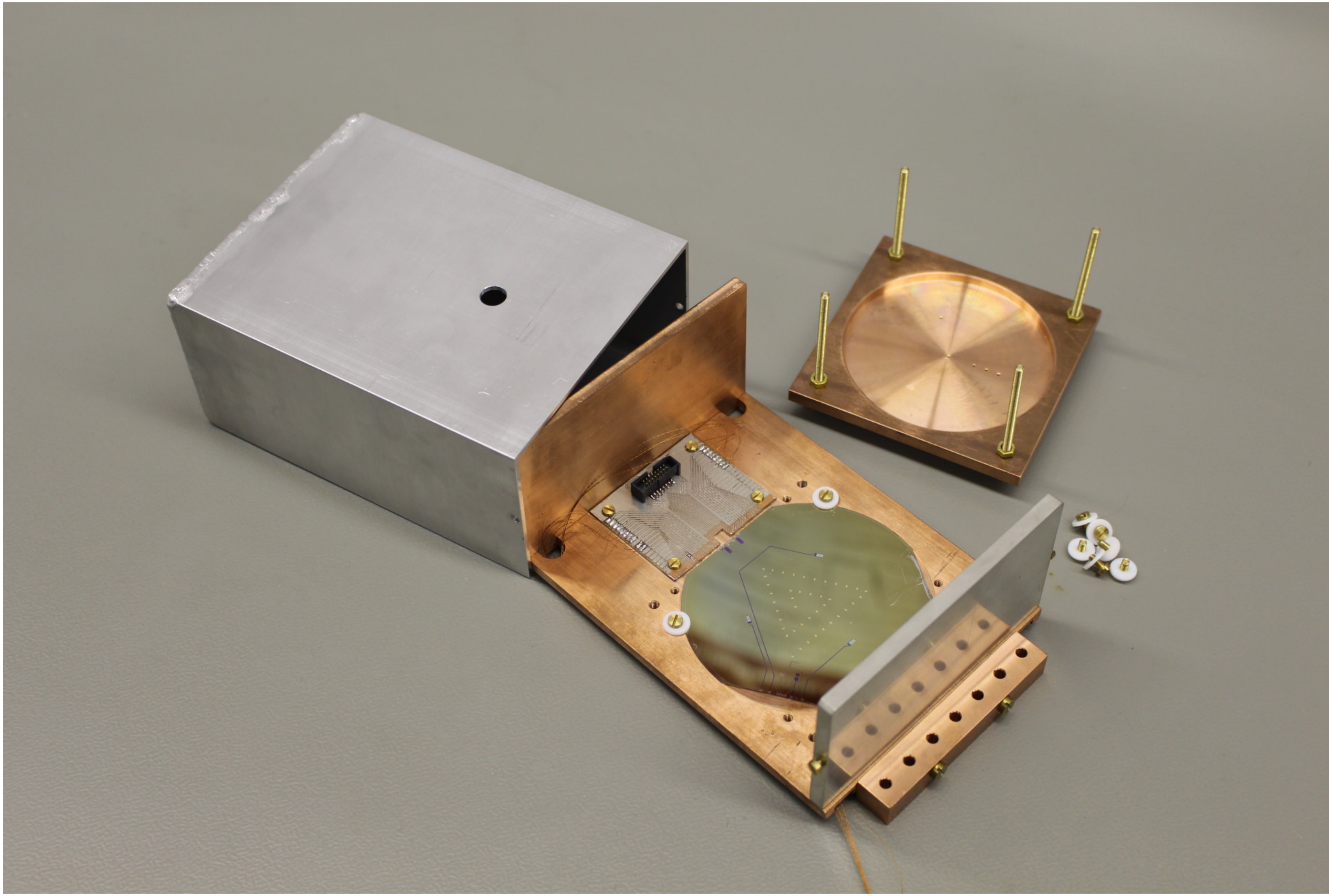

Experimental set-up for P2

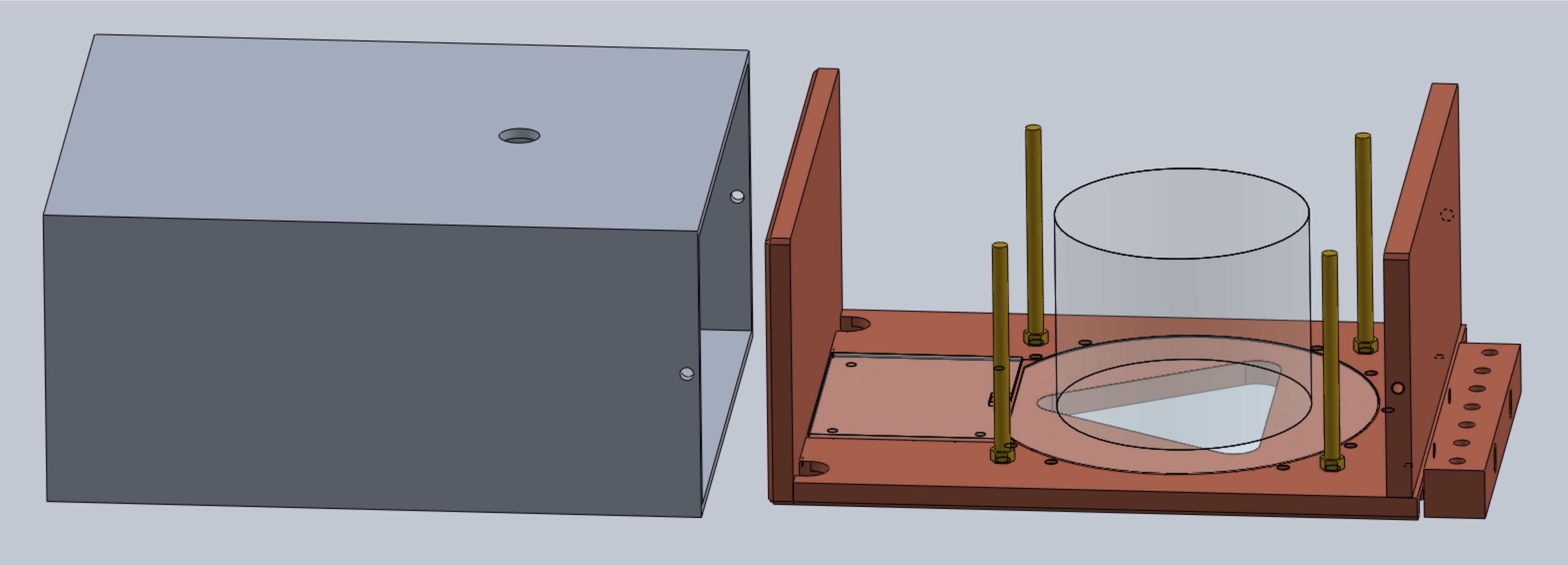

Photon detector: First tests with 6keV x-rays

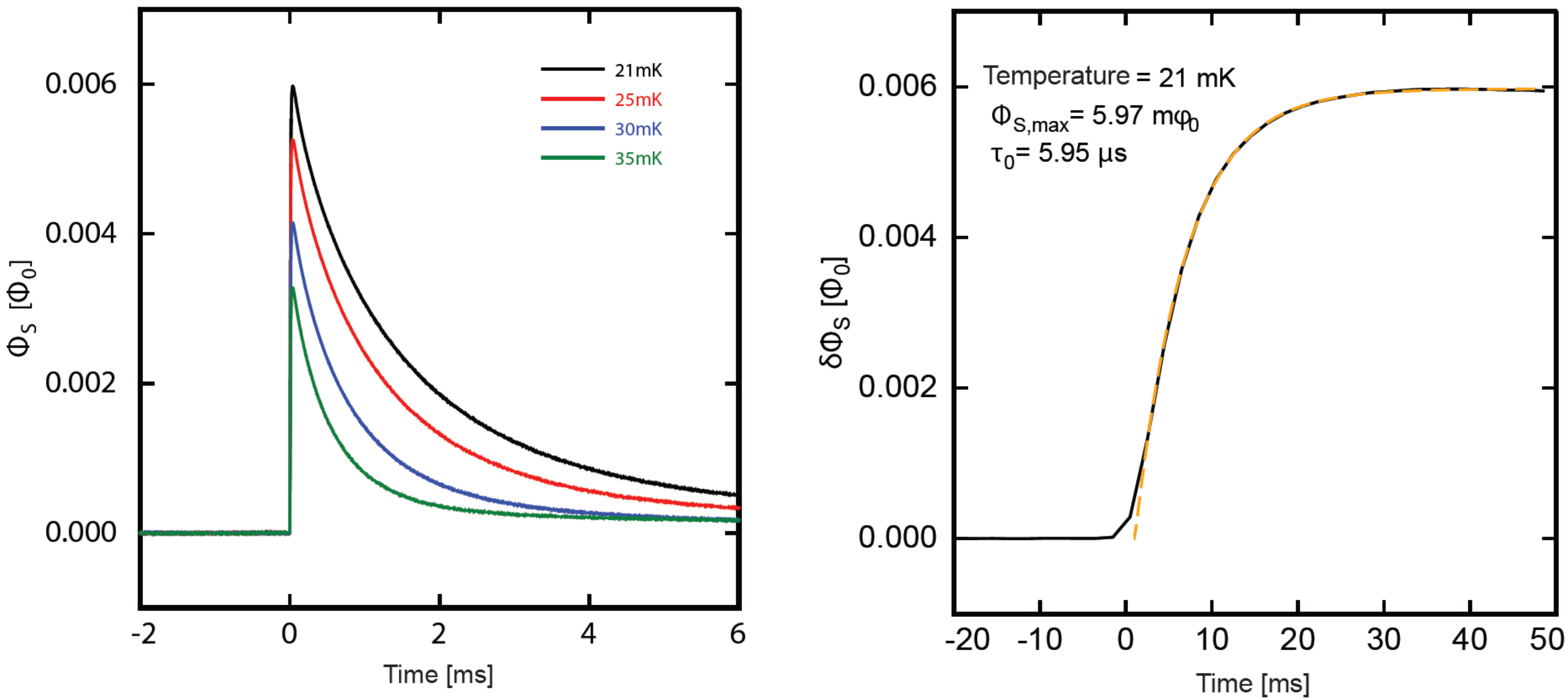

Risetimes:	**direct x-rays**	**~ 6 µs**
	for scintillation light	~ 250–350 µs (Saclay)

D. Gray et al., JLTP 184 3-4 (2016) 904

Conclusions and outlook

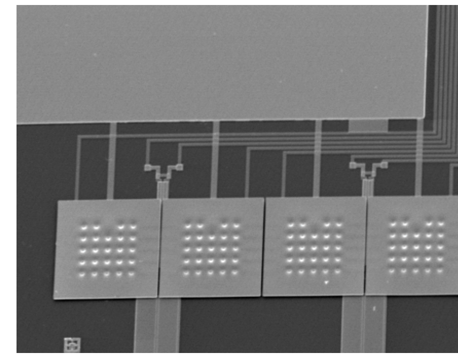

- Metallic magnetic calorimeters are reliable and versatile detectors
  - high resolution for all kinds of particles
  - wide range of energies
  - Fast signal rise time

- Direct determination of the electron neutrino mass using ^{163}Ho
  MMC have proved to fulfil requirements

- eV-scale and keV-scale sterile neutrinos can be investigated through calorimetric measurement of EC spectra

ν

- MMC-based photon and phonon detectors could bring significant benefit for large mass ^{100}Mo-based DBD experiments

Take-home messages

- Working principle of MMCs and their performance

- Where a finite electron neutrino mass affects the ^{163}Ho EC spectrum
  Experimental methods (advantages and disadvantages)

- How to search for sterile neutrino signature in EC spectra

- Benefits of scintillating crystals and
  detector requirements for DBD experiments

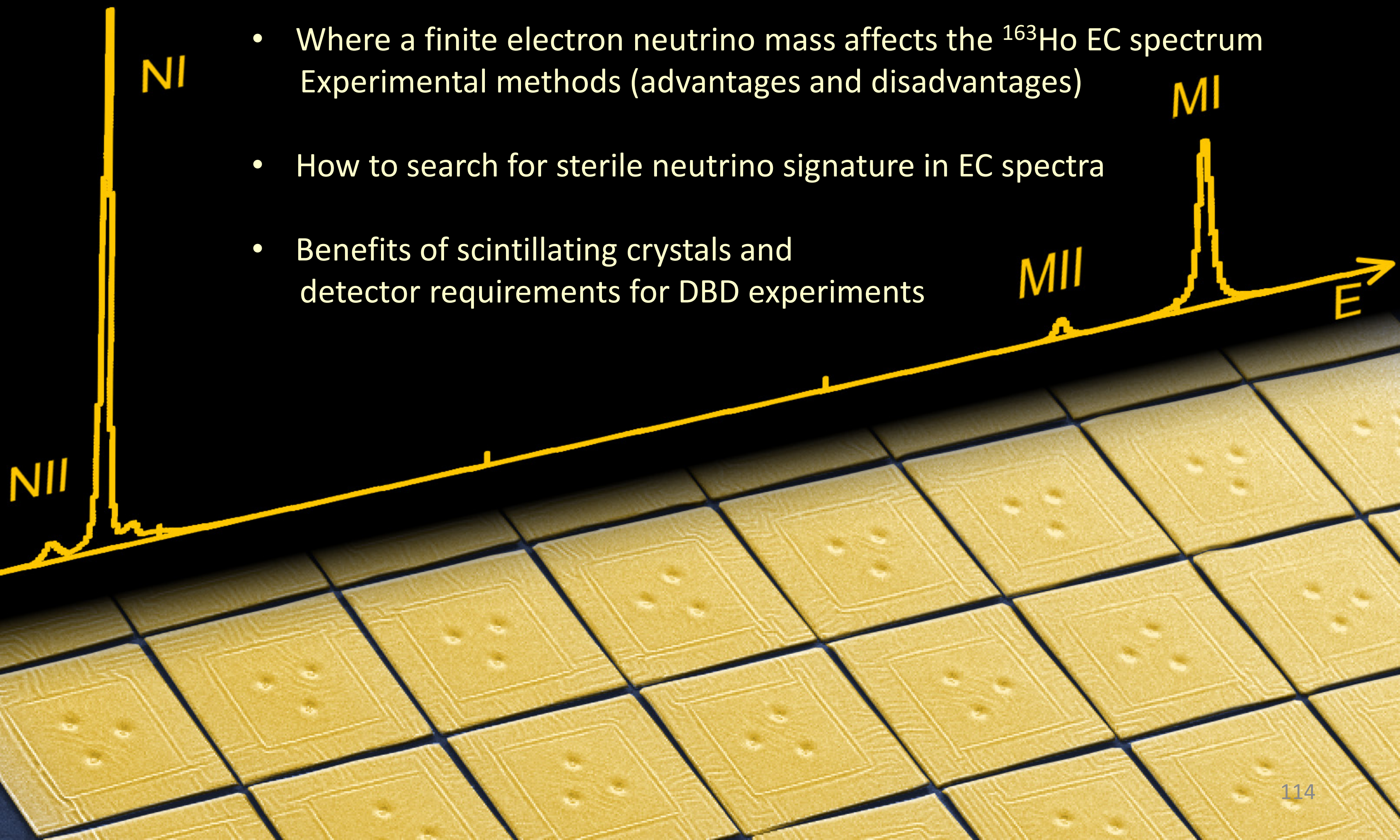

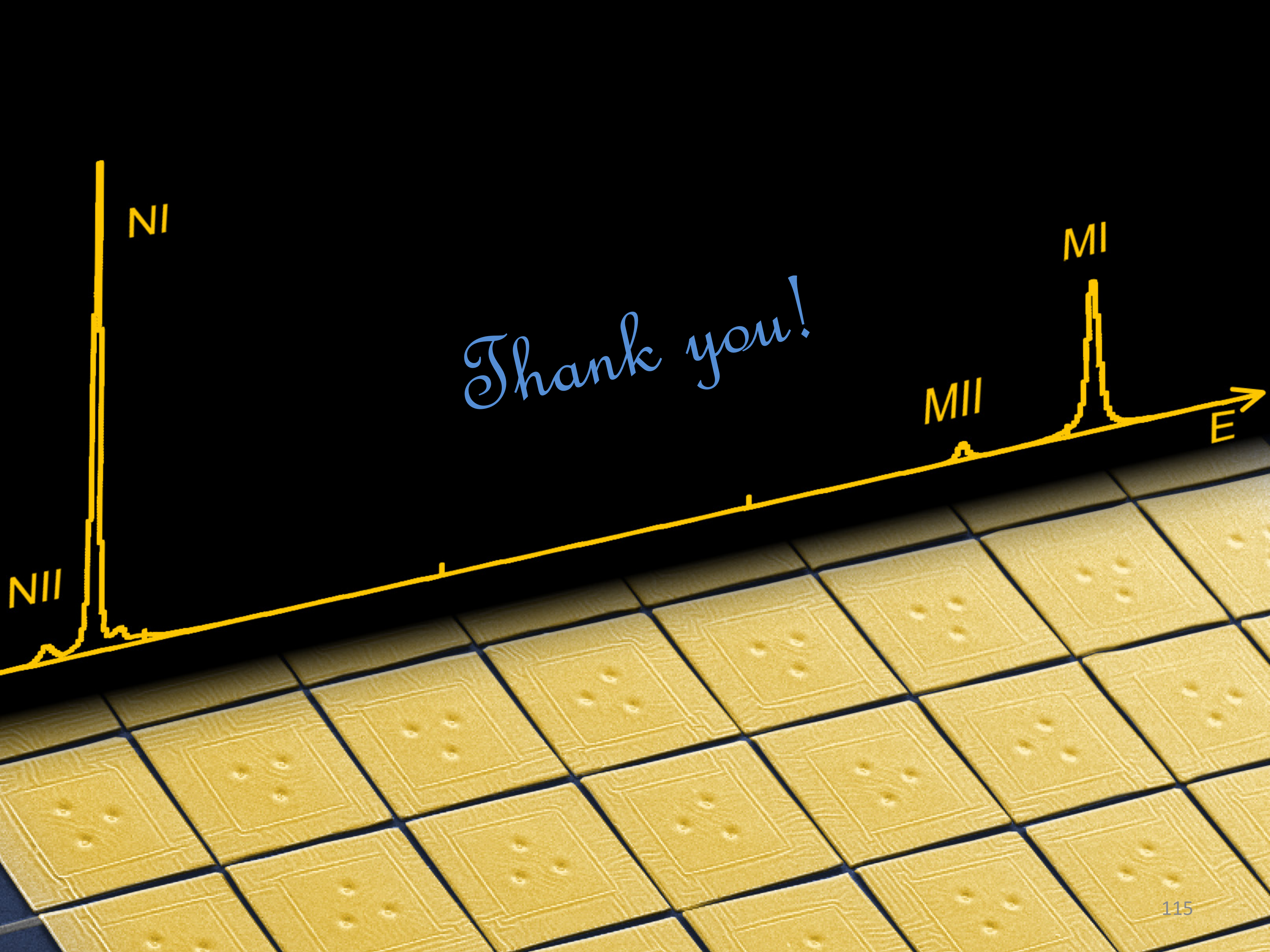
NI
NII
MI
MII
E
Thank you!

MMCs: Microwave SQUID multiplexing

measurement of the spectrum of ^{55}Fe to determine the energy resolution

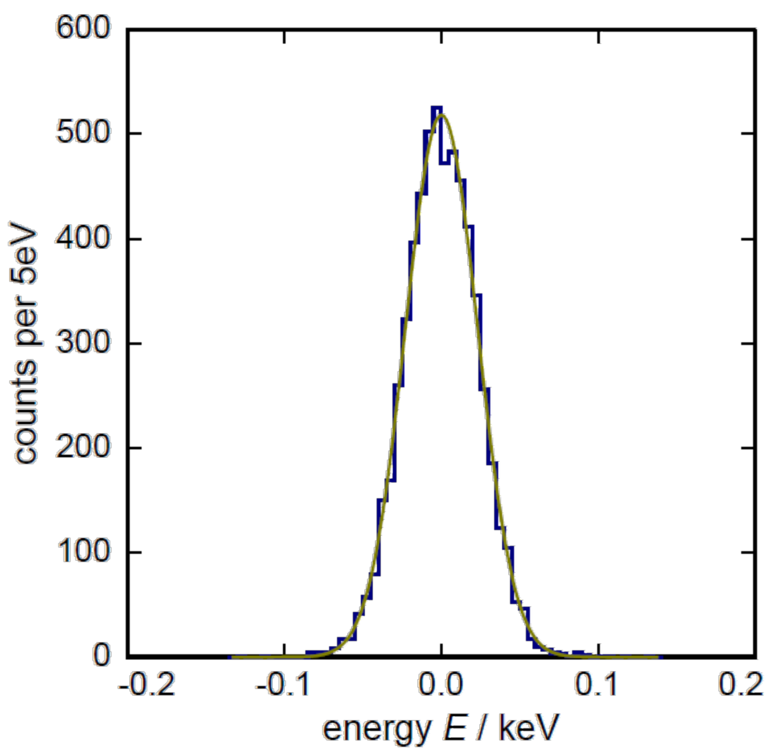

ΔE_{FWHM} = 54. eV

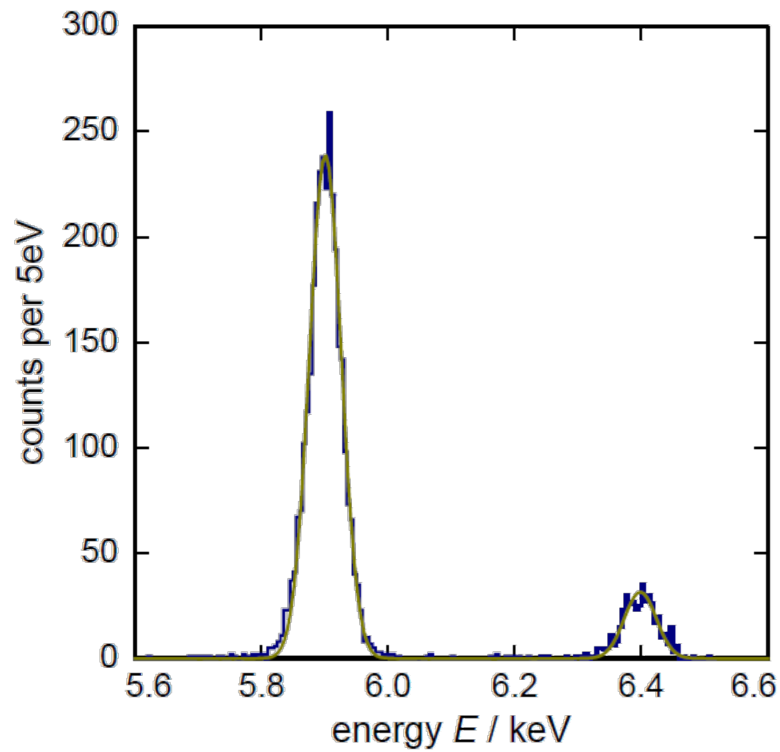

ΔE_{FWHM} = 59. eV

Electron capture in ^{163}Ho: Q_{EC} determination

- ● Calorimetric measurements
- ■ Measurements of x-rays
- ★ $Q_{EC} = m(^{163}\mathrm{Ho}) - m(^{163}\mathrm{Dy})$

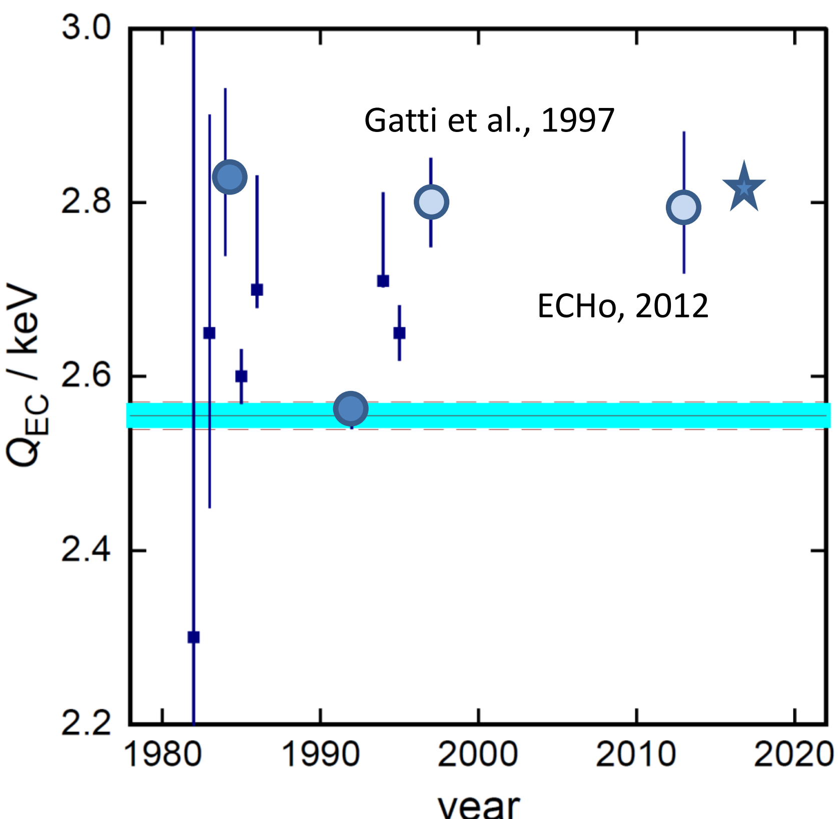

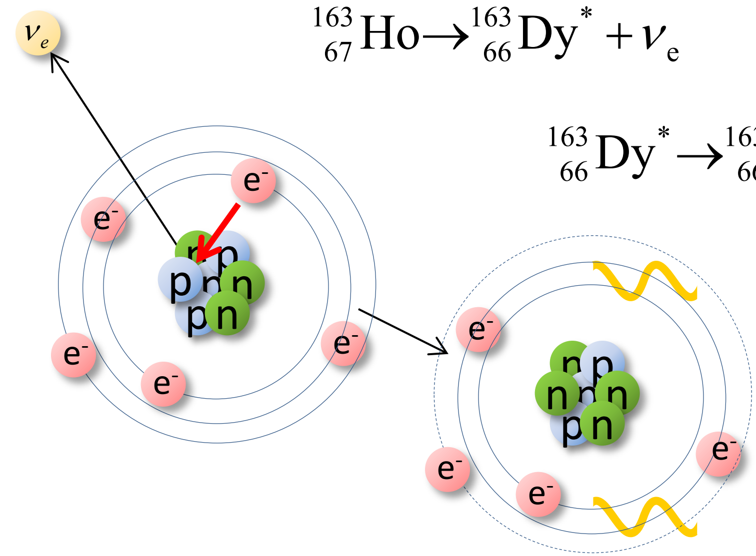

$$^{163}_{67}\mathrm{Ho} \rightarrow ^{163}_{66}\mathrm{Dy}^* + \nu_e$$

$$^{163}_{66}\mathrm{Dy}^* \rightarrow ^{163}_{66}\mathrm{Dy} + E_C$$

- $\tau_{1/2} \cong$ 4570 years (2*10^{11} atoms for 1 Bq)
- Q_{EC} = $(2.833 \pm 0.030^{stat} \pm 0.015^{syst})$ keV

S. Eliseev et al., *Phys. Rev. Lett.* **115** (2015) 062501

Electron capture in ^{163}Ho: Q_{EC} determination

- Calorimetric measurements
- Measurements of x-rays
- $Q_{EC} = m(^{163}\text{Ho}) - m(^{163}\text{Dy})$

Penning Trap Mass Spectroscopy

@TRIGA TRAP (Uni-Mainz) (*)

@SHIPTRAP (GSI – Darmstadt) (**)

$$^{163}_{67}\text{Ho} \rightarrow {}^{163}_{66}\text{Dy}^{*} + \nu_e$$

$$^{163}_{66}\text{Dy}^{*} \rightarrow {}^{163}_{66}\text{Dy} + E_C$$

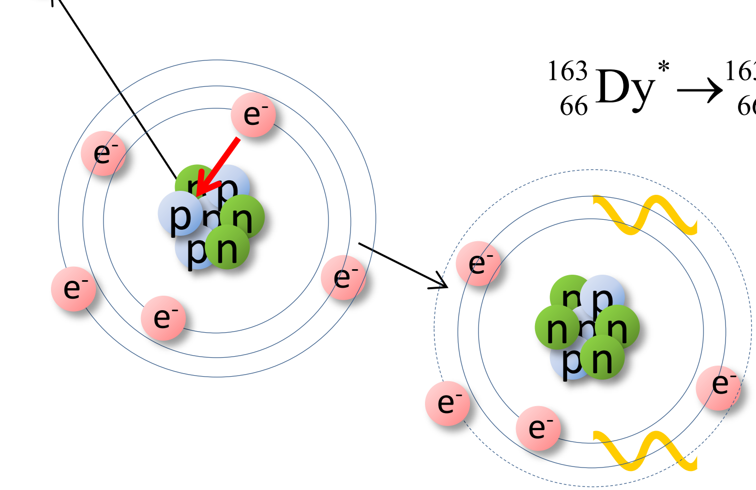

$$\nu_c = \frac{qB}{m}$$

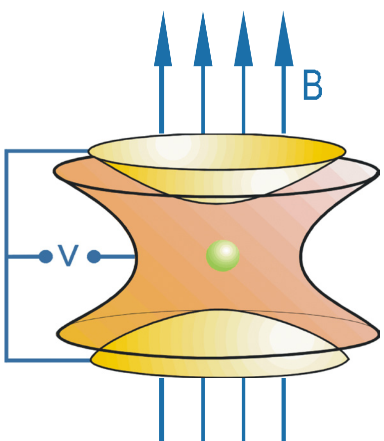

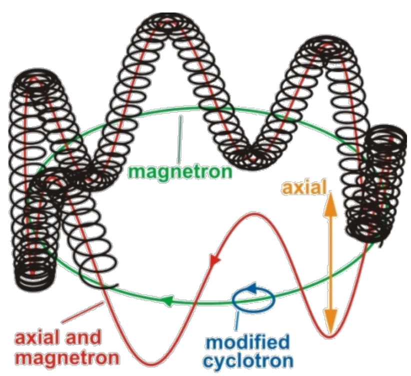

- $\tau_{1/2} \cong 4570$ years (2*10^{11} atoms for 1 Bq)
- Q_{EC} = **(2.833 ± 0.030^{stat} ± 0.015^{syst}) keV**

S. Eliseev et al., *Phys. Rev. Lett.* **115** (2015) 062501 (**)
F. Schneider et al., Eur. Phys. J. A **51** (2015) 89 (*)

High purity ^{163}Ho source in ECHo

Requirement : >10^6 Bq → >10^{17} atoms

- (n,γ)-reaction on ^{162}Er
  - High cross-section
  - Radioactive contaminants

Er161 3.21 h 3/2- EC	Er162 0+ 0.14	Er163 75.0 m 5/2- EC	Er164 0+ 1.61	Er165 10.36 h 5/2- EC	Er166 0+ 33.6
Ho160 25.6 m 5+ * EC	Ho161 2.48 h 7/2- * EC	Ho162 15.0 m 1+ * EC	Ho163 4570 y 7/2- * EC	Ho164 29 m 1+ * EC,β-	Ho165 7/2- 100

- Excellent chemical separation
  Only ^{166m}Ho

- Available ^{163}Ho source:
  ~ 10^{18} atoms

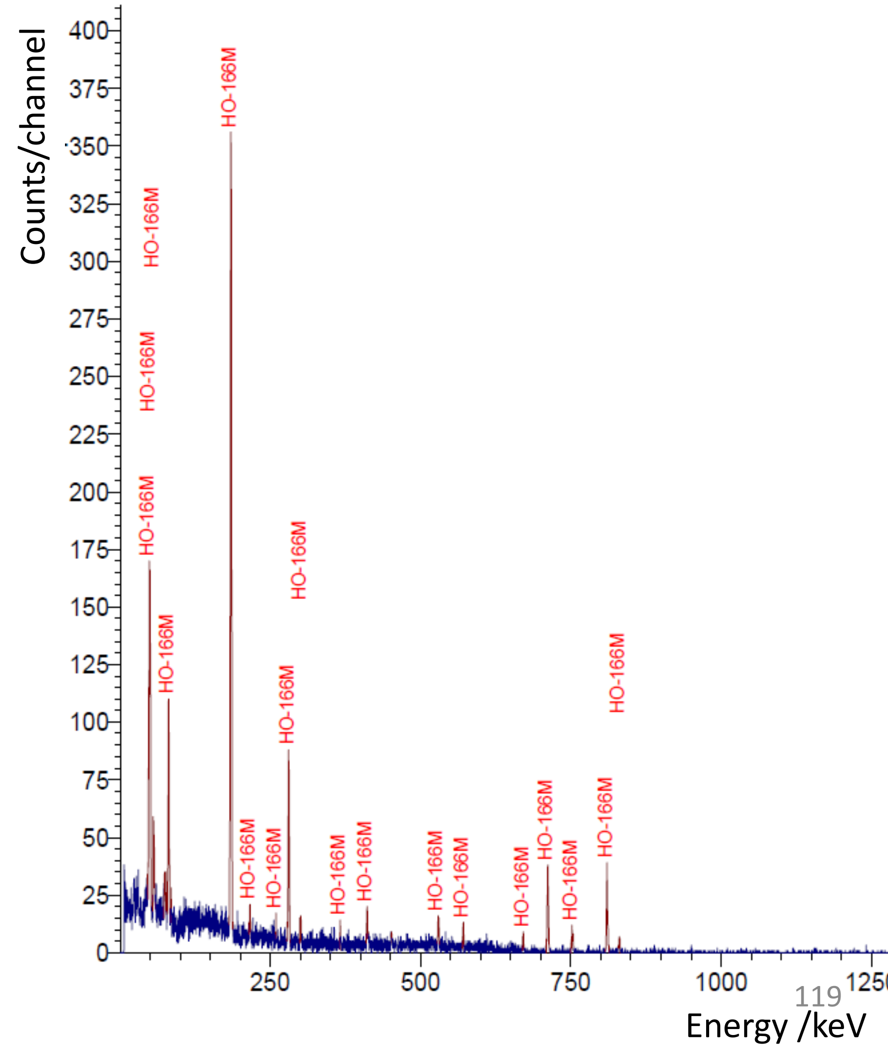

The ECHo Collaboration EPJ-ST 226 8 (2017) 1623

High purity ^{163}Ho source in ECHo

Requirement : $>10^6$ Bq → $>10^{17}$ atoms

- (n,γ)-reaction on ^{162}Er
  - High cross-section 
  - Radioactive contaminants 

Er161 3.21 h 3/2- EC	Er162 0+ 0.14	Er163 75.0 m 5/2- EC	Er164 0+ 1.61	Er165 10.36 h 5/2- EC	Er166 0+ 33.6
Ho160 25.6 m 5+ * EC	Ho161 2.48 h 7/2- * EC	Ho162 15.0 m 1+ * EC	Ho163 4570 y 7/2- * EC	Ho164 29 m 1+ * EC,β-	Ho165 7/2- 100

- Excellent chemical separation
  Only ^{166m}Ho
- Available ^{163}Ho source:
  ~ 10^{18} atoms

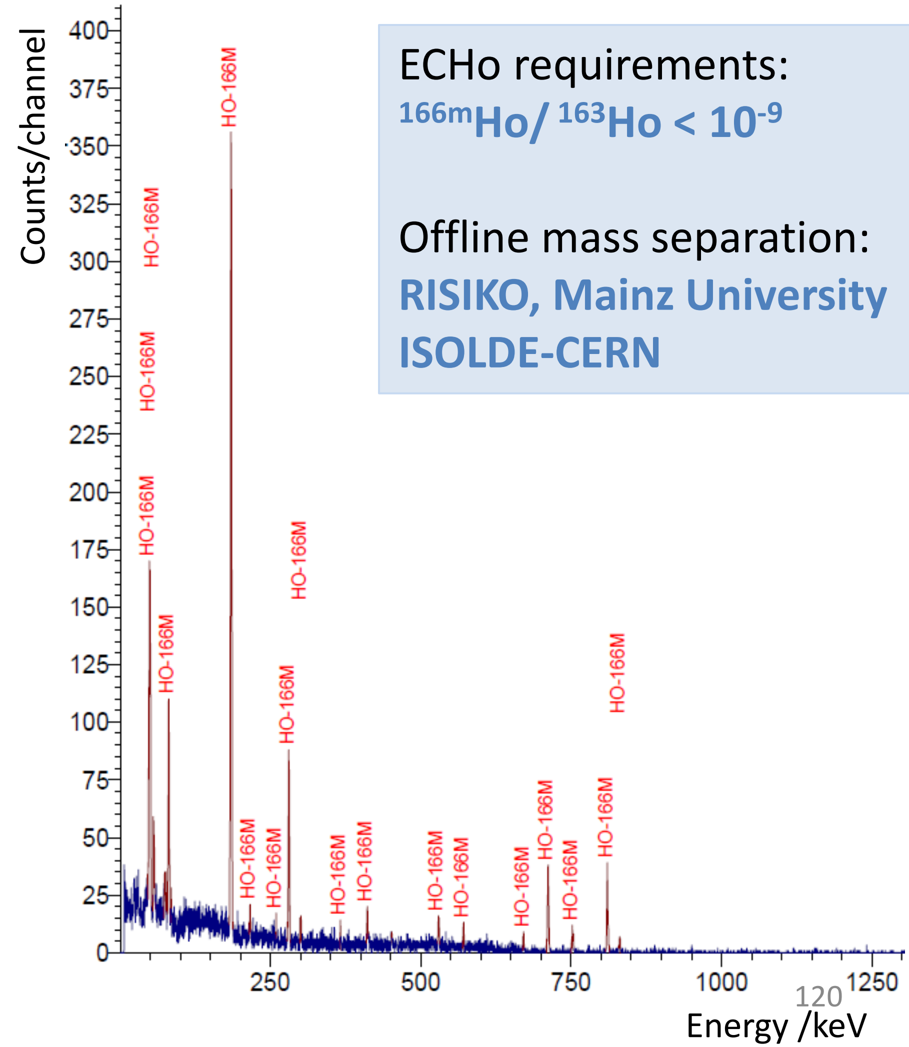

ECHo requirements:
^{166m}Ho/ ^{163}Ho < 10^{-9}

Offline mass separation:
RISIKO, Mainz University
ISOLDE-CERN

The ECHo Collaboration EPJ-ST 226 8 (2017) 1623

Mass separation and ^{163}Ho ion-implantation

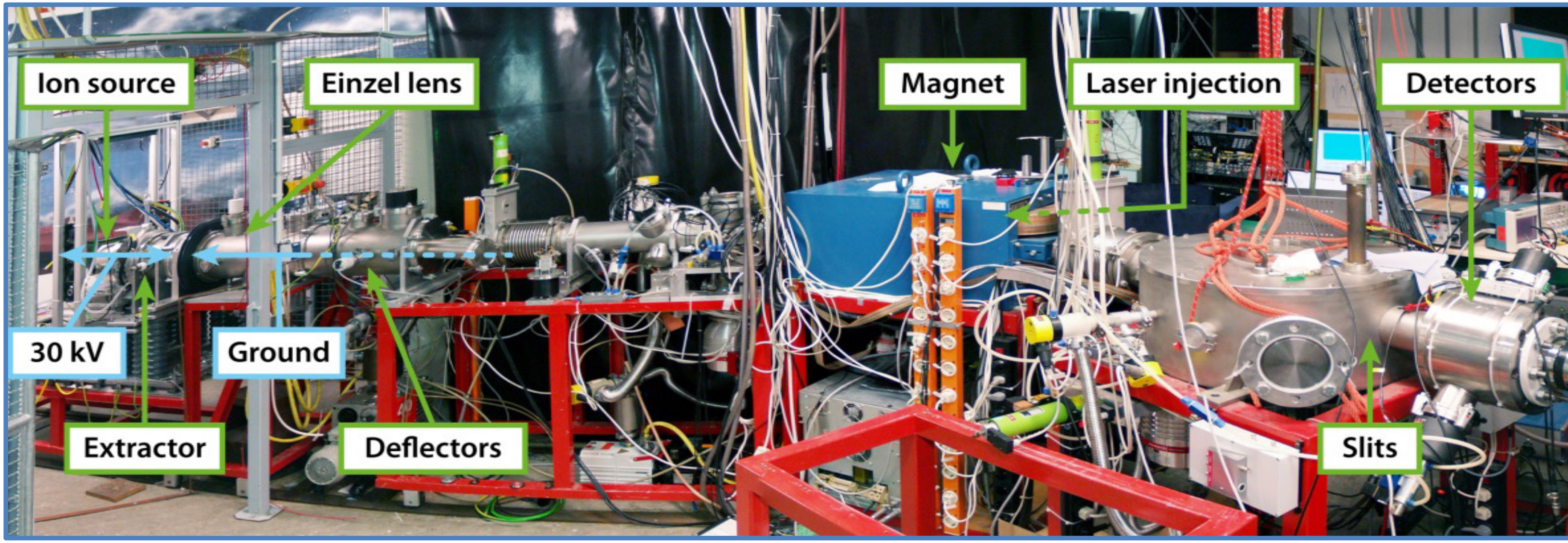

RISIKO @ Physics Institute, Mainz University

- Resonant laser ion source efficiency **42%**
- Suppression of neighboring masses > 700

  → ^{166m}Ho/^{163}Ho $< 10^{-5}$

- Optimization of beam focalization

F. Schneider et al ., *NIM B* **376** (2016) 388

MMCs: Microwave SQUID multiplexing

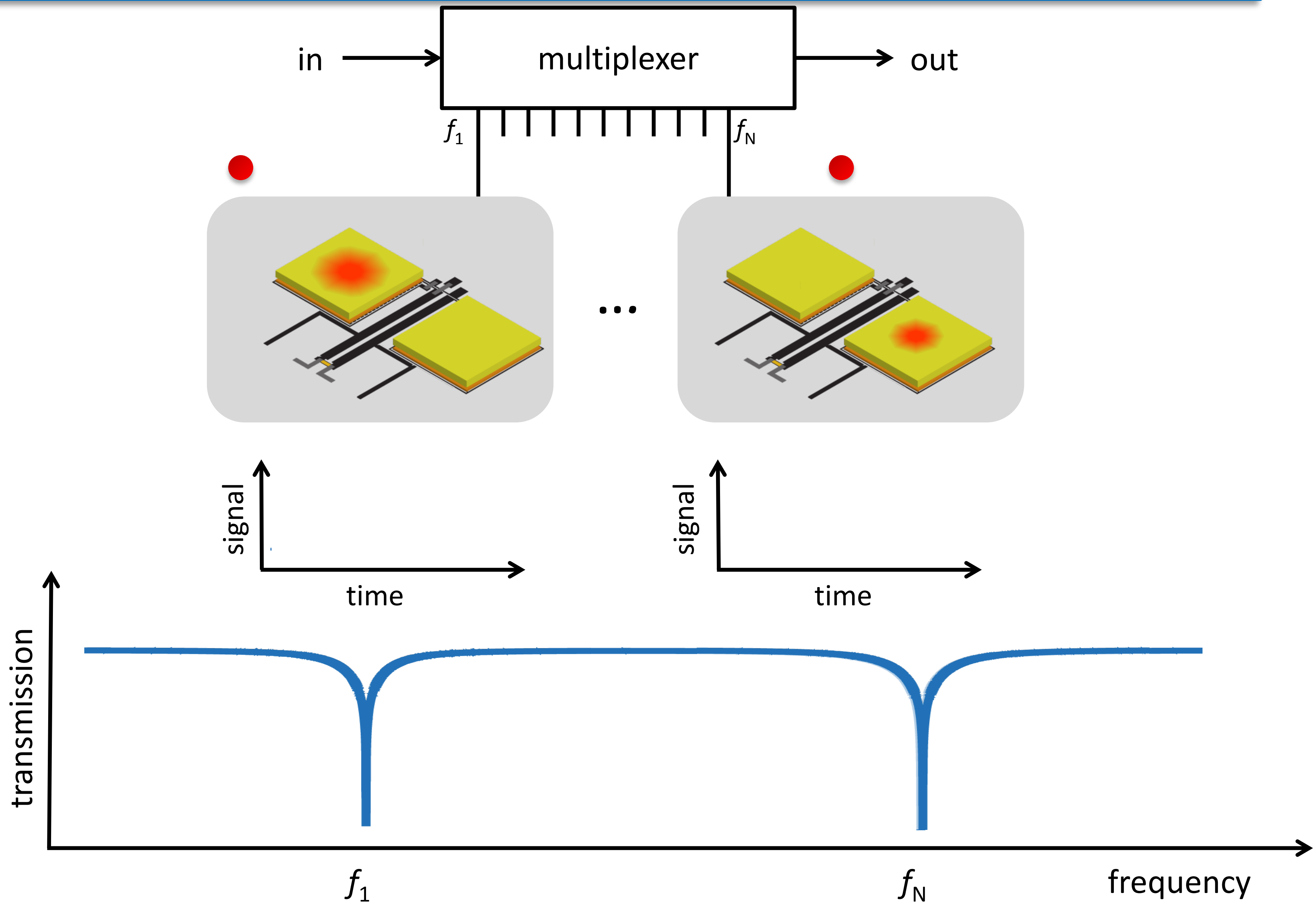

MMCs: Microwave SQUID multiplexing

simultaneous acquisition of signals from two indepedent detectors using a µMUX

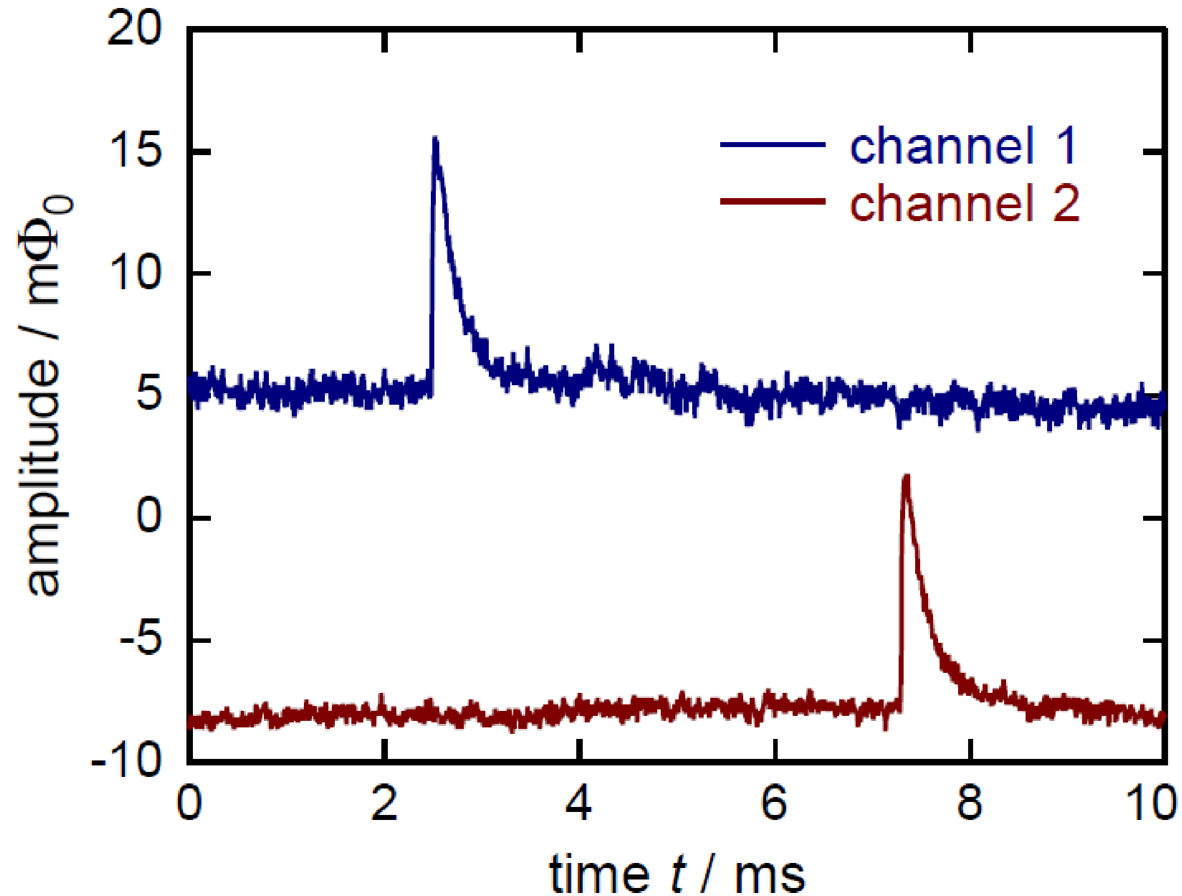

very first demonstration of multiplexed MMC readout

163Ho off-line implantation: results

1 pixel about 2 days

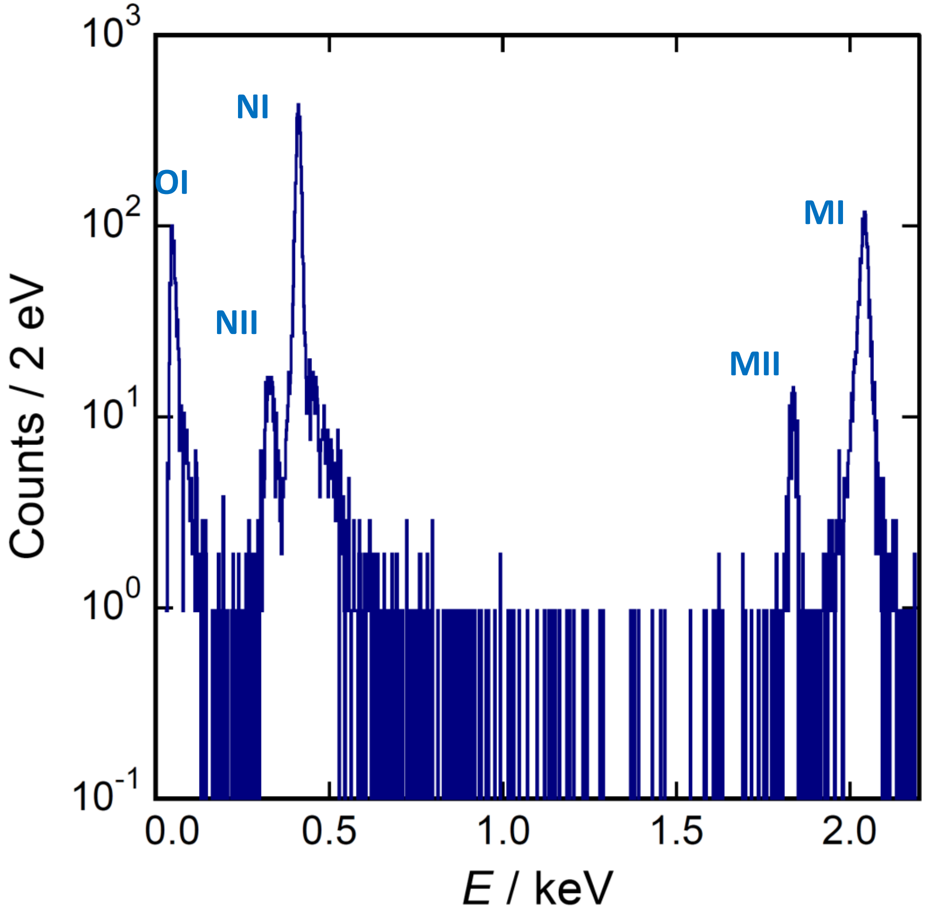

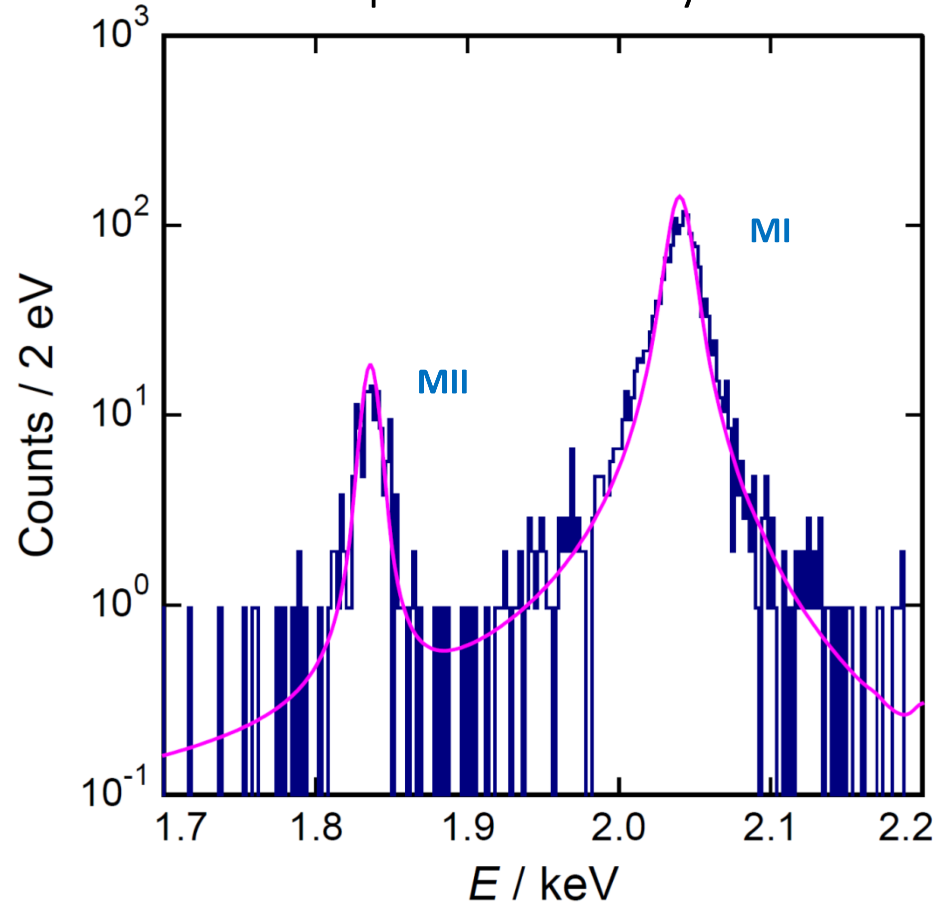

- Activity per pixel $A \sim 0.1$ Bq
- Energy resolution $\Delta E_{FWHM} \sim 10$ eV
- No strong evidence of radioactive contamination in the source
- Symmetric detector response

C. Hassel et al.,JLTP (2015)

Where to improve

High purity ^{163}Ho source:

- Background reduction

Detector design and fabrication:

- Increase activity per pixel
- Stems between absorber and sensor

Understanding of the ^{163}Ho spectrum:

- Investigate undefined structures

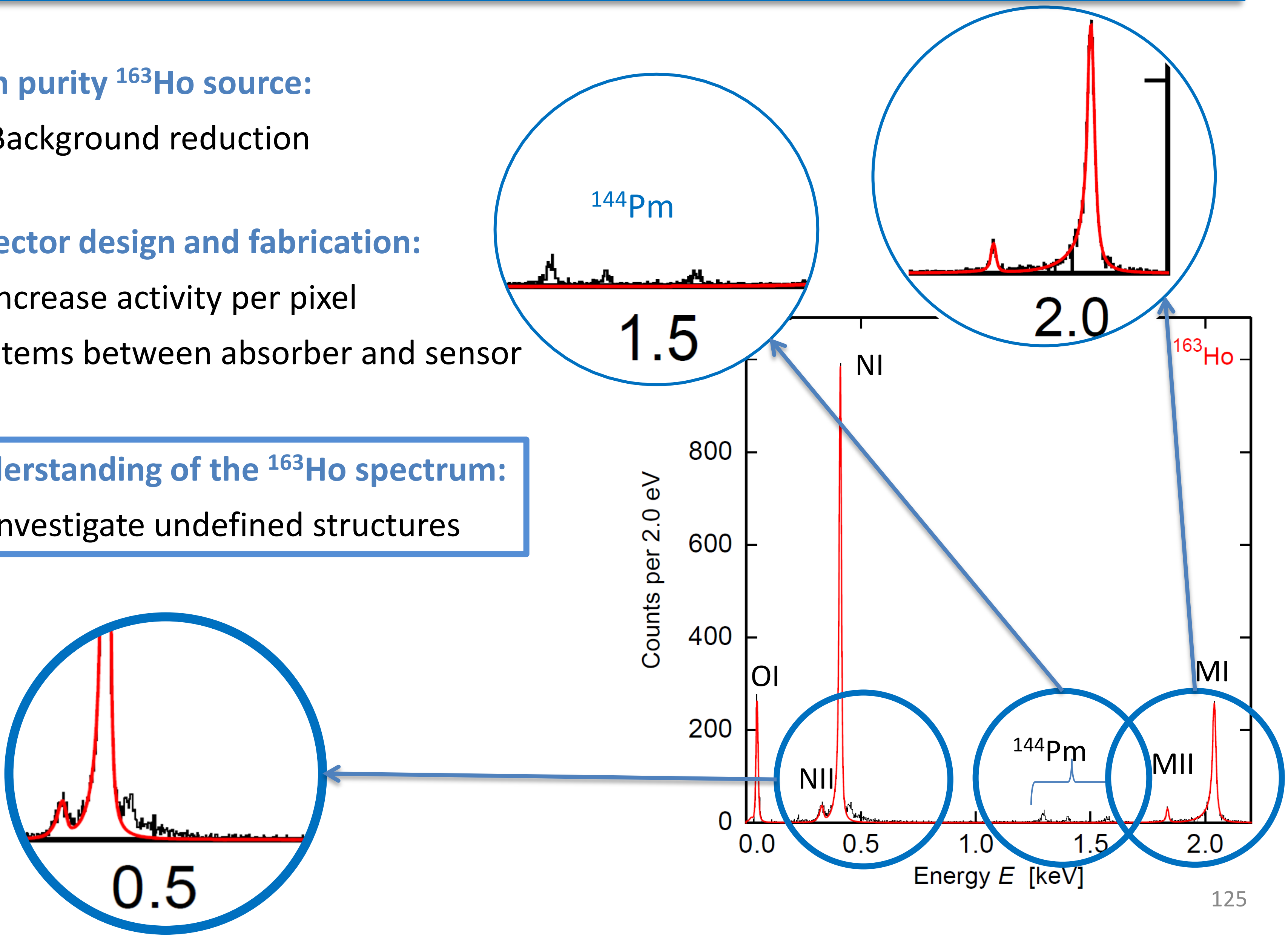

Characterisation of spectral shape

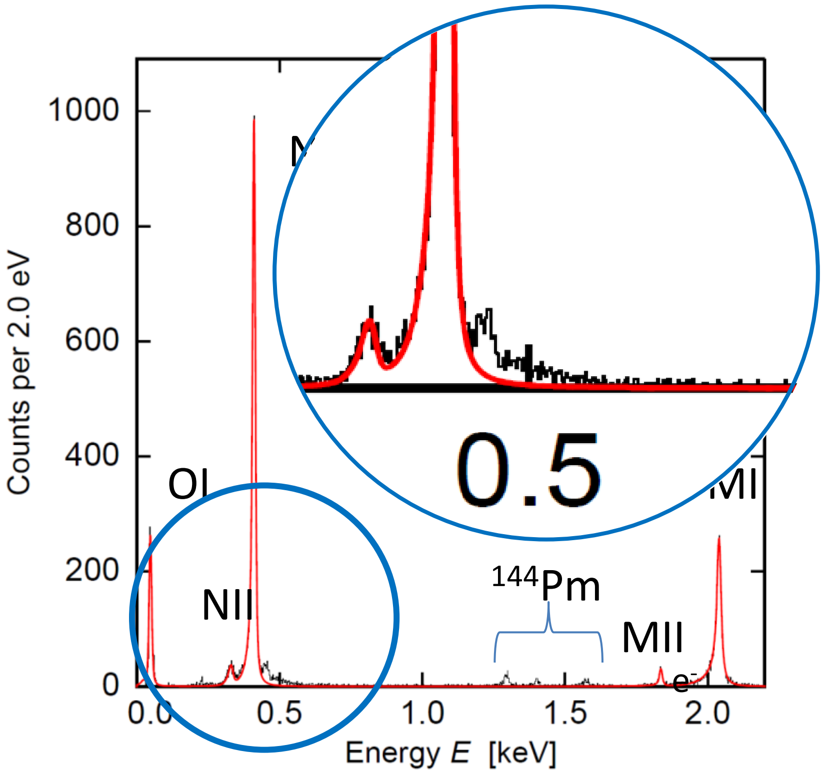

Structures present also in new data

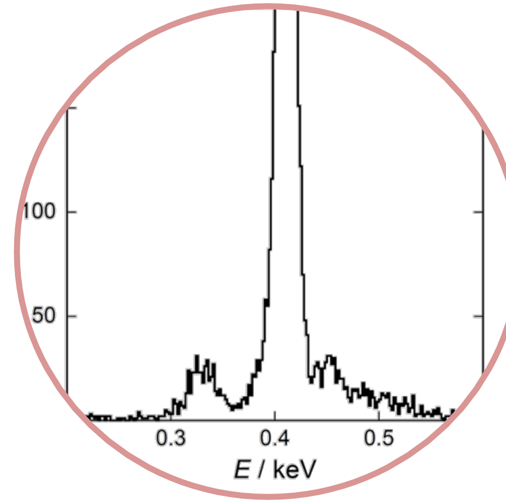

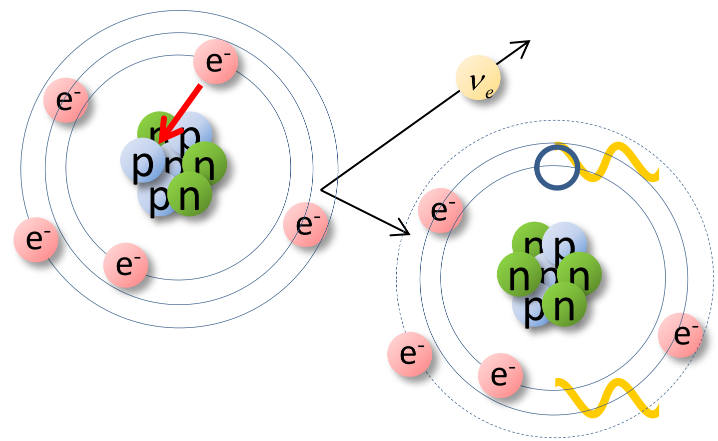

Characterisation of spectral shape

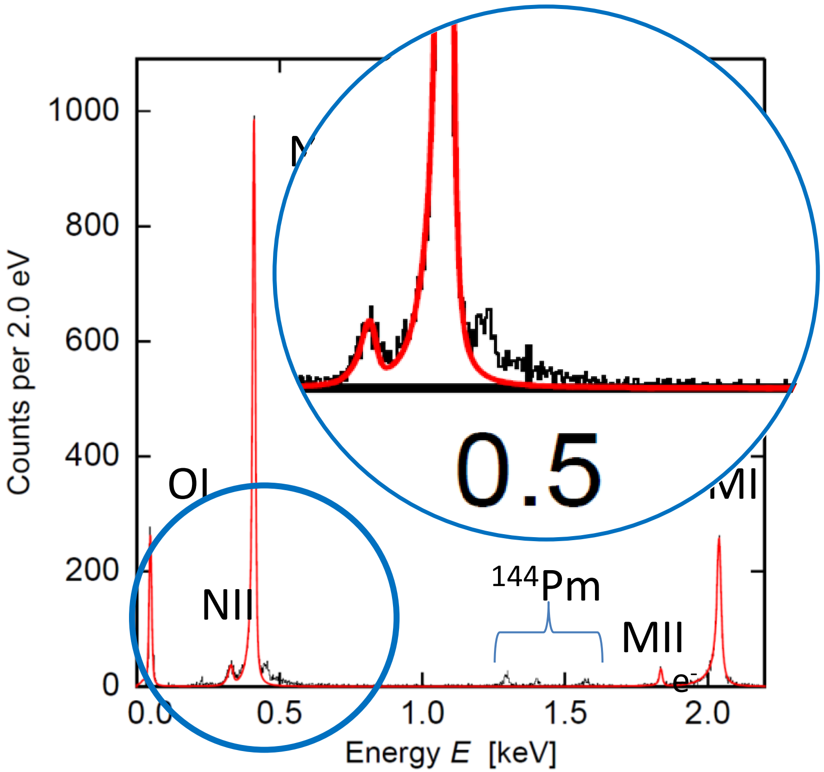

- A. Faessler et al.
  J. Phys. G **42** (2015) 015108
- R. G. H. Robertson
  Phys. Rev. C **91**, 035504 (2015)
- A. Faessler and F. Simkovic
  Phys. Rev. C **91**, 045505 (2015)
- A. Faessler et al.
  Phys. Rev. C **91**, 064302 (2015)
- A. De Rujula and M. Lusignoli
  arXiv:1601.04990v1 [hep-ph] 19 Jan 2016
- A. Faessler et al.
  Phys. Rev. C **95**, (2017) 045502

Two-holes excited states: shake-up

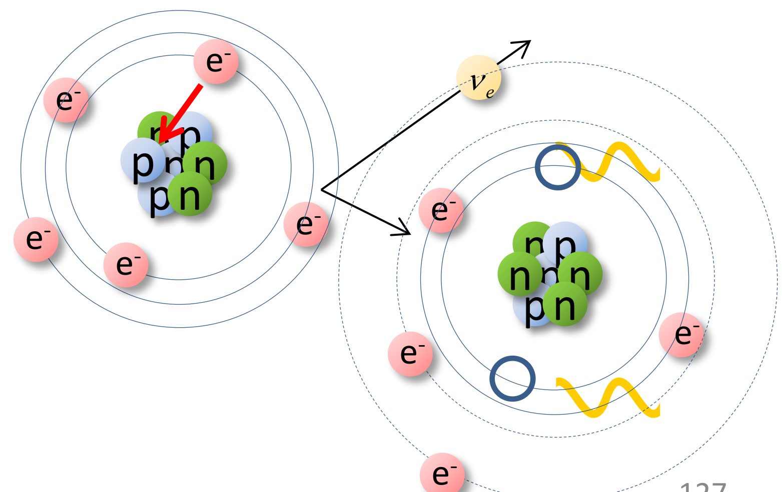

Characterisation of spectral shape

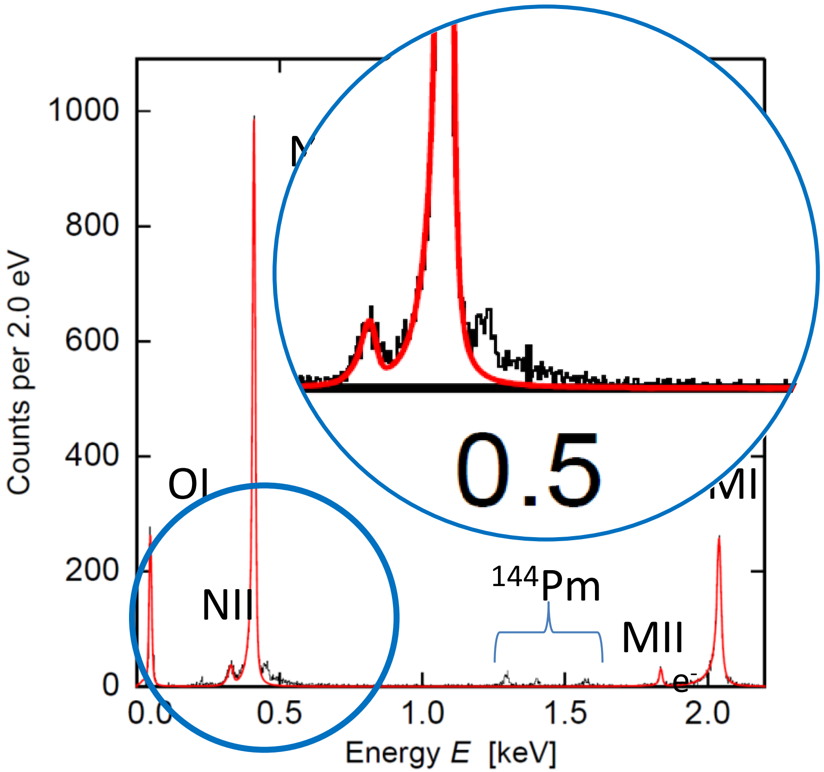

- A. Faessler et al.
  J. Phys. G **42** (2015) 015108
- R. G. H. Robertson
  Phys. Rev. C **91**, 035504 (2015)
- A. Faessler and F. Simkovic
  Phys. Rev. C **91**, 045505 (2015)
- A. Faessler et al.
  Phys. Rev. C **91**, 064302 (2015)
- A. De Rujula and M. Lusignoli
  arXiv:1601.04990v1 [hep-ph] 19 Jan 2016
- A. Faessler et al.
  Phys. Rev. C **95**, (2017) 045502

T

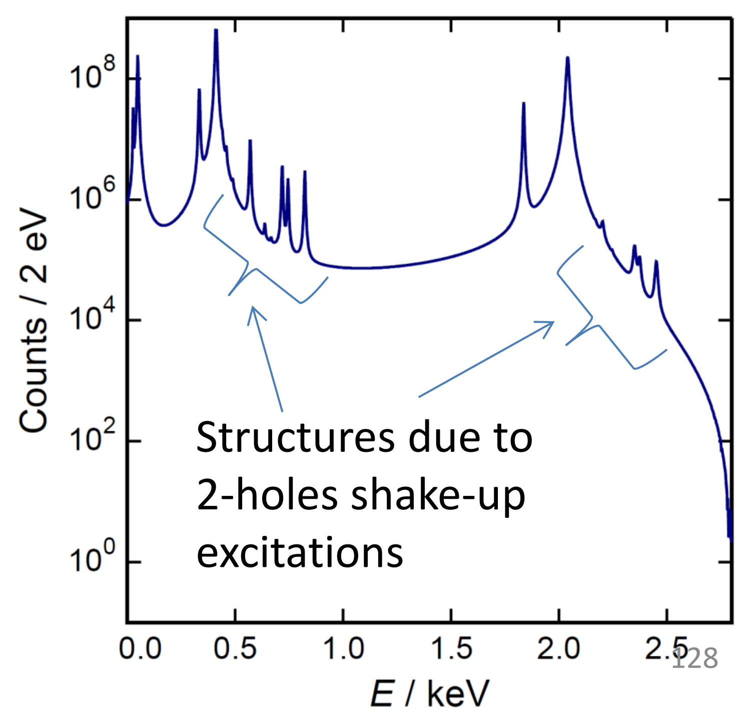

Two-holes excited states: shake-up

Characterisation of spectral shape

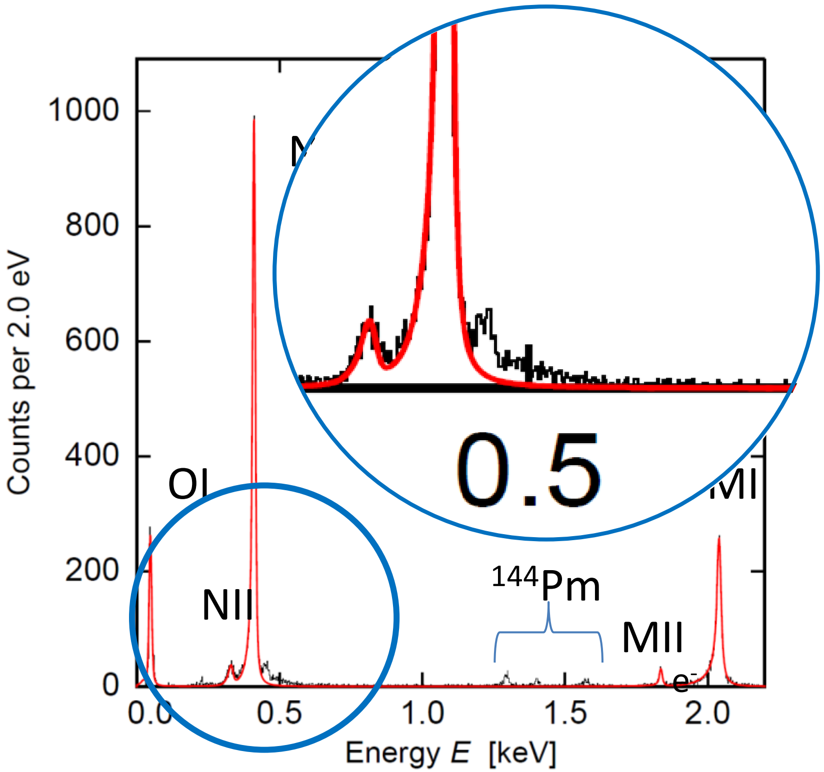

- A. Faessler et al. *J. Phys. G* **42** (2015) 015108
- R. G. H. Robertson Phys. Rev. C **91**, 035504 (2015)
- A. Faessler and F. Simkovic Phys. Rev. C **91**, 045505 (2015)
- A. Faessler et al. Phys. Rev. C **91**, 064302 (2015)
- A. De Rujula and M. Lusignoli arXiv:1601.04990v1 [hep-ph] 19 Jan 2016
- A. Faessler et al. Phys. Rev. C **95**, (2017) 045502

T

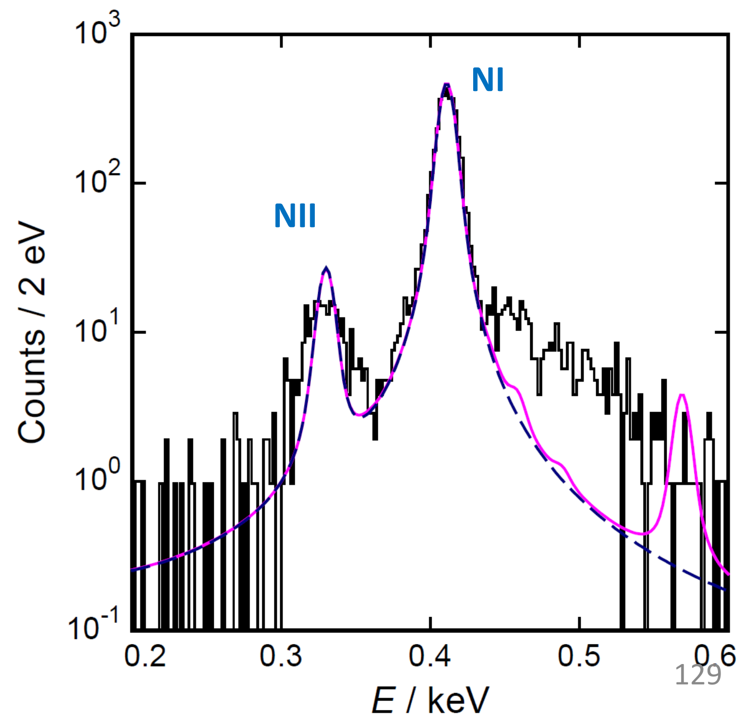

Two-holes excited states: shake-up

Characterisation of spectral shape

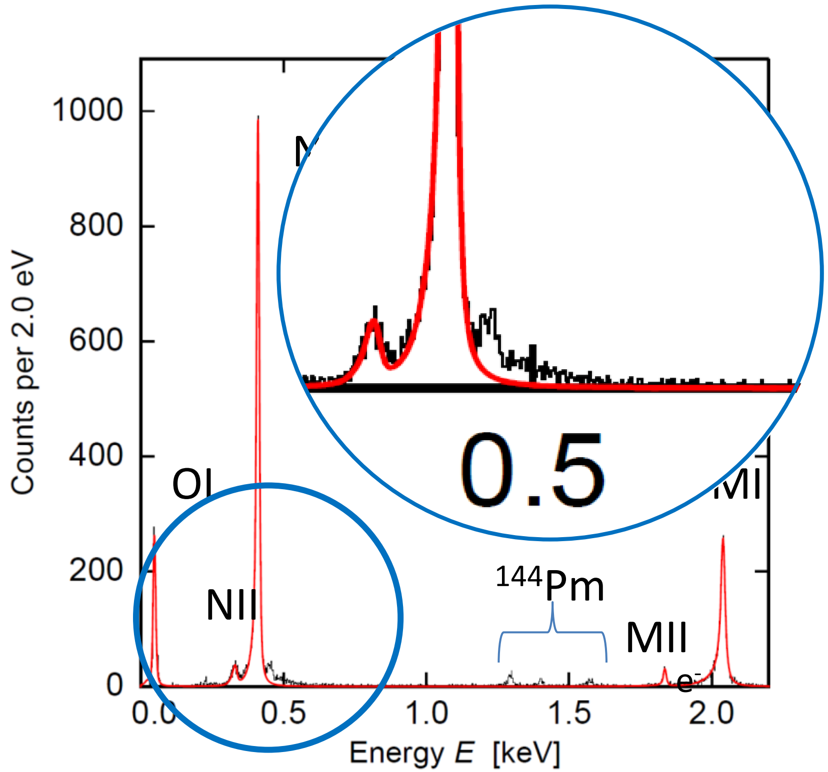

- A. Faessler et al. *J. Phys. G* **42** (2015) 015108
- R. G. H. Robertson Phys. Rev. C **91**, 035504 (2015)
- A. Faessler and F. Simkovic Phys. Rev. C **91**, 045505 (2015)
- A. Faessler et al. Phys. Rev. C **91**, 064302 (2015)
- A. De Rujula and M. Lusignoli arXiv:1601.04990v1 [hep-ph] 19 Jan 2016
- A. Faessler et al. Phys. Rev. C **95**, (2017) 045502

Two-holes excited states: shake-up
shake-off

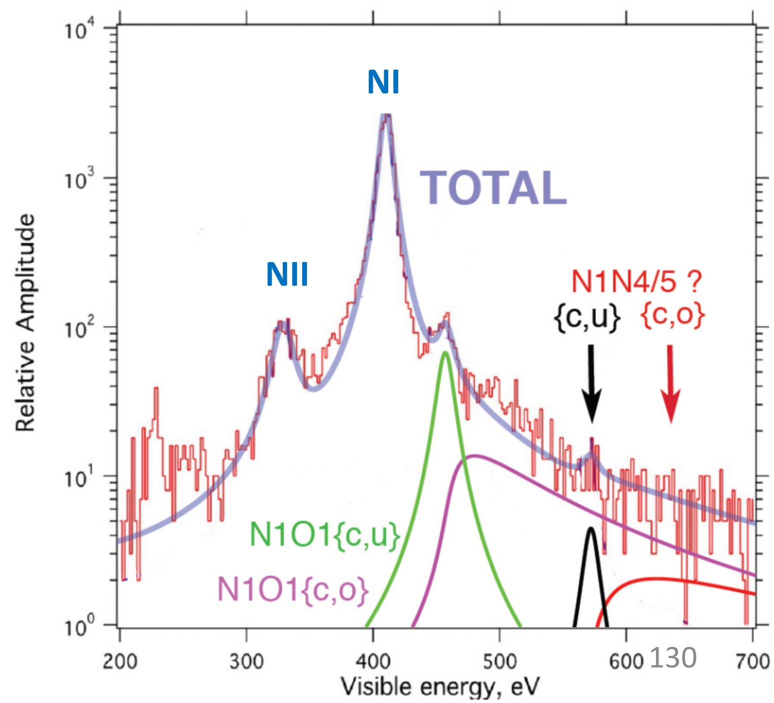

High statistics and high energy resolution spectra will provide information on the spectral shape

Characterisation of spectral shape

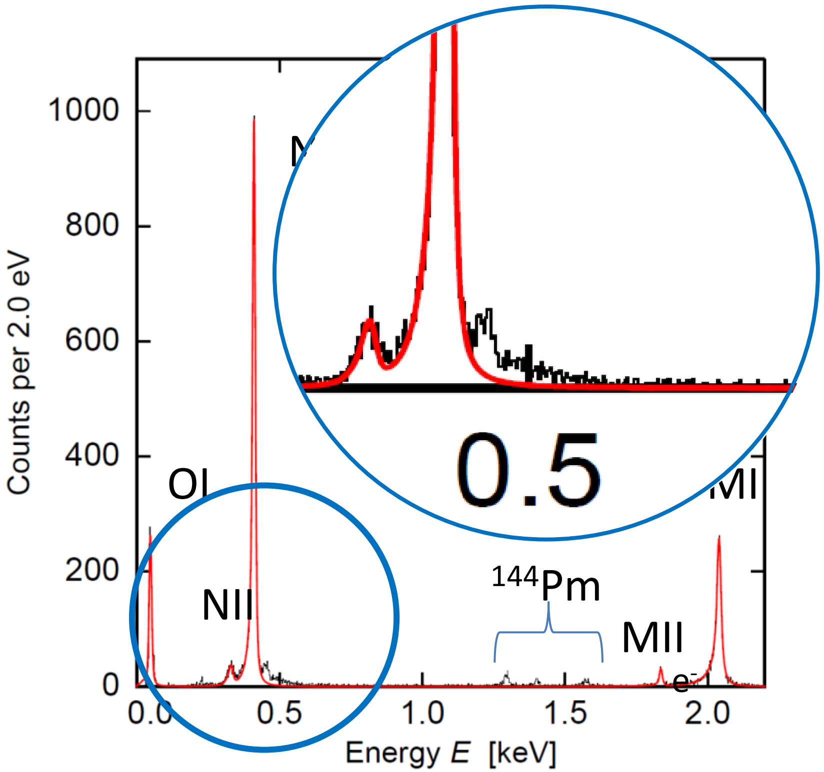

- A. Faessler et al. *J. Phys. G* **42** (2015) 015108
- R. G. H. Robertson Phys. Rev. C **91**, 035504 (2015)
- A. Faessler and F. Simkovic Phys. Rev. C **91**, 045505 (2015)
- A. Faessler et al. Phys. Rev. C **91**, 064302 (2015)
- A. De Rujula and M. Lusignoli arXiv:1601.04990v1 [hep-ph] 19 Jan 2016
- A. Faessler et al. Phys. Rev. C **95** (2017) 045502

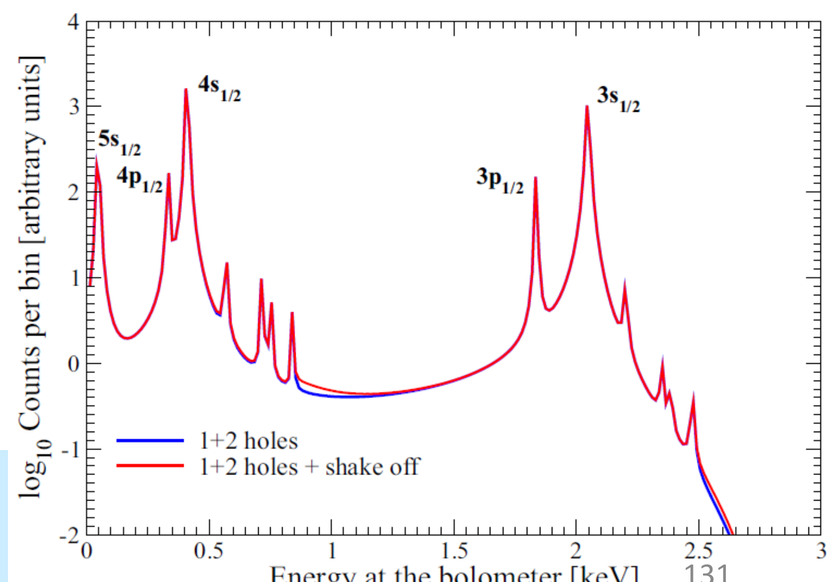

Two-holes excited states: shake-up shake-off

High statistics and high energy resolution spectra will provide information on the spectral shape

Neutrinoless double beta decay - ν mass

The halflife for $0\nu2\beta$ decay depends on the neutrino mass

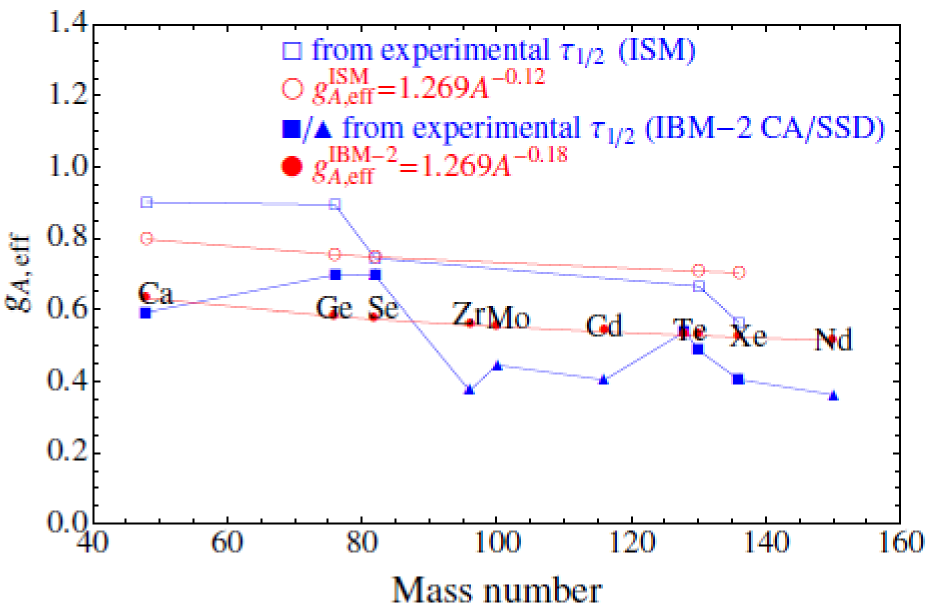

F. Iachello et al., PoS(NEUTEL2015)047

Phase space term

Nuclear matrix element

$$\left(\tau_{1/2}^{0\nu}\right)^{-1} = \left|\frac{m_{\beta\beta}}{m_e}\right|^2 \left|M_\nu^{0\nu}\right|^2 G^{0\nu}$$

$$m_{\beta\beta}^2 = \left|\sum U_{ei}^2 m(\nu_i)\right|^2$$

Uncertanties to evaluate the effective Majorana mass due to:

- Nuclear matrix element
- Quenching of the axial vector coupling constant gA

Neutrinoless double beta decay - ν mass

The halflife for $0\nu2\beta$ decay depends on the neutrino mass

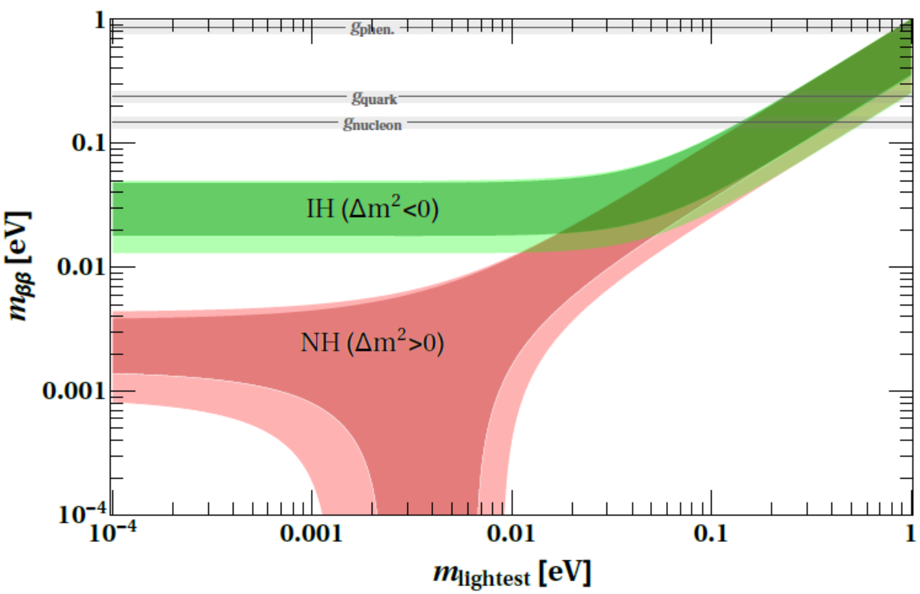

F. Iachello et al., PoS(NEUTEL2015)047

Phase space term

Nuclear matrix element

$$\left(\tau_{1/2}^{0\nu}\right)^{-1} = \left|\frac{m_{\beta\beta}}{m_e}\right|^2 \left|M_\nu^{0\nu}\right|^2 G^{0\nu}$$

$$m_{\beta\beta}^2 = \left|\sum U_{ei}^2 m(\nu_i)\right|^2$$

Uncertanties to evaluate the effective Majorana mass due to:

- Nuclear matrix element
- Quenching of the axial vector coupling constant gA

Neutrinoless double beta decay - ν mass

The halflife for 0ν2β decay depends on the neutrino mass

Phase space term

Nuclear matrix element

$$\left(\tau_{1/2}^{0\nu}\right)^{-1} = \left|\frac{m_{\beta\beta}}{m \ldots}\right|^2 \left|M^{0\nu}\right|^2 \ldots$$

$$m_{\beta\beta}^2 = \left|\sum U_{ei}^2 m(\nu_i)\right|^2$$

F. Iachello et al., PoS(NEUTEL2015)047

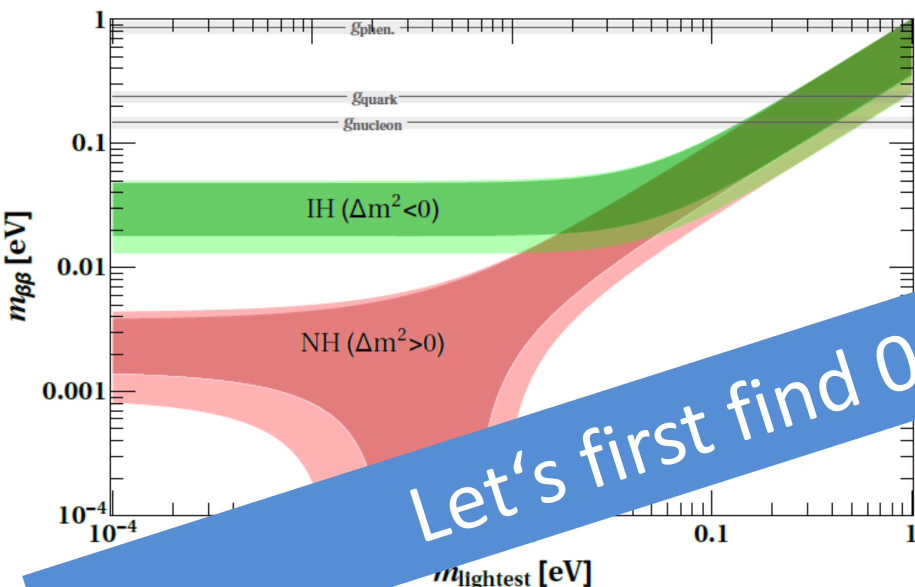

Let's first find 0ν2e events!!!

Uncertainties to evaluate the effective Majorana mass due to:

- Nuclear matrix element
- Quenching of the axial vector coupling constant gA

Fight against background

Direct reduction of background activity

- Select and use ultra-pure materials
- Minimize all passive (non “source”) materials
- Avoid material re-contamination (machining, manipulation, storage)
- Fabricate ultra-clean materials (underground fab if needed)
- underground labs — reduced muon flux & related induced activations

Discrimination techniques

- Energy resolution
- Active veto detector
- Tracking (topology)
- Particle ID, angular, spatial, time correlations
- Fiducial Fits
- Granularity (arrays)
- Pulse shape discrimination (PSD)
- Ion Identification

Methods	
TPCs (liquid, gas)	^{136}Xe
Doped Liquid Scintillators	^{136}Xe, ^{130}Te
Solid state detectors	^{76}Ge, ^{116}Cd
Bolometers (+ enhancements)	^{130}Te, ^{82}Se, ^{100}Mo, ^{116}Cd
Foils with tracking chambers	^{82}Se, ^{150}Nd, ^{100}Mo

Both approaches are needed

Experimental set-up for P2

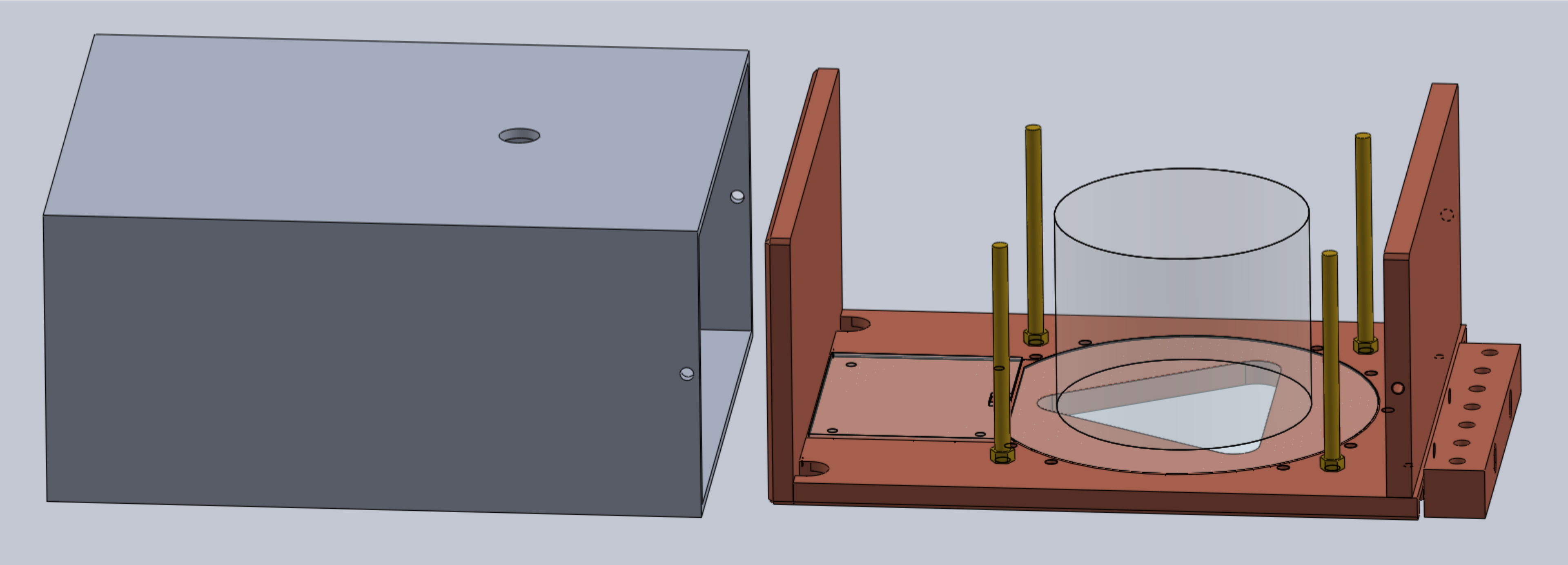

First prototype of photon detector

Top view:

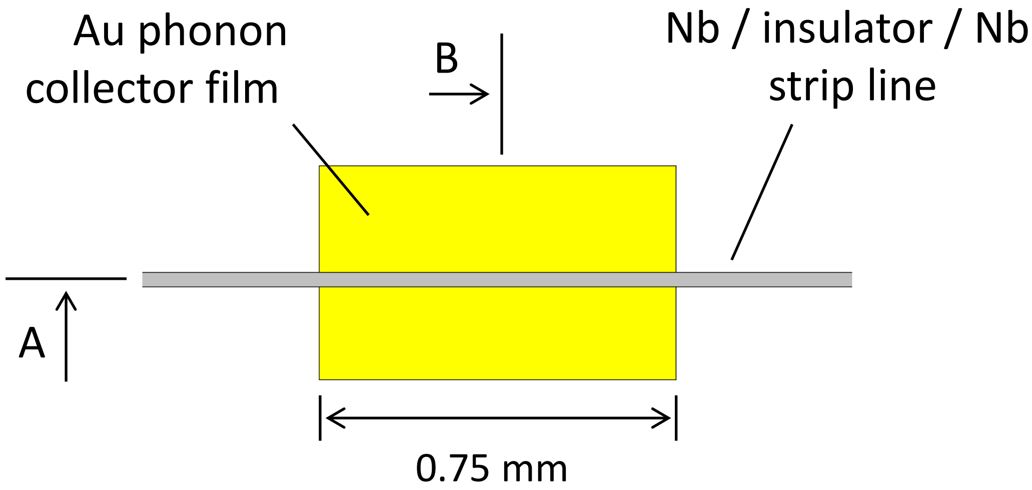

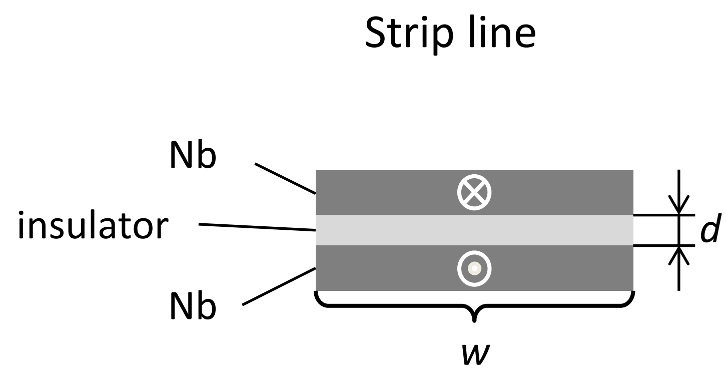

Cross section:

A

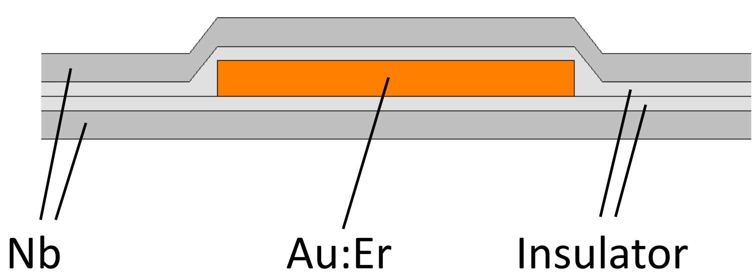

B

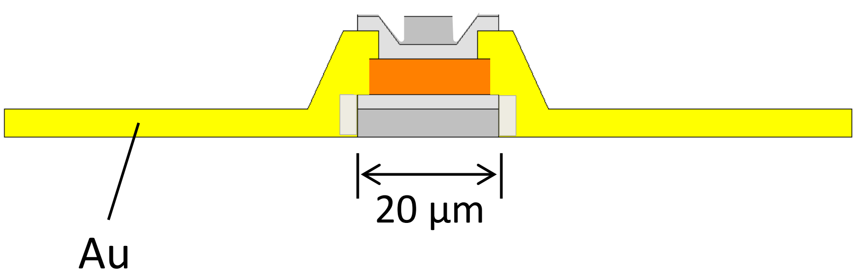

Wärme- & Lichtdetektor